UNCLASSIFIED

AD NUMBER
AD815473
LIMITATION CHANGES

TO:

Approved for public release; distribution is unlimited.

FROM:

Distribution authorized to U.S. Gov't. agencies and their contractors; Critical Technology; MAR 1967. Other requests shall be referred to Air Force Materials Laboratory, Attn: MAMP, Wright-Patterson AFB, OH 45433. This document contains export-controlled technical data.

AUTHORITY

USAF ltr, 12 Jan 1972

THIS PAGE IS UNCLASSIFIED

AD815473

INVESTIGATION OF THERMAL EMBRITTLEMENT IN 18Ni(250) MARAGING STEEL

C. J. BARTON
B. G. REISDORF
P. H. SALMON COX
J. M. CHILTON
C. E. OSKIN, JR.

U. S. STEEL CORPORATION
APPLIED RESEARCH LABORATORY
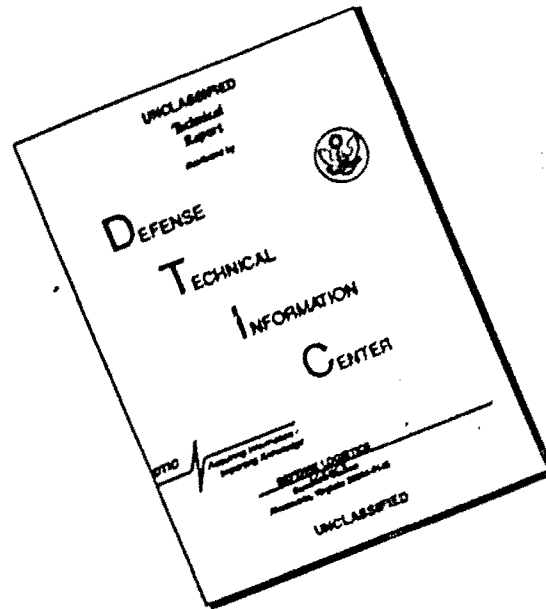
TECHNICAL REPORT AFML-TR-67-34

MARCH 1967

AIR FORCE MATERIALS LABORATORY
RESEARCH AND TECHNOLOGY DIVISION
AIR FORCE SYSTEMS COMMAND
WRIGHT-PATTERSON AIR FORCE BASE, OHIO

DISCLAIMER NOTICE

THIS DOCUMENT IS BEST QUALITY AVAILABLE. THE COPY FURNISHED TO DTIC CONTAINED A SIGNIFICANT NUMBER OF PAGES WHICH DO NOT REPRODUCE LEGIBLY.

NOTICES

When Government drawings, specifications, or other data are used for any purpose other than in connection with a definitely related Government procurement operation, the United States Government thereby incurs no responsibility nor any obligation whatsoever; and the fact that the Government may have formulated, furnished, or in any way supplied the said drawings, specifications, or other data, is not to be regarded by implication or otherwise as in any manner licensing the holder or any other person or corporation, or conveying any rights or permission to manufacture, use, or sell any patented invention that may in any way be related thereto.

Copies of this report should not be returned to the Research and Technology Division unless return is required by security considerations, contractual obligations, or notice on a specific document.

INVESTIGATION OF THERMAL EMBRITTLEMENT IN 18Ni(250) MARAGING STEEL

C. J. BARTON
B. G. REISDORF
P. H. SALMON COX
J. M. CHILTON
C. E. OSKIN, JR.

FOREWORD

This report was prepared by the United States Steel
Corporation, Applied Research Laboratory, Monroeville,
Pennsylvania, under USAF Contract No. AF 33(615)-2780.
The contract was initiated under Project No. 7351,
"Metallic Materials," Task No. 735105, "High Strength
Metallic Materials." The work was administered by the
Air Force Materials Laboratory, Research and Technology
Division, Wright-Patterson Air Force Base, Ohio, with
Lt. F. J. Gurney acting as project engineer.

This report covers work performed during the period
30 June 1965 to 31 October 1966.

This work was conducted under the supervision of
G. E. Pellissier, Manager, Advanced Applied Research,
U. S. Steel Applied Research Laboratory.

Manuscript released by the authors December 1966
for publication as an RTD Technical Report.

This technical report has been reviewed and is
approved.

I. PERLMUTTER
Chief, Metals Branch
Metals and Ceramics Division
Air Force Materials Laboratory

ii

ABSTRACT

The ultrahigh-strength 18Ni maraging steels may be severely
embrittled by certain high-temperature thermal treatments
involved in processing and fabrication. The objectives of this
investigation by the Applied Research Laboratory were to (1)
systematically survey the thermal embrittlement characteristics
of a commercial 18Ni(250) maraging steel; (2) determine the
thermal treatments that result in a maximum degree of embrittle-
ment; (3) discover the metallurgical sources of the embrittle-
ment; and (4) improve the resistance of the steel to thermal
embrittlement. The mechanical properties of a commercial steel,
in both the unaged and aged conditions, were evaluated after a
variety of thermal treatments consisting of heating at tempera-
tures of 2000 to 2400°F, cooling to temperatures of 1300 to
1800°F and holding for times up to 4 hours, and then air cooling.
The most severe embrittlement resulted from heating for 1 hour
at 2200 to 2400°F, cooling to 1500 to 1800°F and holding for
4 hours, air cooling, and aging. The major source of embrittle-
ment was found to be the precipitation of small particles of
TiC,N at austenite grain boundaries during isothermal holding in
the range 1500 to 1800°F following the high-temperature heating.
Marked austenite grain coarsening during the high-temperature
heating was an important contributing factor. Based on these
findings, efforts were made to increase the resistance of the
steel to embrittlement by modifications of alloy composition
and reduction of residual element content. Significant improve-
ments resulted from substitution of aluminum for titanium as
the supplemental strengthening element in an 18Ni(250) maraging
steel of low-residual element content; similar benefits were
obtained by adding 0.2 percent columbium to a steel of normal
alloy composition and low-residual element content. There is
reason to believe that the two effects may be additive, and this
attractive possibility should be explored.

TABLE OF CONTENTS

iv

TABLE OF CONTENTS (cont'd)

TABLE OF CONTENTS (cont'd)

ILLUSTRATIONS

x

xi

TABLES

xviii

I. INTRODUCTION

A number of investigations (References 1 and 2) have indicated that 18Ni(250) maraging steel exhibits substantial loss of notch toughness when subjected to certain thermal cycles; heating to temperatures in excess of 2000°F and slow-cooling, or isothermal holding, in the temperature range 1400 to 1800°F has been found to provide the conditions for a so-called "thermal embrittlement." This problem becomes of prime importance in the processing of heavy sections of maraging steel (Reference 3). Additionally, it was known that certain residual elements in maraging steel (that is, carbon, phosphorus, silicon, manganese, and sulfur) reduced the fracture toughness of the steel, and were therefore limited by specification (Reference 4). The effect of these residual elements upon the thermal embrittlement response of maraging steel was not known.

This Applied Research Laboratory project was undertaken, therefore, with the following aims:

(1) To determine the extent of this thermal embrittlement; this part of the program included a comprehensive series of thermal schedules to be performed on specimens from a large piece of commercial plate. This was done to determine the trends of notch toughness, ductility, and strength, as a function of time and temperature of the various portions of the thermal embrittlement cycle, and to determine the most embrittling heat treatment.

(2) To investigate the mechanism by which the steel is embrittled; microstructural investigations and diffraction analyses were performed on embrittled specimens to isolate the causes of the deterioration of toughness.

(3) To attempt to prevent or minimize the embrittlement by making composition adjustments, including reduction of residual elements.

(4) To make major design changes in the composition of the steel to reduce or eliminate susceptibility to thermal embrittlement.

The body of this report is separated into two main sections: (1) the Commercial Plate investigation, which includes the results of a comprehensive series of heat treatments and their interpretation, and (2) the Experimental

1

Compositions section, which contains the results of the
different attacks made upon the embrittlement problem.

II. COMMERCIAL PLATE

a. Purpose

This section of the report deals with an investigation
of a commercial heat of 18Ni(250) maraging steel. The purpose
of the investigation was twofold: (1) to determine the thermal
conditions that result in embrittlement of this steel, and (2)
through microstructural examinations, to determine the mechanism
of embrittlement. Subsequent sections of the report deal with
attempts to modify the steel's susceptibility to thermal embrit-
tlement through changes in the steel composition.

b. Materials and Experimental Work

(1) Processing of Commercial Plate
USS Heat No. X-53541

The chemical analysis of the plate used in this inves-
tigation is shown in Table 1. The plate was processed from a
20-ton ingot which was poured from an 85-ton air-melted arc-
electric-furnace heat. The ingot (average cross section, 32 by
60 inches) was bloomed to a thickness of 18 inches, reheated,
and rolled to an 8-inch-thick slab. The slab was sectioned and
cross-rolled to approximately 0.7-inch-thick plate with 25
percent of the final reduction made under 1750°F. The plate
was double annealed in the mill—1-1/2 hours at 1650°F and air-
cooled, and 1-1/2 hours at 1530°F followed by air cooling. The
subsequent machining and heat treatment of mechanical-test
specimens were performed at the Applied Research Laboratory.

The embrittling cycles investigated consisted of
annealing for 1 hour at a temperature in the range 2000 to
2400°F, quenching to an intermediate annealing temperature in
the range 1300 to 1700°F, holding for 1/2 or 4 hours, and air
cooling. Most of the high-temperature annealing treatments
were performed in a furnace employing a cracked-ammonia atmos-
phere. During the course of the investigation, it became
apparent that this atmosphere induced hydrogen embrittlement,
at least for some of the thermal treatments. To determine the
extent to which the mechanical properties resulting from various
thermal treatments were influenced by hydrogen embrittlement,

2

and to isolate the purely thermal embrittlement response,
several of the thermal treatments were repeated using an inert
atmosphere (high-purity argon) in the high-temperature anneal-
ing furnace.

After the high-temperature anneal, the specimen blanks
were quenched into a molten salt bath, which was held at a
temperature in the range 1300 to 1700°F. A few specimens were
given an intermediate anneal at 1800°F, and, because of tempera-
ture limitations of the available salt-pot, this treatment was
performed in an atmosphere furnace using either cracked ammonia
or argon as the atmosphere. Specimens were tested in both the
aged and unaged conditions. Unless otherwise stated, "aged"
means that the specimen blanks were aged in air at 900°F for
3 hours and air-cooled. Subsequent to being heat-treated, the
specimen blanks were machined to 0.357-inch-diameter tension-
test specimens and Charpy V-notch (CVN) impact test specimens.
The effect of selected embrittling treatments on plane-strain
fracture toughness also was determined, using bend-test speci-
mens.

The dimensions of the bend-test specimens were 0.60 by
1.10 by 7 inches. A notch was machined in the specimen, perpen-
dicular to the plate surface and to a depth of 0.500 inch. The
notch root-radius was 0.003 inch. The notched specimens were
fatigue-precracked 0.05 inch, so that the length of the notch
plus fatigue crack was about one-half the specimen width. The
specimens were tested using 3-point loading, a 6-inch span, and
lubricated roller-type "frictionless" supports. Strain measure-
ments were made with a double cantilever clip-in gage (linearity
better than 1/2 percent) with a sensitivity of 0.0010 inch of
crack opening displacement per linear inch. Plane-strain frac-
ture toughness (K_{I_C}) values were computed according to the
following expression (Reference 5):

$$K_{I_C} = \frac{[1.931 - 3.067(\frac{a}{W}) + 14.56(\frac{a}{W})^2 - 25.11(\frac{a}{W})^3 + 25.80(\frac{a}{W})^4]6Ma^{1/2}}{B\,W^2}$$

in which   M = bending moment
           B = thickness of specimen in inches
           a = depth of machined notch plus fatigue crack in inches
           W = width of sample in inches

where $M = \frac{PL}{4}$ and P = "pop-in" load
                      L = span length

3

(2) Microstructural Investigations

The gross microstructural features of the steel, for a·
variety of heat-treated conditions, were examined first by
light microscopy. Prior austenite grain-size measurements were
made for specimens annealed at temperatures over the range 1500
to 2400°F.

Extraction replicas were prepared from the fracture
surfaces of broken CVN specimens (in the region of flat frac-
ture just below the notch); these were examined by electron
microscopy to determine the morphology and distribution of
particles in the fracture surfaces, and the extracted particles
were identified by electron diffraction. Two somewhat different
electron diffraction techniques were used. In the first, which
will be referred to as "gross-area electron diffraction," all
the extracted particles contained in the replica over an area
of several squares of a 200-mesh specimen-support grid were
exposed to the electron beam and contributed to the diffraction
pattern. This method provides a rough, semiquantitative
estimate of the relative abundance of different compounds if
more than one is found. "Selected-area diffraction" was also
employed, whereby only a single particle, or a small group of
particles, provided the diffraction pattern. This method
permits direct correlation of crystalline identity with particle
morphology.

c. Results and Discussion

(1) Effects of Thermal Treatments on Mechanical Properties of Commercial Plate

The schedule of heat treatments given the commercial
plate, to investigate the thermal embrittlement of this steel,
is presented in Table 2. The tensile properties shown in
Table 2 are the average of duplicate tests, and the CVN energies
are the average of triplicate tests. Four heat-treating variables
are represented in the table: (1) the high-temperature annealing
temperature; (2) the intermediate-annealing temperature; (3) the
time of holding at the intermediate temperature; and (4) the
final heat-treated condition of the specimens, whether aged or
unaged. To facilitate comparisons of the effects of the several
parameters on impact toughness, the data of Table 2 are plotted
in various forms in Figures 1 through 12.

Figure 1 shows the effect of high-temperature annealing
on CVN toughness. The specimens were annealed for 1 hour at the

4

indicated temperatures, air-cooled, and tested in the unaged condition. The increase in impact toughness with annealing temperature (up to 2300°F) was not reflected in specimens that were aged after the simple annealing treatment; instead, the aged specimens (Figure 2) exhibited a steady decline in toughness as the annealing temperature was increased.

The CVN results plotted in Figure 3 are for specimens that were annealed at a high temperature, quenched to an intermediate temperature, held for 1/2 hour, and air-cooled. Corresponding curves are presented in Figure 4 for specimens held for 4 hours at the intermediate temperatures. With only a few minor exceptions evident in Figure 3, the predominant effect of the intermediate annealing temperature was to decrease impact toughness as the intermediate annealing temperature was increased. In some instances, the isothermal hold at 1300 or 1400°F resulted in somewhat better notch toughness than that of the continuously air-cooled specimens. For example, CVN specimens air-cooled from the 2200°F annealing temperature absorbed 77 ft-lb, whereas the specimens that were annealed at 2200°F, quenched to 1300°F and held for 1/2 hour, absorbed 88 ft-lb; as will be discussed shortly, the aged specimens did not reflect this improvement in toughness. The thermal treatments that produced the most severe embrittlement in the unaged specimens were the combination of a high annealing temperature (above 2200°F) followed by quenching to, and holding at, an intermediate annealing temperature of 1600 to 1800°F.

The effect of holding time at the intermediate annealing temperatures on CVN toughness is shown in Figures 5 through 9. In these figures, the data points plotted at zero time represent the values obtained from specimens that were air-cooled after the high-temperature anneal. For the combination of annealing temperatures that produced the most severe embrittlement—2300 or 2400°F followed by holding at 1500 to 1800°F (Figures 8 and 9)—the impact toughness was reduced drastically by a 1/2-hour intermediate anneal, and there was not much difference between the effects of the 1/2-hour anneal and the 4-hour anneal. Although no data were obtained for very short intermediate annealing times, the drastic reduction of toughness that occurred in 1/2 hour suggests that only a very few minutes in the range 1500 to 1800°F would result in a significant reduction in impact toughness, if the steel were first subjected to very high temperatures, say over 2000°F. Thus, in practice it would seem to be particularly important to avoid high temperature heating of thick sections which cannot be cooled rapidly through the embrittling temperature range.

5

Figures 10 and 11 show the effect of the various embrittling treatments on the impact toughness of specimens that were aged after they were given the embrittling treatments. From Figure 10, which shows the CVN results for specimens held for 1/2 hour at the intermediate annealing temperatures, it is apparent that the impact toughness decreased as either the high- or the intermediate-annealing temperature was increased. As was observed for the unaged specimens, very severe embrittlement resulted when both of the annealing temperatures were at the upper limits of their ranges.

Except where the 1/2-hour intermediate anneal had already resulted in very low CVN values (about 5 ft-lb), annealing for 4 hours instead of 1/2 hour caused a further reduction of the impact toughness (Figure 11). The 1/2-hour intermediate anneal at 1300°F did not result in any embrittlement, as compared to the specimens that were air-cooled after the high-temperature anneal. This is apparent when the data of Figure 10 is replotted in the form shown in Figure 12. The circled points in Figure 12 were obtained from specimens that were continuously air-cooled after the high-temperature anneal, and these points are virtually identical with those obtained from specimens given a 1/2-hour intermediate anneal at 1300°F.

The specimens with code No. 8 through No. 12 in Table 2 show the effect of a 1500°F re-anneal on specimens previously aged at high temperatures and air-cooled. Comparing the CVN values before the re-anneal (code No. 3 through No. 7) with those obtained after the re-anneal, little difference is noted for either the unaged or the aged specimens. However, when the reduction of area (RA) values are examined, there are three observations worthy of note: (1) whereas the CVN values for the unaged specimens of code No. 3 through No. 7 were relatively constant, the corresponding RA values exhibited a drastic decrease as the annealing temperature was increased (from 58.0% RA for the 2000°F anneal to 13.3% RA for the 2400°F anneal); (2) although the 1500°F re-anneal did not affect the CVN values very much, the RA values, that were quite low after the high-temperature anneal, showed a marked improvement; (3) the 1500°F re-anneal had little, if any, effect on the tensile ductility of the aged specimens.

The large discrepancy between the impact values and the tensile ductility values that were obtained from the specimens given a single high-temperature anneal suggested that the observed "toughness" values depended on the speed of the test (strain-rate sensitivity). Hydrogen embrittlement, which is

6

the most common source of such strain-rate sensitivity, appeared to be a likely explanation of the discrepancy, especially because the specimens were annealed in a hydrogen-rich (cracked ammonia) atmosphere, at high temperatures. Observations (2) and (3) mentioned above suggested that, after re-annealing at 1500°F or aging at 900°F for 3 hours, the suspected hydrogen embrittlement was no longer the primary factor controlling the tensile ductility; either the hydrogen content of the steel was decreased or, in the case of the aged specimens, its effect was masked by some other, stronger embrittling reaction.

A number of the thermal treatments and tests shown in Table 2 were repeated using an inert (99.996% pure argon) atmosphere; the impact and tension test results are shown in Table 3. For ease of comparing the effect of annealing atmospheres, the CVN and RA results from Tables 2 and 3 are presented side-by-side in Table 4. The most striking effect of annealing atmosphere is evident in the RA values for the specimens given a single high-temperature anneal at 2200°F or above. The RA values for specimens annealed in argon at 2200, 2300, and 2400°F were 64.8, 64.8, and 68.6 percent, respectively, whereas the corresponding values for specimens annealed in cracked ammonia were 23.2, 16.6, and 13.3 percent, respectively—clearly a result of hydrogen embrittlement. Neither the aged CVN specimens nor the aged tension test specimens showed any clear evidence of an annealing atmosphere effect; although two of the RA results for specimens annealed in argon (treatments 4 and 5, Table 4) were higher than those obtained from specimens tested in cracked ammonia, the reverse was true for two other treatments (8 and 10). The unaged specimens that were given an intermediate anneal subsequent to a high-temperature anneal in argon (treatments 8 through 19) generally exhibited somewhat higher CVN and RA values than the specimens annealed in cracked ammonia. The reason for this is not known, but is unlikely to be hydrogen embrittlement, (1) because the CVN test results would not be expected to reflect hydrogen embrittlement, and (2) because of the low hydrogen content found in one of the steels by chemical analysis.

Table 5 shows hydrogen determinations for specimen blanks given various thermal treatments. After the indicated thermal treatment, the specimens were immersed in liquid nitrogen until they were analyzed. In the as-received condition (mill-annealed in air), the steel contained only 0.49 ppm hydrogen. After a 1-hour anneal at 2300°F in a cracked-ammonia atmosphere followed by a water-quench, the steel contained 4.72 ppm hydrogen. Air-cooling from 2300°F reduced the hydrogen content to 3.89 ppm, but this hydrogen level was sufficient to severely embrittle the

7

steel. Re-annealing the specimen for 1 hour at 1500°F further reduced the hydrogen content to 2.53 ppm, and eliminated most of the hydrogen embrittlement. A single 1-hour anneal at 1500°F in cracked ammonia resulted in a hydrogen content in the steel of 2.14 ppm, and at this hydrogen level the tension test specimens did not exhibit any evidence of hydrogen embrittlement. Aging for 3 hours at 900°F reduced the hydrogen content to about 0.3 ppm in specimens that had previously been water-quenched, or air-cooled, from a 2300°F anneal in a cracked-ammonia atmosphere.

Finally, a specimen that was annealed at 2300°F in cracked ammonia and quenched into salt at 1500°F, held for 4 hours and air-cooled, contained only 0.78 ppm of hydrogen. Although the aging of hydrogen-charged specimens does reduce the hydrogen content to a low level, damage (cracking) may occur if the aging is not done promptly. Two tension test blanks and three CVN blanks were annealed at 220 °F for 1 hour in a cracked-ammonia atmosphere and water-quenched. A similar set of specimen blanks were given the same thermal treatment in an argon atmosphere. No cracks were observed in any of the specimens on the day the heat treatments were performed, but, on the following day, gross cracks were observed in all five specimen blanks that had been annealed in cracked ammonia, whereas a microscopical examination of the specimens annealed in argon did not reveal any cracks, even when re-examined several days later. No cracks were observed in any of the air-cooled specimens; presumably the slower cooling rate had permitted some reduction of the hydrogen level in the steel at the lower temperatures, and also decreased the intensity of the thermal stresses.

The tensile ductility values, as measured by the reduction of area of tension test specimens, reflected the same general adverse effects of the various thermal embrittlement treatments as the CVN energy values.

The effects of some of the thermal embrittlement treatments (argon furnace atmosphere) on plane-strain fracture toughness, K_{IC}, are shown in Table 6. Although specimens were tested in triplicate, in most instances only two K_{IC} values are reported in Table 6; in these cases, one of the triplicate specimens did not provide a distinct "pop-in" on the load-deflection curve and was discarded. Figure 13 is a plot of K_{IC} values versus CVN values; the nearly linear correlation between the K_{IC} values and the CVN energy values is rather surprising, in view of the different nature of the two tests.

8

(2) Effects of Thermal Treatments on
Microstructure of Commercial Plate

Figures 14a to 14j are photomicrographs of heat No.
X-53541 annealed for 1 hour at various temperatures and air-
cooled subsequent to the mill-annealing treatments. The most
apparent effect of annealing temperature on microstructure is
the effect on the prior austenite grain size. In comparing
grain size, note that the magnifications of the various micro-
graphs are not the same. Below an annealing temperature of
1700°F the prior austenite grain boundaries were not well delin-
eated in this steel by any of the several etchants tried, and,
in order to reveal the grain size in a specimen annealed at
1500°F, it was necessary to age the specimen and prepare elec-
tron micrographs from replicas of the etched surface. The
electron micrograph of Figure 15 is from a specimen aged for
1 hour at 950°F after being air-cooled from a 1-hour anneal at
1500°F. The average prior austenite grain size is plotted as
a function of annealing temperature in Figure 16. The average
austenite grain "diameter" in a specimen annealed for 1 hour at
1500°F was about 9 microns, which corresponds to ASTM grain
size No. 11, the grain diameter increased exponentially with
annealing temperature, so that after annealing for 1 hour at
2400°F, the grain diameter had increased to almost 2 mm, or
ASTM No. -5.

Figure 17 is an electron micrograph of a carbon-
extraction replica prepared from the fracture surface of a
specimen that had received the normal annealing and aging treat-
ment—1 hour at 1500°F, air-cooled, and aged 3 hours at 900°F
and air-cooled. In most areas of the fracture surface, only a
few small particles were observed, but in occasional areas there
were more massive particles, such as that shown in Figure 18.

Figures 19, 20, and 21 are extraction fractographs of
broken impact specimens that had been quenched to 1600°F and
held for 4 hours, after a 1-hour anneal at 2000, 2100, and
2200°F, respectively. The corresponding CVN absorption energies
were 41, 31, and 24 ft-lb. Although wide variations in the
number and size of particles were observed in different regions
of a single replica, which made it difficult to compare particle
content among the different specimens, the general impression
was that the particle size and particle distribution density
increased with the degree of embrittlement. Figure 22 is an
extraction fractograph of a specimen that was annealed for 1
hour at 2200°F, quenched to 1600°F, held for 1/2 hour, and
air-cooled. The treatments for specimens of Figures 21 and 22

9

were the same, except for the time that they were held at the intermediate annealing temperature. The CVN energy value for the specimen of Figure 21 was less than helf that of the specimen of Figure 22 (24 versus 51 ft-lb). It was apparent from an examination of many areas of the replicas from the two specimens that the fracture surfaces of the higher toughness specimen contained fewer and smaller particles than that of the lower toughness specimen.

The extraction fractograph of Figure 23 was obtained from a CVN specimen that absorbed only 8 ft-lb in the unaged condition. This fractograph is typical of specimens given a severe thermal embrittling treatment. The treatment consisted of annealing the specimen for 1 hour at 2300°F, quenching it into salt at 1700°F, holding it for 4 hours, and finally air-cooling the specimen. A very high proportion of the fracture surface was covered by particles after the severe embrittling treatments.

The extraction fractographs prepared from embrittled-and-aged specimens appeared about the same as those obtained from the embrittled-but-unaged specimens, as shown by a comparison of the fractographs of Figure 21 (unaged) and Figure 24 (aged).

The fracture surfaces of severely embrittled specimens had a flat, granular appearance that strongly suggested that fracture had occurred along prior austenite grain boundaries. Fairly conclusive evidence was obtained that fracture proceeded predominantly along the prior austenite grain boundaries. Extraction replicas were prepared from polished and etched specimen surfaces, rather than from fracture surfaces, to permit observation of the particle distribution in relation to the microstructure. Figures 25, 26, and 27 are electron micrographs of such replicas, that were obtained from three differently treated specimens. These micrographs show that precipitation of the particles occurred preferentially at the prior austenite grain boundaries, and that these boundaries were the only regions in which the particles had precipitated as profusely as in the fracture surfaces.

To identify the particles, the extraction replicas prepared from the fracture surfaces of CVN specimens coded 20, 39, 40, 40A, and 52 (Table 2) were examined by gross-area electron diffraction. All the replicas provided strong ring diffraction patterns that corresponded to Ti(C,N), and, except

10

for the replica from specimen No. 52, the diffraction patterns
did not contain any lines in addition to the Ti(C,N) diffrac-
tion lines. This finding demonstrated that the vast majority
of the particles extracted from fracture surfaces of the
embrittled specimens were Ti(C,N). The diffraction patterns
from the replica of specimen No. 52 contained several weak rings,
in addition to the Ti(C,N) rings; Table 7 provides a tabulation
of the diffraction rings obtained from specimen No. 52. The
rings obtained, in addition to the Ti(C,N) lines, could have
arisen from τ-Ti$_2$S, but the fit is not sufficiently good for
positive identification.

The identification of the particles as Ti(C,N) requires
some discussion. Both TiC and TiN have a face-centered-cubic
crystal structure, and their lattice parameters are not very
different in comparison to the accuracy of electron diffraction
measurements. Also, there is not necessarily a fixed stoichio-
metric relationship between the numbers of titanium and carbon
or nitrogen atoms in the compound. For example, the cubic form
of TiC exists over the range 11 to 20 weight percent carbon with
attendant changes in lattice parameter (Reference 6). The mixed
compound, Ti(C,N), also exists and doubtless has a range of
lattice parameters depending upon the specific proportions of
Ti, C, and N. Because of the limited accuracy of electron
diffraction measurements, and the ambiguity that would exist
even if the measurements were precise, the compound is specified
as Ti(C,N), with the understanding that the proportion of the
three elements in each case was not determined.

The extraction replicas obtained from broken impact
test specimens coded 30 and 40 in Table 2 were examined exten-
sively by selected-area electron diffraction, whereby only one
particle or a small group of particles, contributed to the
diffraction pattern. The results of the selected-area-diffraction
analysis established that the dendritic, or "fern-shaped," parti-
cles invariably were Ti(C,N). Two examples of Ti(C,N) selected-
area-diffraction patterns, together with micrographs of the
particles that produced the patterns, are shown in Figures 28
and 29. The thin Ti(C,N) particles constituted, by far, the
major portion of the particles observed on the fracture surfaces,
but occasionally, larger and thicker particles were noted that
could not be identified merely by their morphology. Some of
the thick particles were Ti(C,N), some were τ-Ti$_2$S, and a few
yielded unidentifiable patterns. Two examples of micrographs
of τ-Ti$_2$S particles, with corresponding selected-area-diffraction
patterns, are shown in Figures 30 and 31.

11

d. <u>Summary</u>

The results of this investigation have shown that the degree of embrittlement, as evaluated by CVN impact tests of specimens of commercially produced plate given various thermal treatments, increased with (1) the temperature of the high-temperature anneal, (2) the temperature of the intermediate anneal, and (3) the holding time at the intermediate temperature. The most severe embrittlement conditions consisted of annealing for 1 hour at temperatures in the range 2200 to 2400°F, quenching to an intermediate temperature and holding in the range 1500 to 1800°F, air cooling, and aging. For these conditions of treatment, the resulting CVN energy was only about 5 ft-lb.

By means of electron microstructural examinations, coupled with electron diffraction analyses, the source of the embrittlement has been found to be the copious solid-state precipitation of fine, plate-like particles of the intermetallic compound Ti(C,N), preferentially along austenite grain boundaries, at the intermediate annealing temperatures. The size of the Ti(C,N) particles observed in the fracture surfaces of CVN impact test specimens, and the extent to which these particles covered the fracture surfaces, increased with the degree of embrittlement.

Metallographic examination at low magnification revealed that the austenite grain size increased quite markedly during the high-temperature anneal, especially at temperatures above 2200°F. In view of the tendency of Ti(C,N) to precipitate preferentially at the austenite grain boundaries, and because of the limited residual amounts of carbon and nitrogen in the steel, it is believed that the observed increase in austenite grain size may have contributed importantly to the observed embrittlement. That is, when the austenite grain size remained small, the grain-boundary surface area was large, and there might have been insufficient carbon and nitrogen available in the steel to permit precipitation of Ti(C,N) over a large fraction of the grain-boundary area; whereas, for the larger grain sizes, resulting from annealing at temperatures above 2200°F, these amounts of carbon and nitrogen might have been adequate for the formation of an almost continuous film of Ti(C,N) over most of the grain surface area.

Calculation has indicated that, if all the carbon in a very low-carbon (0.004%) maraging steel were available for formation of a TiC film of about the same thickness (about

12

1000 Å) as that of the Ti(C,N) particles found in the fracture
surfaces of embri tled specimens, the film could cover the
entire grain surface area of a steel having a grain size of
ASTM No. -3; this grain size is developed by annealing at 2300°F
for 1 hour. However, for a steel with a grain size of ASTM
No. 4, which results from annealing at about 1?00°F, the steel
would have to contain about 0.04 percent carbon, to effect
complete coverage of the grain surface area by TiC. The contri-
bution of nitrogen was neglected in this calculation, and,
therefore, the amounts of carbon indicated possibly should be
somewhat lower; on the other hand, probably not all of the
carbon and nitrogen in the steel is available for precipitation
as Ti(C,N).

        Based on the results of this investigation, the follow-
ing mechanism of embrittlement is postulated:

    (a) As a result of the high-temperature anneal (>2000°F),
         most of the carbon and nitrogen (in the form of
         carbide and nitride particles) becomes redissolved
         in the matrix, because of increased solubility and
         diffusion rates.

    (b) Upon slow cooling, or interrupted cooling and holding
         at some intermediate temperature (1500 to 1800°F),
         Ti(C,N) precipitates at austenite grain boundaries
         because of the marked chemical affinity of titanium
         for carbon and nitrogen, because of the decrease in
         solubility of Ti(C,N) in the austenite with decreas-
         ing temperature and possibly because of the segrega-
         tion of one or all of the constituent elements in
         grain boundary regions at the lower temperature (or
         perhaps, the easier nucleation of Ti(C,N) in these
         regions).

    (c) For still lower intermediate holding temperatures
         (<1500°F), the degree of embrittlement is not as
         severe for reasonable holding times, even though the
         solubility of Ti(C,N) would be expected to decrease
         further with decrease in temperature, because the
         diffusion rates of the precipitating elements become
         so low that significant nucleation and growth of
         Ti(C,N) particles does not take place in the times
         considered.

13

1. THE EFFECT OF CARBON

a. Purpose

The thermal embrittlement characteristics of low-residual element maraging steels with varying amounts of carbon were investigated. From the commercia plate study described in the previous section, the identification of Ti(C,N) in the fracture surfaces of thermally embrittled maraging steels indicated a cause-and-effect relationship. High- and low-carbon steels were made with low-residual element content, the purpose of this approach being to determine the effects of carbon on thermal embrittlement with a minimum of complicating effects from other elements, such as sulfur and phosphorus which also are believed to have adverse effects on toughness. One of these two heats (V-8858) had a carbon level of 0.027 percent, whereas the other (V-8497) had a very low carbon content (0.004%). In this way, the effect of very low residual element levels, in both a low-carbon steel and a steel of commercial carbon level, could be determined; also, any contributions of residual elements to the thermal embrittlement of these steels would be minimized, and thus a more accurate evaluation of the effect of carbon on the thermal embrittlement of these steels could be made. A series of thermal cycles was employed to investigate the relative susceptibility of low- and commercial-carbon 18Ni(250) maraging steel to thermal embrittlement treatments and to determine the microstructural features that were associated with any changes in toughness.

b. Materials and Experimental Work

(1) Materials

The results of the chemical analyses of the steels investigated are given in Table 8. The residual element levels of these heats were held as low as possible to isolate the effect of carbon on thermal embrittlement with a minimum of interference from other variables. Heat V-8497 contained a very low carbon content (0.004%), whereas V-8858 contained a carbon level approximating that found in commercial maraging steels (0.027% C). Except for this large difference in carbon content, the two heats were essentially identical in composition.

14

(2) Heat Treatment

The results of the conventional heat treatments, numbered 1, 2, 3, and 4 in Table 9, were used as a basis of comparison for determining the effects of the thermal embrittlement treatments, numbered 5 through 10.

Mechanical properties were determined from duplicate 0.252-inch-diameter tensile specimens and triplicate Charpy V-notch specimens tested at room temperature.

The high-temperature portion of each embrittling treatment was carried out in a cracked-ammonia atmosphere furnace, and the intermediate anneal was conducted in a molten salt bath. The cracked-ammonia atmosphere was used for treating these specimens prior to recognition of the hydrogen embrittlement problem. Not enough material remained to permit repeating all the treatments and mechanical testing, so that the results, particularly the reduction of area values, may have been influenced to some degree by hydrogen embrittlement. The impact test results, however, are believed to accurately reflect the influence of the thermal embrittling treatments alone, judging from the results obtained in the commercial plate investigation. In fact, enough material did remain to repeat several of the high-temperature treatments in argon for impact test specimens. The results were essentially the same as those obtained on specimens heat-treated in cracked ammonia; however, no tensile tests could be made to check the yield and tensile strengths.

For heat treatments 7 and 8, the specimens were taken from the high-temperature treatment furnace and placed directly in the preheated molten salt bath; that is, interrupted cooling from the high-temperature treatment was used because previous work indicated that a more severe embrittlement condition was caused by the interrupted cooling. In heat treatments 9 and 10, the specimens were allowed to air-cool to room temperature, and then they were reheated to the intermediate temperature. All combinations of the thermal treatments used in this investigation are listed in Table 9.

(3) Specimen Preparation

(a) Extraction Replicas

The fracture surfaces of impact-test specimens in the central regions of flat fracture were examined by an extraction-replica technique for the possible presence of a second phase.

15

Carbon was evaporated on the fracture surface and the carbon film, along with any second-phase particles present, were loosened electrolytically in a methanol solution of 1 percent bromine. Films obtained in this way were mounted on microscope grids for examination in the electron microscope. Electron-diffraction ring patterns and selected-area diffraction patterns were obtained to identify the extracted phase(s).

(4) Analysis of Diffraction Patterns

Extraction replicas of fracture surfaces yielded specimens containing a high density of second-phase particles. Electron-diffraction ring patterns obtained from these particles were measured and analyzed in the usual manner.

Single-crystal patterns also were obtained by selected-area diffraction techniques in the Siemens electron microscope. For the most part, this technique was used in conjunction with thin foil specimens, although it was sometimes helpful in the examination of extraction replicas. The spot-type patterns obtained yielded information on angular relationships between crystallographic planes, as well as interplanar spacings (d-spacings); these data, in addition to ring patterns, are necessary if the precipitate to be identified is noncubic. Information on angles between planes is helpful even in identifying cubic materials, since it provides a check on the results of the ring-pattern analyses. A computer program was developed for the calculation of angles between planes, when the appropriate lattice parameters are provided, for all orthoganol crystal systems, as well as for the hexagonal system; d-spacings can be calculated, which aids in such analysis.

c. Results and Discussion

(1) Mechanical Properties

Table 9 contains the mechanical properties for the two steels investigated. The reference heat treatments employed for heats V-8497 and V-8858 included the as-rolled and the as-rolled-and-aged conditions (heat treatments 1 and 2). In comparing the results of these two treatments with those of the 1500°F anneal (No. 3), and with those of the 1500°F anneal-and-age (No. 4), it is evident that the latter two treatments substantially increased the notch toughness of both steels. The as-rolled condition, however, is difficult to define, and the resulting properties may vary widely depending on the particular rolling schedule employed.

16

Another significant point is that, for each of these four treatments, the notch toughness of the low-carbon steel was at least twice as high as that of the high-carbon steel. After treatment 4, the values of impact energy and tensile ductility of the high-carbon steel were decidedly inferior to those of the low-carbon steel; however, the yield strength of the low-carbon steel was somewhat lower (approximately 4%) than that of the high-carbon steel, which may account for some of the difference in toughness.

After heating to 2200°F for 1 hour, both steels exhibited significantly lower notch toughness than specimens annealed at 1500°F. Steels V-8497 and V-8858 exhibited approximately the same percent reduction in impact-energy values, when the results of the 2200°F heat treatment were compared to those of the 1500°F anneal. After aging (treatment 6), a further reduction in toughness occurred; for both the high- and low-carbon steels, reductions in yield strength as well as in impact energy occurred, compared to the results of the 1500°F anneal-and-age treatment (No. 4). It is interesting to note that, although the notch toughness of the low-carbon steel was always substantially greater than that of the high-carbon steel, the impact energy values decreased by a higher percentage in the low-carbon steel.

The interrupted cooling treatments (No. 7 and 8) reduced the notch toughness of both steels drastically. The interrupted cooling from 2200°F (heat treatment No. 7) resulted in much lower toughness when compared with the results of heating to 2200°F and air cooling. This decrease was more pronounced for the low-carbon steel; however, it is curious that the impact values for both steels were reduced to the same low level as a result of heat treatment No. 7.

Both steels responded to the full embrittling and aging treatment (No. 8) with a marked reduction in strength, tensile ductility, and notch toughness from the levels resulting from conventional annealing and aging (No. 4). It is interesting to note that this thermal embrittling treatment reduced these values to approximately the same low level for both the high- and low-carbon steels; that is, despite the superior properties of the low-carbon steel in the as-rolled condition (No. 1 and No. 2) and in the annealed condition (No. 3 and No. 4), the mechanical properties of both steels were about the same after treatment No. 8. This comment is especially pertinent considering the low-residual element content of these steels.

17

In addition to the embrittling treatment involving interrupted cooling from the high temperature and holding at an intermediate temperature (No. 7 and No. 8), the effects of reheating to 1500°F after air cooling from 2200°F to room temperature (heat treatments 9 and 10) were investigated. In comparing the results of treatment No. 10 with those of treatments No. 6 and No. 8, it is evident that reannealing at 1500°F for 1 hour after air cooling from 2200°F increased not only the notch toughness but also the yield and tensile strengths. The 1500°F anneal reaustenitized these specimens and established a new austenite grain size (and a new grain boundary network location) from that which existed after the 2200°F heat treatment.

(2) Metallography

Figures 32 through 35 are light micrographs of specimens of steels V-8497 and V-8858 that had been subjected to various heat treatments. When examined in the as-rolled condition (Figure 32), the grain size of the high-carbon (0.027%) steel was clearly revealed, but that of the low-carbon steel was not. The grain size of the high-carbon steel (V-8858) was approximately ASTM No. 6, but it was nonuniform, and many small grains were evident. This observation is consistent with the deformation process employed, that is, hot rolling to a low finishing temperature. It is not definitely known why the grain boundaries were revealed only in the high-carbon steel (V-8858).

After annealing for 1 hour at 1500°F (Figure 33), the prior austenite grain boundaries were no longer revealed in either steel, which is the usual situation for annealed maraging steel. The reaustenitization probably resulted in a smaller grain size than that observed in the as-rolled condition. After heating to 2200°F for 1 hour, the grain size was at least as large as ASTM No. 1 in both the low- and the high-carbon steels (Figure 34). Finally, the prior austenite grain sizes of specimens of both steels after heating to 2200°F for 1 hour, holding at 1500°F for 4 hours and air cooling are shown in Figure 35. It is evident that the high-temperature treatment (2200°F) caused a large increase in grain size but that no further change occurred upon holding at 1500°F for 4 hours during the interrupted cooling.

Extraction replicas of the fracture surfaces of broken CVN impact test specimens provided information on the presence of second-phase particles in the fracture path. Figures 36 through 43 are electron micrographs of extraction replicas

18

prepared from the fracture surfaces of Charpy V-notch impact specimens of steels V-8858 and V-8497. Figure 36 is an electron micrograph of an extraction replica of the fracture surface of a specimen of steel V-8858 (0.027% C) that had been annealed 1 hour at 1500°F; the volume fraction of extracted particles was quite small. After heating for 1 hour at 2200°F (Figure 37), large particles were found in the fracture surface, which presumably had formed upon cooling from 2200°F; these particles evidently fragmented during fracture of the impact test specimen. When specimens of steel V-8858 were heated to 2200°F for 1 hour, then cooled to 1500°F and held for 4 hours, the density of particles extracted from the fracture surface of a broken impact specimen greatly increased, as shown in Figure 38. The density of particles contained on the fracture surfaces of embrittled specimens appeared about the same whether the specimens were aged or unaged (compare Figures 38 and 39). A high-magnification micrograph showing the morphology of some of the extracted particles found in the fracture surfaces of embrittled and aged impact specimens is presented in Figure 40.

Extraction replicas of the fracture surfaces of CVN specimens of the low-carbon steel (V-8497) were similar in appearance to those of the high-carbon steel (V-8858), but the concentration of particles was much lower. Figure 41 shows the fracture surface of a specimen of V-8497 that had been heated to 2200°F for 1 hour and air-cooled; indications of only a few particles associated with the fracture surface could be found in this replica (see lower right-hand corner of micrograph). The concentration of extracted particles in the fracture surfaces of specimens heated to 2200°F for 1 hour, then cooled to 1500°F and held for 4 hours (Figure 42), increased substantially over that of specimens that had been heated to 2200°F and air-cooled; the concentration of such particles was about the same after aging (Figure 43). However, the concentration of extracted particles in the fracture surface of this specimen was much lower than was found in the fracture surface of the higher carbon steel after the same treatment (Figure 39), despite the fact that the strength and toughness of the two steels were reduced to approximately the same low level by the thermal embrittling treatment.

The fracture surfaces of all embrittled specimens contained a considerable concentration of these particles,

which strongly suggested that they were the cause of the
embrittlement, particularly in view of the semiquantitative
correlation between particle concentration and the degree of
thermal embrittlement.

(3)   Diffraction analyses

Analyses of both gross and selected-area diffraction
patterns obtained from the particles extracted in the replicas
of fracture surfaces were made.   Electron-diffraction ring
patterns from extraction replicas of steels V-8858 and V-8497
in an embrittled condition have resulted in the identification
of two different compounds in the fracture surface—Ti(C,N)
and τ-Ti$_2$S.   Table 10 lists the diffraction rings, in terms of
interplanar spacings (d), that were obtained from extraction
replicas of the two steels by the gross diffraction technique,
together with standard ring patterns for Ti(C,N) and τ-Ti$_2$S.
Two patterns are listed for steel V-8858; one pattern was
identified as being predominantly that of Ti(C,N), whereas the
other corresponded mainly to that of τ-Ti$_2$S.   It is evident
that each pattern possesses one or two rings belonging to the
other, probably because minor amounts of the other compound
were present.   The data for steel V-8497 showed that both
Ti(C,N) and τ-Ti$_2$S were present.   In general, the Ti(C,N)
patterns appeared with greater frequency than those of τ-Ti$_2$S.
Both Ti(C,N) and τ-Ti$_2$S were present in the fracture surfaces
of V-8858 and V-8497, despite the low carbon content of steel
V-8497 and the low sulfur levels in both steels.   Other diffrac-
tion rings also were occasionally observed, however, that did
not originate from either compound, but they could not be
positively identified.   Thus, although the diffraction evidence
indicated that the extracted particles consisted mainly of
Ti(C,N) and τ-Ti$_2$S, minor amounts of some other unidentified
compound probably were present.

The selected-area diffraction technique was used to
confirm the identification of Ti(C,N) and τ-Ti$_2$S.   Since
Ti(C,N) is cubic, its identity can be checked quite easily by
comparing angles between crystallographic planes with those
calculated for the cubic system.   Angles between planes in
the tetragonal, orthorhombic and hexagonal crystal systems,
however, depend upon the lattice parameters and, therefore,
are different for each compound.   A review of the intermetallic
compounds and precipitate phases that are possible in these
steels, from consideration of composition alone, has shown that
a majority are noncubic; this includes τ-Ti$_2$S, which is hexag-
onal.   A computer program, therefore, was prepared that would

20

calculate and print out angles between crystallographic planes for all orthogonal crystal systems and for the hexagonal system. The only computer inputs required were the specific crystal system, the lattice parameters, and the maximum values of the Miller indices (h, k, and l) to be calculated.

Typical spot patterns, from which Ti(C,N) and τ-Ti$_2$S were identified, are shown in Figures 44 and 45. The first pattern (Figure 44), that of Ti(C,N), was obtained from a thin foil of a specimen of an experimental maraging steel (T-6110) very similar in composition to that of steel V-8497 (Reference 7); it had been heated to 2200°F for 1 hour, then cooled to 1400°F for 4 hours; the identification system is indicated in the accompanying sketch. The camera constant, obtained by identifying the matrix zone, was used in calculating the d-spacings of the three reflections. When these planes had been tentatively identified, the measured angles were checked with the table of angles between planes in the cubic system and were found to agree. The second pattern (Figure 45) was obtained from an extraction replica of a specimen of V-8858 that had been heated 1 hour at 2200°F and air-cooled. The identification was made as in the previous example; the d-spacings of three reflections were calculated, and indices were tentatively assigned. The angles between reflections were measured and compared with the data calculated for τ-Ti$_2$S, and were found to agree. This τ-Ti$_2$S diffraction pattern was obtained from particle "A" of Figure 46. All the particles in this field were τ-Ti$_2$S; they could be distinguished from Ti(C,N) particles by their massive, angular appearance. In contradistinction, the Ti(C,N) particles usually appeared as dendritic or fan-shaped particles, as shown in Figure 40.

(4) Differential Thermal Analysis— Effluent Gas Analysis Results

Another corroborative approach to the correlation of the presence of Ti(C,N) and τ-Ti$_2$S with thermal embrittlement was attempted by means of Differential Thermal Analysis— Effluent Gas Analysis (DTA-EGA). This technique can be used to identify and quantitatively determine certain intermetallic compounds that occur in steels. The technique is performed on an extracted residue which is obtained in various ways, depending upon the type of compound for which the analysis is conducted; for example, titanium nitride is extracted by an ester-halogen technique, whereas electrolytic extraction is used for titanium carbide and titanium sulfide. The DTA is the qualitative portion of the procedure and, briefly, consists

21

of the determination of the rate of change of heat content, using a programmed constant rate of heating (in this case, 10°C/minute). Discontinuities occur in the heat content curves that correspond to energy absorption or release. These energy changes can be caused by chemical reactions, phase changes, or changes of state. This technique can be calibrated with pure TiN, TiC, etc., and a DTA "fingerprint" can be determined for the various compounds. The EGA part of the procedure consists of gas chromatographic analysis of the effluent gases from the DTA. This is the quantitative portion of the analysis and can relate back to the original amount of compound in the steel.

Preliminary results on specimens of steels V-8858 and V-8497 agreed in trend with the results of extraction replication and analysis. A comparison of the DTA-EGA results on the two steels was made before and after embrittlement, i.e., for treatments 3 and 7 (Table 9). The analysis was performed on unaged specimens to avoid diluting the extracted residues with strengthening precipitates. The results are not refined enough to allow quantitative comparisons between steels; therefore, a descriptive presentation of the results will be made. The extracted residue from the low-carbon steel (0.004%) contained only TiN by this method of analysis; it was not possible to determine whether the relative amounts of TiN were different for specimens treated according to 3 or 7. Because of the very low carbon content of this steel, the method evidently was not sensitive enough to detect any TiC or Ti(C,N). In the higher carbon steel (0.027%), TiC, TiN, and Ti_2S* were detected in specimens subjected to both treatments 3 and 7; it was not possible to make reliable quantitative determinations of the amounts of these compounds present in the steel, but, relatively, the amounts seemed to be higher after treatment 7 than treatment 3.

d. Summary

Two experimental heats of maraging steel, containing very low levels of the residual elements but different levels of carbon, were melted and rolled to plate. Specimens were heat-treated according to several different schedules that included embrittling treatments, and their mechanical properties were determined both before and after aging. The low-carbon steel (0.004%) possessed good notch toughness after annealing and after annealing plus aging; in contrast, the

---

*The distinction between the different forms of Ti_2S cannot be made.

22

toughness of the steel containing 0.027 percent carbon was considerably lower and about the same as that for the commercial plate. After the full thermal-embrittlement treatment (2200°F for 1 hour + 1500°F for 4 hours), however, the notch toughness was drastically reduced in both steels, and a significant reduction in strength was also observed.

Metallographic examination showed that considerable austenitic grain growth occurred in the two steels during heating at 2200°F for 1 hour and that little additional grain growth resulted from subsequent isothermal annealing (interrupted cooling) at 1500°F for 4 hours. This grain growth is believed to be a contributing factor to the observed embrittlement.

Extraction replication and diffraction analysis revealed plate-like particles of the titanium compounds—Ti(C,N) and τ-Ti$_2$S—in the fracture surfaces of the CVN specimens; the concentration of these particles increased with the degree of thermal embrittlement. The concentration also was higher in the steel of higher carbon level (0.027%) than in the steel with low carbon content (0.004%). However, even the low-carbon, low-residual steel could be rather thoroughly embrittled (CVN energy of 6 ft-lb) by heating to 2200°F for 1 hour, cooling to 1500°F and holding for 4 hours, air cooling, and aging at 900°F for 3 hours. Evidently, a carbon content as low as 0.004 percent is still sufficient to cause complete embrittlement as a result of this particular thermal treatment.

2. THE EFFECT OF ALUMINUM SUBSTITUTION

a. Purpose

The previously reported results suggested that one method of eliminating the precipitation of particles of Ti(C,N) in maraging steel would be to omit titanium from the steel and to substitute a supplemental hardening element that does not form a carbide. Accordingly, a series of steels was made in which titanium was entirely replaced by aluminum. In the first of the steels (T-6109) the aluminum recovery was incorrectly estimated in melting, so that a somewhat lower strength material was obtained than for similar steels containing about 0.4 percent titanium. For this reason and because its resistance to thermal embrittlement appeared to be improved, additional experimental heats (W-8135-2, W-8068, and W-8598) containing 0.4 percent aluminum were melted; W-8135-2 contained 0.02 percent carbon, whereas W-8068 and W-8598 contained minimum levels of carbon.

23

Another split heat (W-8252-1A, -1B, and -1C) containing different levels of manganese was investigated to determine whether, in the absence of titanium, manganese might have a beneficial effect on ductility and toughness by combining with the residual sulfur to form innocuous, globular manganese sulfides in place of platelets of τ-Ti_2S that occasionally were found in the fracture surfaces of embrittled titanium-bearing steels. In addition to these steels, a heat (W-8263) containing 1 percent aluminum was melted to determine the embrittlement characteristics at a higher strength level.

b. Materials and Experimental Work

The chemical analyses of these experimental heats (T-6109, W-8068, W-8135-2, W-8598, W-8252-1A, -1B, -1C, and W-8236) are shown in Table 11. These steels were 300-pound vacuum-melted heats poured into 100-pound ingots measuring 3 by 8 by 14 inches. All ingots were soaked at approximately 2200°F for 6 hours, and then straightaway-rolled to 1-1/4-inch-thick plate in five passes and water-sprayed; this plate was sectioned into three pieces, heated to approximately 2160°F, cross-rolled to 1/2-inch-thick plate in five passes, and water-sprayed. The plate temperature before the third pass was approximately 1800°F.

Mechanical properties were determined from duplicate 0.252-inch-diameter tensile specimens and triplicate CVN test specimens tested at room temperature. All specimens were heat-treated before final machining in an argon atmosphere with the exception of some of the blanks from T-6109, which were treated in a cracked-ammonia atmosphere.

The gross microstructural features of the steels in a variety of heat-treated conditions were examined by light microscopy. In addition, extraction replicas were prepared from the fracture surfaces of broken CVN specimens (in the region of flat fracture just below the notch); these were examined by electron microscopy to determine the morphology and distribution of particles in the fracture surfaces. The extracted particles were identified by electron diffraction. Two somewhat different electron-diffraction techniques were used which were described in detail earlier in this report. Briefly, gross-area electron diffraction was employed, in which all the extracted particles contained in the replica over an area of several squares of a 200-mesh specimen-support grid were exposed to the electron beam, and this contributed to the diffraction pattern. This method provided a rough, semiquantitative estimate of the relative abundance of different compounds,

24

if more than one was present. Selected-area diffraction also
was employed, whereby only a single particle, or a small group
of particles, contributed to the diffraction pattern. This
method permitted direct correlation of crystalline identity
with particle morphology.

c. Results and Discussion

(1) Steel T-6109

The experimental steel (ARL heat No. T-6109) contained
0.19 percent aluminum, in place of the 0.4 percent titanium
normally present in commercial 18Ni(250) maraging steel, but it
contained only very small amounts of residual elements. The
effects of several different thermal treatments on the mechanical
properties of this experimental steel are shown in Table 12.

As in the experiments on the commercial steel, the possi-
bility of the occurrence of hydrogen embrittlement in this
experimental steel during annealing at high temperatures (above
2100°F) in cracked ammonia was not anticipated at the time this
work was done. In consequence, experiments involving six thermal
treatments were repeated using argon as a furnace atmosphere.
The results, also reported in Table 12, showed that hydrogen
embrittlement was a significant factor only in the specimens
that had been annealed at 2100°F and air-cooled. For these
specimens, the effect of the argon atmosphere was to produce a
marked increase in both the annealed and the annealed-and-aged
tensile ductility. Conversely, the effect of furnace atmosphere
on the tensile ductility of specimens that had been quenched
into salt at 1500°F after the high-temperature anneal was not
significant. Although all the aged specimens, which had been
heat-treated in argon, exhibited somewhat higher toughness
values than those heat-treated in cracked ammonia, this increase
in toughness was offset by a decrease in yield strength.

The strength levels achieved in this steel were consider-
ably lower than those for similar steels of conventional composi-
tion containing about 0.4 percent titanium and given similar
thermal treatments. The intention had been to substitute aluminum
for titanium on an equivalent weight-percent basis (0.4%), but
the aluminum recovery was incorrectly estimated in melting this
experimental heat of modified composition. The comparatively
low content of this supplemental strengthening element is
believed to be the reason for the lower strength. Despite the
relatively lower strength, the data of Table 12 indicate that
this steel was not as susceptible to thermal embrittlement as
the titanium-strengthened steels investigated.

25

For example, in the annealed condition (1500°F for 1 hour), this steel exhibited a CVN energy of 194 ft-lb (at 113 ksi yield strength), and in the annealed-and-aged (900°F for 3 hours) condition, the CVN energy was 33 ft-lb (at 225 ksi yield strength). After a thermal embrittling treatment (2200°F for 1 hour, quenched to 1500°F and held for 4 hours), the CVN energy was 153 ft-lb (at 111 ksi yield strength), and after aging (900°F for 3 hours) the value was 33 ft-lb (at 214 ksi yield strength). In contrast to this behavior, the commercial steel (X-53541), when subjected to the same thermal treatment, exhibited a CVN energy before aging of 48 ft-lb (at 116 ksi yield strength) and only 6.5 ft-lb (at 234 ksi yield strength) in the aged condition.

The low-magnification (100X) light micrographs of Figure 47a-h show the microstructures that developed in steel T-6109 on annealing for 1 hour at temperatures of 1700 to 2400°F (at 100°F intervals). Below 2000°F, the prior austenite grain size appeared to be relatively insensitive to annealing temperature, the grain size increasing from ASTM No. 6 at 1700°F to ASTM No. 5 at 2000°F. Some difficulty was experienced in measuring these grain sizes since the boundaries were not always clearly delineated, especially after the 1700 to 1800°F anneals. For temperatures in excess of 2000°F, the grain size increased sharply with increase in annealing temperature; for 2100°F the ASTM grain size number was 3, and for 2300°F the number was -1.

Comparison of the grain sizes of this steel with those of the commercial steel (heat No. X-53541) after the same annealing treatments showed that the grain sizes were similar above 2100°F but that in the temperature range 2100 to 1900°F steel T-6109 had a finer prior austenite grain size. Since aluminum can act as both a grain refiner and a grain growth inhibitor, it is believed that the smaller grain size of T-6109 in this temperature range was a direct result of the substitution of aluminum for titanium. Evidently, aluminum does not inhibit grain growth above 2100°F.

(2) Steels W-8068 and W-8135-2

Steel W-8068 contained 0.44 percent aluminum and low levels of carbon and other residual elements, whereas steel W-8135-2 contained 0.38 percent aluminum and 0.018 percent carbon with low levels of the other residual elements. The titanium content in both of these steels was less than 0.01 percent. The effects of several different thermal treatments

BEST AVAILABLE COPY

on the mechanical properties of W-8068 and W-8135-2 are shown in Tables 13 and 14, respectively. Both steels were aged for 1 hours at 900°F to develop the required strength.

In comparing the results of as-rolled and the as-rolled-and-aged treatments with those of the standard anneal and annealed-and-aged treatments, it is evident that the latter two treatments did not improve the yield-strength—toughness relationship for either steel. Also, for each of these four treatments, the notch toughness of the low-carbon steel (W-8068) was only marginally greater than that of the high-carbon steel (W-8135-2), although exact comparisons are difficult because of the varying yield strengths of the two steels.

After being heated to 2200°F for 1 hour and aged, both steels exhibited decreases in toughness and yield strength when compared with specimens annealed at 1500°F and aged. It is interesting to note that, as in the case of the standard annealing and aging treatments, the toughness and the strength of the low-carbon steel were not significantly different from those of the high-carbon steel.

The interrupted-quench experiments from 2200°F reduced the notch toughness of both steels compared with that obtained by heating to 2200°F only; the decreases in toughness were significantly less for the low-carbon steel than for the high-carbon steel. For example, heating to 2200°F and quenching to 1500°F for 4 hours and aging reduced the toughness of the low-carbon steel to 12 ft-lb, whereas the value for the high-carbon steel was 6 ft-lb. The results of the interrupted-quench experiments from 2400°F produced more drastic reductions in toughness for both steels. As before, the reductions in toughness were less for the low-carbon steel.

In addition to the heat treatments described, some specimens were air-cooled from 2200°F to room temperature, and then reheated to 1500°F for either 1/2 or 4 hours. The results show that the toughness and strength of the low-carbon steel were somewhat lower when compared with these for the standard annealing and annealing-and-aging treatments; in the case of the high-carbon steel, similar reductions were evident only for one treatment, that is, after reheating to 1500°F for 4 hours and aging.

Comparison of the results for steel W-8068 with those of the low-carbon, low-residual steel V-8497 containing titanium (see Table 9) shows that the substitution of aluminum for titanium improved the resistance of the steel to thermal embrittlement.

For example, after a thermal embrittling treatment (2200°F for 1 hour, quenched into salt at 1500°F for 4 hours, air-cooled and aged), steel V-8497 exhibited a CVN energy value of 6 ft-lb, tensile elongation of 4.5 percent, and a tensile reduction of area of 10 percent, at a yield strength of 218 ksi; whereas, the comparable values for the aluminum-substituted steel (W-8068) were 12 ft-lb, 5.8 and 22.3 percent, respectively, at a yield strength of 235 ksi.

Comparison of the results of aluminum-substituted steel W-8135-2 with those of the high-carbon, low-residual steel W-8858 containing titanium (see Table 9) show that the toughness of steel W-8135-2 was significantly greater for the standard annealing and annealing-and-aging treatments. However, the susceptibility of steel W-8135-2 to thermal embrittlement (2200°F for 1 hour, quenched into salt at 1500°F for 4 hours, air-cooled and aged) was about the same.

The low magnification (100X) light micrographs (Figures 48 and 49) show the microstructures that developed in steels W-8068 and W-8135-2 after the standard 1500°F anneal and after two of the thermal embrittling treatments (2200°F for 1 hour, or 2400°F for 1 hour, followed by cooling to 1500°F and holding for 4 hours). After annealing at 1500°F, the prior austenite grain boundaries in steel W-8068 were not well delineated, whereas in steel W-8135-2 the boundaries were evident, but the grains were of irregular shape and elongated in the rolling direction. In both steels, the ASTM grain size was estimated to be between 5 and 6. After heating at 2200°F for 1 hour, the ASTM grain size of both the high- and low-carbon aluminum-substituted steels was 1/2, which is not significantly different from that observed for the low- and high-carbon titanium-bearing steels (V-8598 and V-8858) after the same treatment. Annealing at 2400°F for 1 hour increased the grain size of both aluminum-substituted steels to ASTM No. -1.

Extraction electron fractographs were prepared from broken CVN test specimens, as previously described. After a heat treatment of 1 hour at 2200°F (or 2400°F), air cooling, and aging for 6 hours at 900°F, the fractographs obtained from the two steels (W-8068 and W-8135-2) were very similar in appearance. Relatively few particles of a segregate phase were evident in the fracture surface, and the fracture mode appeared to be one of dimpled rupture, except in microscopic regions containing particles, where the fracture surface was smoother (Figure 50). Figure 51 is an extraction replica of the fracture surface of a specimen of steel W-8068 (low carbon level) that

28

had been heated to 2200°F for 1 hour, then cooled to 1500°F for 4 hours and aged. It is evident that the fracture surface of this specimen contained many thin, platelike precipitate particles; furthermore, the microscopic surface topography was smoother than that observed in the specimens heated only to 2200°F and air-cooled, and was more characteristic of an intergranular type of fracture. After holding at 2400°F for 1 hour, cooling to 1500°F and holding for 4 hours and aging, the concentration of particles in the fracture surface was still greater, and the microscopic surface topography was quite smooth (Figure 52).

To identify these particles, both selected-area electron-diffraction and "bulk" electron-diffraction patterns were obtained from these extraction replicas. Analyses of ring electron-diffraction patterns obtained from gross areas of the extraction replicas showed that the interplanar spacings closely matched those of aluminum nitride (AlN), (Table 15). Selected-area diffraction patterns obtained from single particles confirmed that the particles contributing to the diffraction pattern were, in fact, those observed microscopically in the replicas.

Figure 53 is an extraction replica of the fracture surface of a specimen of steel W-8135-2 (high carbon) that had been heated to 2200°F for 1 hour, then cooled to 1500°F and held for 4 hours, and then aged. Two different types of particles were present in this replica, namely, thin platelike particles, similar to those identified as aluminum nitride in steel W-8068, and thicker, electron-opaque particles. As in the case of the low-carbon steel (W-8068), the fracture surface was quite smooth and characteristic of an intergranular fracture. After holding at 2400°F for 1 hour and then cooling to 1500°F and holding for 4 hours and aging, the concentration of the precipitate particles in the fracture surface was considerably greater (Figure 54). Examination of an extraction replica of a polished-and-etched section of an embrittled specimen of this steel revealed that both types of precipitate particles were located in the prior austenite grain boundaries (Figure 55).

Analyses of ring electron diffraction patterns obtained from gross areas of these extraction replicas showed that the interplanar spacings closely matched those of aluminum nitride (AlN), but that additional rings not attributable to AlN also were present (Table 16). Because of the higher carbon content of steel W-8135-2, it was suspected that a carbide phase might also have precipitated on austenite grain boundaries during the thermal embrittling treatments. Further analysis in fact revealed that these extra lines could be satisfactorily identified with a molybdenum carbide (Mo_2C).

The presence of particles of aluminum nitride and molybdenum carbide in the fracture surface of specimens that had been subjected to an interrupted-quench, indicated that these particles had precipitated during the 1500°F holding portion of the thermal treatments, since they were not present in specimens which had been merely heated to 2200 or 2400°F and air-cooled. Thus, it is believed that the precipitation of AlN in the low-carbon steel (W-8068), and of both AlN and Mo_2C in the high-carbon steel (W-8135-2), accounts for both the intergranular type of fracture and the lower fracture toughness of these steels that resulted from the thermal embrittling treatments. Presumably, the greater susceptibility of steel W-8135-2 to thermal embrittlement compared with that of steel W-8068 was a consequence of the additional precipitation of molybdenum carbide.

(3) Steel W-8598

This steel was similar in composition to steel W-8068, but contained slightly less aluminum—0.40 compared with 0.44 percent (see Table 11). The effects of several different thermal treatments on the mechanical properties are shown in Table 17. An excellent combination of strength and toughness (CVN) was obtained in the as-rolled and aged condition (70 ft-lb at a yield strength of 222 ksi). The susceptibility of this steel to thermal embrittlement appeared somewhat less than that of steel W-8068 (see Table 13), although an exact comparison is difficult because of the different yield strengths of the two steels. The most severe embrittlement occurred upon heating at 2200°F for 1 hour, quenching into salt at 1500°F for 4 hours, air cooling, and aging; this treatment resulted in a yield strength of 214 ksi, an elongation of 10.0 percent, a reduction in area of 45.9 percent and a CVN value of 23 ft-lb. These values are very similar to those of steel T-6109 when subjected to the same treatment (see Table 12).

Electron fractographic examination of the fracture surfaces of CVN specimens of this steel, in various embrittled conditions, revealed that the fractures were relatively flat and intergranular and contained particles similar in appearance to those found in steel W-8068.

(4) Effects of Different Aging Treatments on the Mechanical Properties of Steels W-8068 and W-8598

Earlier work had indicated that aging at 900°F for 6 hours was necessary to develop the full strength of the aluminum-substituted steels, but the effects of the different

30

aging treatments on toughness was not explored.

In view of the limited data previously available on the aging characteristics of aluminum-substituted maraging steels, a brief survey of the effects of different aging times and temperatures on the mechanical properties of steels W-8068 and W-8598 was carried out to determine the aging conditions that would provide optimum combinations of strength and toughness. The results of aging at 900, 800, and 700°F for various times are presented in Table 18. The most interesting combinations of strength and toughness were obtained by aging for 1 hour at 900°F. Steel W-8068 exhibited a CVN energy value of 89 ft-lb at a yield strength of 212 ksi whereas steel W-8598, which contained slightly less aluminum (0.40%), exhibited a value of 122 ft-lb at a yield strength of 195 ksi; these combinations of strength and toughness are exceptionally good. Even at the higher yield strength level of 237 ksi, steel W-8068 aged for 3 hours at 900°F exhibited very good toughness (CVN energy of 50 ft-lb).

Aging these steels at lower temperatures considerably reduced the toughness for a given strength level. For example, aging steel W-8068 for 3 hours at 800°F resulted in a CVN energy value of 37 ft-lb at a yield strength of 212 ksi, whereas aging for 1 hour at 900°F provided the same yield strength but a value of 89 ft-lb—an increase of a factor of two. After aging at an even lower temperature, namely, 700°F for 24 hours, steel W-8068 exhibited a yield strength of 220 ksi and a CVN energy value of 20 ft-lb. A similar decrease in the toughness—yield-strength ratio with decreasing aging temperature was observed for steel W-8598 (see Table 18). Thus, it is concluded that, although a given strength level may be attained by several different aging treatments, the associated toughness (CVN) values are not necessarily comparable. Judging from the results of this short survey, better combinations of strength and toughness can be achieved by aging for relatively short times (1 to 3 hours) at 900°F than by aging at lower temperatures for longer times.

(5) Steels W-8252-1A, -1B, -1C

This experimental steel was made as a split heat containing 0.4 percent aluminum, low levels of residual elements, and three levels of manganese: 0.1, 0.2, and 0.3 percent (W-8252-1A, -1B, -1C, respectively). The chemical analyses of these steels are shown in Table 11. The effects of several different thermal treatments on the mechanical properties of these steels are shown in Tables 19, 20, and 21. In the annealed-and-aged condition

31

(1 hour at 1500°F, air-cooled, 6 hours at 900°F, air-cooled),
the mechanical properties of the steels containing 0.1, 0.2,
and 0.3 percent manganese were not significantly different,
that is, the CVN toughness values were 26, 25, and 24 ft-lb
at yield strengths of 253, 252, and 252 ksi, respectively
(Tables 19, 20, and 21). These values are similar to those
obtained from steel W-8068 (29 ft-lb at a yield strength of
248 ksi), which contained similar levels of aluminum and
residual elements, but only 0.007 percent manganese.

The response of each of these steels to thermal embrit-
tlement treatments was very similar, and not markedly different
from the embrittlement susceptibility of steel W-8068. For
example, after heating for 1 hour at 2200°F, quenching into
salt at 1500°F and holding for 4 hours, air cooling and aging
at 900°F for 6 hours and air cooling, the CVN toughness values
of steels W-8252-1A, -1B, -1C, and W-8068 were 12, 12, 11, and
12 ft-lb, respectively, at yield strengths of 240, 235, 242,
and 235 ksi, respectively (see Tables 19, 20, 21, and 13). On
the basis of these results, it appears that manganese, in
amounts up to at least 0.3 percent, in the aluminum-substituted
steel does not significantly alter its resistance to thermal
embrittlement.

In view of the similarity of these results to those of
W-8068, a detailed microstructural examination of steels
W-8252-1A, -1B, and -1C was not carried out.

(6) Steel W-8236

This steel was a low-carbon, low-residual steel contain-
ing 1.06 percent aluminum (see Table 11). The effects of several
different thermal treatments on the mechanical properties of this
steel are shown in Table 22. In the annealed-and-aged condition,
a CVN toughness value of 20 ft-lb was recorded at a yield
strength of 283 ksi. This level of toughness is remarkably good
for a steel of this high strength level, and it is considerably
better than that obtained in commercial 18Ni(280) maraging
steel plate containing about 0.8 percent titanium.

After an embrittling treatment (heating at 2200°F for
1 hour, quenching into salt at 1500°F for 4 hours, air cooling,
and aging), the yield strength was reduced to 264 ksi and the
CVN energy to 10 ft-lb. The results of this and other treatments
(shown in Table 22) indicated that the degree of embrittlement
even at this higher strength level was no greater than that
observed in the steels of lower yield strength, which contained

32

approximately 0.4 percent aluminum. Furthermore, the CVN energy values of this steel in the embrittled condition were significantly higher than those obtained from the lower strength steels containing 0.4 percent titanium (commercial plate, steel No. V-8497 and steel No. V-8858) after the same embrittling treatments (see Tables 2 and 9).

A detailed metallographic examination of this steel was not carried out.

d. Summary

The substitution of aluminum for titanium in experimental 18Ni maraging steels, containing only very small amounts of carbon (0.001 to 0.003%) and other residual elements, considerably improved their resistance to thermal embrittlement. This reduced susceptibility was observed for steels containing 0.2 or 0.4 percent aluminum, and particularly for a higher strength steel containing 1 percent aluminum. The addition of 0.1, 0.2, or 0.3 percent manganese to a low-residual steel containing 0.4 percent aluminum did not further improve its resistance to thermal embrittlement. The substitution of aluminum for titanium in a steel having a higher carbon content (0.018%) did not result in improved resistance to thermal embrittlement, as compared to the behavior of steels of similar low-residual element content that contained 0.4 percent titanium.

Some embrittlement did occur, however, in all of these steels. Electron fractographic examination revealed that the fractures of the embrittled steels were mainly intergranular, rather than of a dimple-rupture nature as observed in fractures of the unembrittled steels. In the embrittled steels of low-carbon content, thin, platelike particles of a segregate phase were found in the extraction replicas of the fracture surfaces; these particles were identified as aluminum nitride (AlN) by means of bulk and selected-area electron-diffraction analyses. In the steel of higher carbon content, which exhibited more severe embrittlement, the concentration of particles in the fracture surface was greater, and two different types of particles could be discerned; the thin, platelike particles were identified as aluminum nitride (AlN), whereas the thicker, blocky particles were found to be molybdenum carbide (Mo_2C). In metallographic sections, the particles were found to be located on grain boundaries.

Evidently, the AlN particles had precipitated during the 1500°F holding portion of the thermal treatments, since they did

33

not appear in specimens which had been merely heated to 2200 or 2400°F and air-cooled. Thus, the precipitation of AlN in these aluminum-substituted steels is analogous to the precipitation of Ti(C,N) in the titanium-bearing steels. The presence of the precipitates at grain boundaries is believed to account for the observed intergranular type of fracture and the decrease toughness of these steels after the thermal treatments. The embrittlement was more severe in the steel of higher carbon content, presumably because of the additional precipitation of Mo_2C.

A subsidiary study of the effects of different aging treatments on the strength and toughness of two of the aluminum-substituted steels (containing about 0.45% aluminum) revealed that aging times of 1 to 3 hours at 900°F yielded the best combinations of properties; aging for 1 hour at 900°F provided exceptionally high levels of toughness at a yield strength level of about 200 ksi.

3. THE EFFECT OF VANADIUM SUBSTITUTION

a. Purpose

As part of the effort to reduce the susceptibility of the 18Ni maraging steels to thermal embrittlement by eliminating titanium from the composition, the possibility of substituting vanadium for titanium as the supplemental strengthening element was explored. For this purpose, steels of low-residual element content having two levels of vanadium (1.6 or 1.0%) were made, and their properties and embrittling characteristics were determined. Normal amounts of molybdenum (5%) and cobalt (7.5%) were used in the 1.6 percent vanadium steel, whereas a somewhat lower molybdenum content (4%) and much higher cobalt content (12.3%) were employed in the 1.0 percent vanadium steel. In some preliminary experiments not reported here, these compositions appeared to provide the most attractive combinations of strength and toughness at the desired yield strength level (240 to 250 ksi). The two steels were melted and processed in duplicate to test the reproducibility of their properties and response to thermal embrittlement.

b. Materials and Experimental Work

The chemical analyses of the four experimental heats are shown in Table 24. The compositions of heats W-8133-1A and W-8133-1C were nearly identical, as were those of heats W-8134-1A and W-8134-1C. These steels were 300-pound, vacuum-induction-

34

melted heats that were poured into 100-pound ingots. Each ingot measured 3 by 8 by 14 inches, with the exception of one ingot from each heat that measured 4 by 4 by 21 inches. All ingots were soaked at approximately 2200°F for 6 hours and the slab ingots (3 by 8 by 14 inches) were reduced to 1-1/4-inch-thick plate in five passes and water-sprayed. The plate was sectioned into three pieces, heated to approximately 2160°F and cross-rolled to 1/2-inch-thick plate in five passes and water-sprayed. The plate temperature before the third pass was approximately 1800°F. The 4- by 4- by 21-inch ingots were straightaway-rolled to 2-inch-thick plate in three passes and water-sprayed. The plate was sectioned into two pieces, heated to approximately 2160°F and cross-rolled to 1-1/8-inch-thick plate in four passes. The plate temperature before the last pass was approximately 1800°F.

Mechanical properties were determined from duplicate 0.252-inch-diameter tension test specimens and triplicate CVN specimens tested at room temperature.

The gross microstructural features and prior austenite grain size of the steels, in a variety of heat-treated conditions, were examined first by light microscopy. Extraction replicas were prepared from the fracture surfaces of broken CVN specimens in the region of flat fracture just below the notch; these replicas were examined by electron microscopy to determine the morphology and distribution of any particles present in the fracture surfaces. The extracted particles then were identified by electron diffraction. Two somewhat different electron-diffraction techniques were used. In the first, which will be referred to as "gross-area electron diffraction," all the extracted particles contained in the replica, over an area of several squares of a 200-mesh specimen-support grid, were exposed to the electron beam and contributed to the diffraction pattern. This method provided a rough, semiquantitative estimate of the relative abundance of different compounds, when more than one was found. "Selected-area diffraction" was also employed, whereby only a single particle, or a small group of particles, contributed to the diffraction pattern. This method permitted direct correlation of crystalline identity with particle morphology.

c. Results and Discussion

The mechanical properties of the 1.6 percent vanadium steels (W-8133-1A and W-8133-1C) after a variety of thermal treatments are shown in Tables 24 and 25, respectively. For each

35

treatment, the resulting strength, ductility, and toughness values for these two steels were very nearly the same, indicating good reproducibility. In the rolled-and-aged and annealed-and-aged conditions, the toughness levels were somewhat higher than for the commercial plate (see Table 2), but only intermediate between those for the high-carbon (0.027%) and low-carbon (0.004%) low-residual, titanium-bearing steels (see Table 9), and, in general, lower than for the aluminum-substituted steels (see Tables 13, 14, 17, and 18). After the thermal embrittling treatments (heating at either 2200 or 2300°F for 1 hour, followed by cooling and holding at 1500°F for 1/2 or 4 hours, and aging), the notch toughness was better than for the commercial steel and the low-residual titanium-bearing steels, but not as good as for the aluminum-substituted steels. As for the other steels previously discussed in this report, heating of these vanadium steels to 2200 to 2400°F for 1 hour, followed by air cooling and aging, resulted in moderate decreases in both strength and toughness, but reannealing at 1500°F for 1/2 or 4 hours, after air cooling from 2200°F, but prior to aging, effected considerable rectification of both losses.

The corresponding properties of the 1.0 percent vanadium steels (W-8134-1A and W-8134-1C) are given in Tables 26 and 27, respectively. Again, the properties of these two steels, after the various thermal treatments, were nearly the same. Although the reductions in strength (aged condition) resulting from continuous air cooling, or interrupted cooling (and holding at 1500°F), from 2200 or 2300°F were not as marked as for the 1.6 percent vanadium steels, the losses in toughness were somewhat greater and were comparable to those for the commercial steel (see Table 2) and the low-residual titanium-bearing steels (see Table 9). The smaller losses in strength possibly were a consequence of the unusually high cobalt content of these 1.0 percent vanadium steels, since variations in the other two strengthening elements (vanadium and molybdenum) have not been observed to have this effect. In common with the other experimental steels, annealing at 1500°F, after air cooling from 2200°F, effected considerable restoration of the losses in strength and toughness that resulted from the high-temperature heating, although perhaps to a somewhat greater degree.

The gross features of the microstructures of the 1.6 percent vanadium steel (W-8133-1A), after annealing at 1500°F and aging, and after two of the embrittling and aging treatments, are shown in the low-magnification (100X) light micrographs of Figure 56. The prior austenite grain size was relatively small (approximately ASTM No. 10) as a result of annealing at 1500°F

36

but became quite large upon heating for 1 hour at 2200°F (ASTM No. 1/2 to 0) and still larger as a consequence of heating at 2300°F for 1 hour (ASTM No. 0 to -1). The prior austenite grain sizes after these thermal treatments for the duplicate 1.6 percent vanadium steel (W-8133-1C) were about the same; this was true also for the 1.0 percent vanadium steels (W-8134-1A and W-8134-1C), as indicated in the light micrographs of Figure 57 for steel W-8134-1A. In general, these grain sizes were nearly the same as for the other steels previously discussed after the corresponding thermal treatments.

Extraction fractographs were prepared from the flat-fracture area of broken CVN specimens of steel W-8133-1A, which had been heated at 2200°F for 1 hour, air-cooled, and aged; although this treatment caused some reduction in strength as compared to the standard annealing treatment, there was no loss of toughness. Electron microscope examination of the fracto-graphs showed that the microscopic fracture topography consisted of relatively shallow dimples with some tendency toward flat intergranular rupture, but only occasional particles of a segregate phase could be found (Figure 58). On the other hand, examination of the extraction replicas obtained from the fracture surfaces of specimens of this steel in an embrittled condition (heated at 2200°F for 1 hour, cooled to 1500°F and held 4 hours, air-cooled, and aged) revealed a flat, intergranular type of fracture topography and the presence of a high concentration of two types of particles in the fracture surfaces; one type was of a dendritic or platelike shape (Figure 59), whereas the other was smaller and chunkier (Figure 60). Essentially, the same findings were obtained from the other vanadium-bearing steels.

From the results of gross-area (or bulk) electron-diffraction analyses of extraction replicas from steels W-8133-1A and W-8134-1A, the particles were identified as vanadium carbide (VC) and/or vanadium nitride (VN), as shown in Table 28. Since these two compounds evidently are isostructural, with only a relatively small difference in lattice parameters, and because small amounts of both nitrogen and carbon were present in these steels, the more general description, $V(C,N)$, is probably more correct.

Thus, the mechanism of thermal embrittlement in these vanadium-substituted steels is believed to be entirely analogous to that of the conventional titanium-bearing steels.

d. Summary

The substitution of vanadium for titanium, as a supple-
mental strengthening element, did not eliminate the suscepti-
bility of the 18Ni maraging steels to thermal embrittlement.
However, the degree of embrittlement of the steels containing
1.6 percent vanadium, with normal amounts of the other alloying
elements, did appear to be somewhat less than for the commercial
steel and the low-residual titanium-bearing experimental steels;
but it was greater than for the aluminum-substituted steels.
The steels that contained 1 percent vanadium, 4 percent molyb-
denum, and 12 percent cobalt exhibited about the same low levels
of toughness in the embrittled conditions as the commercial
steel, although the strength levels were somewhat higher, possi-
bly because of the higher cobalt content.

The embrittlement in these steels was associated with an
intergranular type of fracture and with the presence of small
particles of vanadium carbonitride, V(C,N), in the fracture
surface of CVN specimens. Evidently, the V(C,N) particles had
precipitated on austenite grain boundaries upon cooling from
2200 or 2300°F and holding at 1500°F. Thus, the mechanism of
the embrittlement is believed to be essentially analogous to
that of the titanium-bearing steels.

4. THE EFFECT OF COLUMBIUM AND TANTALUM ADDITIONS

a. Purpose

Another attempt was made to overcome the sensitivity of
the 18Ni maraging steels to thermal embrittlement by adding other
elements that possibly might have a greater propensity for carbide
and nitride formation than titanium to maraging steels of conven-
tional composition. The two elements chosen for this investiga-
tion were columbium and tantalum. In employing this approach,
it was hoped that (1) the columbium or tantalum would combine
preferentially with the residual amounts of carbon and nitrogen
in the steel and thus preclude the formation of embrittling
films of Ti(C,N) during the various thermal treatments and (2)
the columbium or tantalum carbides and nitrides formed would not
dissolve and reprecipitate as intergranular films, in a manner
analogous to Ti(C,N), during the thermal treatments.

b. Materials and Experimental Work

Three low-residual 18Ni(250) maraging steel laboratory
heats were made by vacuum-induction melting; one contained 0.2

percent columbium (0.2% specified), the second contained 0.21 percent tantalum (0.3% specified), and the third contained no columbium or tantalum and served as a control. The levels of all other alloying and residual elements in these heats were maintained as nearly the same as possible. The chemical compositions of each of these steels is shown in Table 29. The melting practice consisted of making all the standard alloying additions, excepting titanium, adding the specified amount of columbium or tantalum, holding the steel in the furnace crucible for 15 to 20 minutes, then making the titanium addition and pouring. In this way it was hoped that sufficient time would be available for the columbium or tantalum to form carbides and nitrides prior to the addition of the titanium.

Each of these heats weighed 200 pounds and was cast into two 4- by 4-inch ingots, each weighing about 100 pounds. The ingots were subsequently soaked at 2200°F, rolled straightaway at temperatures between 2000 and 1800°F to 1-1/2-inch-thick plates, and spray-quenched. After reheating to 2200°F, the plates were cross-rolled to 1/2-inch thickness, with at least 20 percent reduction in the temperature range 1800 to 1700°F followed by spray-quenching.

Duplicate 0.252-inch-diameter tensile and triplicate impact specimen blanks were prepared, and heat treating was carried out in an argon atmosphere. The thermal cycles employed in the embrittling treatments were selected from among those used in the experiments on the commercial plate as being representative of those that would most likely be encountered in processing and fabricating these steels; they are listed in Table 30.

Extraction replicas were prepared from the fracture surfaces of CVN specimens of each steel in the aged condition after (1) heating at 2200°F for 1 hour and air cooling; (2) heating at 2200°F for 1 hour, cooling to 1500°F and holding for 1/2 hour and air cooling; and (3), heating at 2200°F for 1 hour, cooling to 1500°F and holding for 4 hours at 1500°F, and air cooling. These replicas were examined in the electron microscope, and any particles appearing on them were analyzed by means of electron diffraction.

c. Results and Discussion

The mechanical properties of the three heats (W-8196, W-8197, and W-8198) that resulted from the various thermal treatments are given in Tables 30 to 32. The properties of

39

steel W-8198 of conventional composition are used as the basis
for judging the effects of the columbium addition (steel W-8196),
and the tantalum addition (steel W-8197) on the susceptibility
to thermal embrittlement.

Because of the differences in strength levels (aged
condition) of the three steels after each thermal treatment, it
is difficult to make precise comparisons of the effects of the
different thermal treatments on the resulting toughness levels.
The strength levels of the columbium-bearing steel (W-8196)
were somewhat lower, but the toughness levels were higher than
those of the control steel (W-8198); whereas, the strength
levels of the tantalum-bearing steel (W-8197) were higher, but
the toughness values were lower than for the control steel
(W-8198). In general, it is clear that the addition of columbium
or tantalum did not provide a major improvement in the resist-
ance of the low-residual titanium-bearing maraging steel to
thermal embrittlement when allowances are made for the differences
in strength. Nevertheless, in comparing the results for the
columbium-bearing steel (W-8196) with those for (1) the low-
residual steels (V-8497 and V-8858) discussed earlier, (2) the
1.65 percent vanadium-substituted steels (W-8133-1A and -1C),
and (3) the aluminum-substituted steels (W-8068 and W-8252-1A,
-1B, -1C), it does appear that the columbium addition did have
some beneficial influence on resistance to thermal embrittle-
ment, which was greater than that for vanadium and comparable
to that of aluminum.

Electron-microscope examination of extraction replicas
prepared from the fracture surfaces of CVN specimens of the
columbium-bearing steel (W-8196) showed that, as a result of
heating at 2200°F for 1 hour (plus air cooling and aging), the
topography of the fracture surface changed from dimpled rupture
to a smoother, more intergranular type of fracture, as shown in
Figure 61; nevertheless, few particles of any segregate phase
were noted in the replicas. Replicas of the fracture surfaces
of specimens that had been more severely embrittled (2200°F for
1 hour, cooled to 1500°F and held for 1/2 hour, air cooled, and
aged) exhibited an even smoother surface appearance, and parti-
cles of some segregate phase were clearly evident (Figure 62).
As a result of still further embrittlement (2200°F for 1 hour,
cooled to 1500°F and held for 4 hours, air-cooled, and aged),
the concentration of platelike particles was greater (Figure 63).
Thus, the increased concentration of particles in the fracture
surfaces coupled with a greater tendency toward flat, inter-
granular rupture appeared to be associated with more severe
embrittlement.

40

The fractographic findings (Figures 64 to 66) for the tantalum-containing steel (W-8197), after the same three embrittling treatments, were very similar to those for steel W-8196, except that the concentration of particles in the fracture surfaces of the most embrittled specimens (2200°F for 1 hour, cooled to 1500°F and held for 4 hours, air-cooled, and aged) appeared greater than for steel W-8196 (Figure 66). Essentially these same microscopic fracture features were displayed by broken CVN specimens of the control steel (W-8198), after the same three embrittling treatments, as shown in Figures 67 to 69. These results also indicate, at least semiquantitatively, a correlation between the concentration of particles in the fracture surface, with the associated microscopic fracture features, and the degree of embrittlement.

Electron diffraction analyses of the particles extracted from the fracture surfaces of CVN specimens of the three steels that had been embrittled (2200°F for 1 hour, cooled to 1500°F and held for 4 hours, air-cooled, and aged) revealed that the particles were titanium carbonitride, Ti(C,N), in all cases. The electron-diffraction data obtained from the three steels is presented in Table 33, together with the standard data for titanium carbide (TiC) and titanium nitride (TiN). The interplanar spacings for steels W-8196 and W-8197 seem to match those of TiC more closely than those of TiN, whereas the reverse situation appears to be true for the control steel (W-8198); however, this difference may not be significant, and, as discussed earlier in this report, the more general identification as Ti(C,N) is probably more correct.

The diffraction rings in the patterns obtained were spotty and of low intensity, particularly for the columbium-bearing steel (W-8196). Furthermore, there appeared to be some preferred orientation of the particles in the replica and fracture surface such that a [111] direction in the crystal lattice of Ti(C,N) was normal to the plane of the platelets and to the fracture surface. These observations would account for the absence of the (200) and (400) reflections in the pattern of steel W-8196, and possibly the absence of the (400) reflection in steel W-8198. There was no evidence in the diffraction patterns of any carbide or nitride of columbium or tantalum, and since these patterns originated from particles covering a relatively large area of the fracture surface, it is concluded that such carbides or nitrides were not present.

In view of these findings, it appears that sufficient amounts of uncombined carbon and nitrogen remained available in

41

these steels to permit formation of some Ti(C,N) during the thermal
embrittling treatments despite the presence of columbium or
tantalum. Evidently titanium has a greater propensity for com-
bination with ¬arbon and nitrogen in the austenite of these
steels than columbium or tantalum. The beneficial influence of
columbium in increasing the resistance of the steel to thermal
embrittlement might be explained by postulating that (1) some
of the residual carbon and/or nitrogen in the molten steel had
combined with columbium during the steelmaking and (2) the
resulting carbides and nitrides, which remained in the solid
steel, were sufficiently massive and stable that they did not
redissolve appreciably during the thermal embrittling treat-
ments, so that the amounts of nitrogen and carbon available for
recombination with titanium were thus reduced. Such massive
particles in low concentrations would not be expected to have
much influence on toughness.

d. Summary

The addition of a small amount (0.2%) of columbium or
tantalum to a low-residual 18Ni maraging steel of otherwise
conventional composition did not effect a major improvement in
the resistance of the steel to thermal embrittlement. The
columbium addition, however, did significantly reduce the degree
of embrittlement; in this respect, it was more effective than
the substitution of 1.6 percent vanadium for titanium and compa-
rable in its effect to the substitution of 0.4 percent aluminum
for titanium.

Fractographic investigation revealed that, as the
embrittlement became more severe in these steels, the micro-
scopic fracture topography changed from dimpled rupture to a
more intergranular type of fracture, and concomitantly the
concentration of segregate phase particles in the fracture
surface increased. The particles were identified as Ti(C,N) by
means of electron diffraction. The concentration of Ti(C,N)
particles in the fracture surfaces of CVN specimens of the
columbium-bearing steel, that had been thermally embrittled,
was considerably less than for the tantalum-bearing steel or
for the control steel; this was particularly true for the most
severely embrittled condition.

Thus, the addition of columbium or tantalum to a low-
residual 18Ni maraging steel did not preclude the formation
of Ti(C,N) during the thermal treatments nor eliminate the
consequent embrittlement. But the addition of columbium did
result in somewhat less embrittlement, possibly by combining

42

with some of the residual carbon and nitrogen in the steel to form rather massive, stable carbides and nitrides that were not deleterious to toughness and which reduced the amounts of carbon and nitrogen available for Ti(C,N) precipitation during the thermal embrittling treatments.

5. THE EFFECT OF SILICON

a. Purpose

It has been known, from the early development work on the 18Ni maraging steels, that an excessive amount of residual silicon impairs their ductility and toughness. For this reason, an upper limit of 0.10 percent was imposed on the residual silicon content of the commercial steels. In view of this influence of silicon, it was considered desirable to investigate the effects of still lower silicon contents on the ductility and notch toughness of the 18Ni(250) maraging steel, and on its susceptibility to thermal embrittlement, in the "absence" of possible interfering effects of other residual elements. For this investigation, three 18Ni(250) maraging steels of the same conventional alloy composition were prepared, having different silicon contents, and low levels of the other residual elements.

b. Materials and Experimental Work

A 300-pound vacuum-induction-melted heat of 18Ni(250) maraging steel, of conventional alloy composition but having low levels of residual elements, was split into three ingots having different silicon contents (0.017, 0.056, and 0.11%, respectively); the silicon level was adjusted by controlled additions of silicon, just prior to pouring each ingot. The chemical compositions of the three steels are given in Table 34. The 4- by 4-inch ingots were rolled to 1/2-inch-thick plate, using the same rolling schedule as for the other experimental steels previously discussed. The plate materials were heat-treated according to the several cycles listed in Table 35; the high-temperature heating (2200 or 2300°F) was carried out in an argon atmosphere. Mechanical properties were determined from duplicate tension test specimens (0.252 inch diameter), and from triplicate CVN test specimens. Extraction replicas were prepared from the fracture surfaces of the CVN specimens by the technique described earlier, and these were examined by means of electron microscopy, and analyzed by electron diffraction.

43

c. Results and Discussion

The mechanical properties of the three steels, that
resulted from the various thermal treatments, are recorded in
Tables 35 to 37. A comparison of the properties of the three
steels, in the rolled-and-aged condition and in the annealed-
and-aged condition, shows that the silicon content within the
range of low silicon levels investigated had no significant
effect on strength, ductility, or notch toughness. After the
various thermal embrittling treatments, the notch toughness of
all three steels in the aged condition was very poor, ranging
from 3 to 8 ft-lb, but the lower silicon steels did have the
higher values; the accompanying decreases in strength also
tended to be somewhat smaller for the lowest silicon steel
(W-8202-A). Thus, lowering the silicon content by a factor of
about 7 slightly improved the resistance of the steel to thermal
embrittlement.

Electron-microscope examination of extraction replicas
of the fracture surfaces of CVN specimens of the three steels
that had been subjected to the same embrittling treatment
(2200°F for 1 hour, cooled to 1500°F and held for 4 hours, air-
cooled, and aged) revealed that the microscopic fracture topog-
raphy was predominantly intergranular, and that the fracture
surfaces contained many small particles of a segregate phase,
as shown in Figures 70 to 72. The concentration of these
particles was greater for the two steels of higher silicon
content (W-8202-B and W-8202-C), as might be expected in view
of the lower notch-toughness values obtained from these two
steels in comparison to those for the steel of lowest silicon
content (W-8202-A). The results of electron-diffraction
analyses of the particles in these replicas (Table 38) showed
that they were titanium carbonitride, $Ti(C,N)$; for two of the
steels, there also was evidence of the presence of minor amounts
of titanium sulfide ($\tau-Ti_2S$).

3. Summary

Reduction of the silicon content (from 0.11 to 0.017%)
of an 18Ni(250) maraging steel, of low-residual element content
but of conventional alloy composition, did not significantly
change the strength or toughness of the steel in the as-rolled—
and-aged condition, or in the annealed-and-aged condition, nor
did it provide a major increase in the resistance of the steel
to thermal embrittlement. The lowest silicon steel (0.017%
silicon) exhibited somewhat better toughness after the embrit-
tling treatments than did the two higher silicon steels (0.056

44

and 0.11% silicon), and fractographic investigation revealed
that fewer particles of the embrittling constituent, Ti(C,N),
were present in the fracture surface of the CVN specimen of
this steel.

If it is assumed that the somewhat better resistance of
the lowest silicon steel to thermal embrittlement can be properly
attributed to its low silicon content, then it is difficult to
understand the effect; it does appear from the fractographic
evidence, that the precipitation of the embrittling Ti(C,N) phase
was inhibited, in some manner, by reduction of the silicon
content to 0.017 percent. The mechanism of such an effect must
be quite complex.

6. THE EFFECT OF CERIUM

a. Purpose

In common with other residual elements, sulfur is believed
to have an adverse influence on the toughness of the 18Ni maraging
steels, and so an upper limit of 0.010 percent sulfur has been
recommended for the commercial steels. Furthermore, in work
previously mentioned in this report and in other related research
by this laboratory, particles of titanium sulfide occasionally
have been found in the fracture surfaces of embrittled CVN
specimens although in much smaller quantities than the main
embrittling Ti(C,N) precipitate. The reduction of residual sulfur
in these steels during steelmaking to sufficiently low levels to
preclude formation of this sulfide is not feasible commercially
and is difficult to achieve in the laboratory.

Another approach to the problem would be to add small
amounts of other elements which might preferentially combine
with the sulfur to form sulfides in a form that would not
adversely influence the toughness of the steel and would preclude
formation of the titanium sulfide particularly during the thermal
embrittling treatments. In some earlier experiments carried out
in this laboratory, manganese in amounts up to 0.5 percent, which
is considerably above the upper limit (0.10%) normally specified
for this residual element, were added to 18Ni maraging steels of
conventional composition for this purpose. However, no signifi-
cant effect, either beneficial or harmful, could be found. More
recently, the experiment was tried again for steels containing
aluminum in place of titanium as the supplemental strengthening
element; as reported in an earlier section, no influence of the
higher manganese content could be clearly discerned. Still
earlier efforts comprised adding mixtures of rare earth elements,

or lanthanum metal, to molten baths of 18Ni maraging steel, to promote formation of stable sulfides of these elements and so metallurgically isolate the sulfur and preclude its participation in solid-state reactions (such as τ-Ti$_2$S formation) during thermal treatments. These experiments likewise were unsuccessful, even though special precautions were taken to avoid loss of the rare earth elements by oxidation during the steelmaking.

As a further attempt to render the residual sulfur in these steels innocuous, through combination with a strong sulfide-forming element, it was decided in the present program to add small amounts of cerium metal to the molten steel. For this purpose, three laboratory heats were prepared of 18Ni(250) maraging steel of normal alloy composition and low-residual element content except for sulfur (which ranged from 0.004 to 0.010%) and the intended cerium additions of 0.15 and 0.5 percent to two of the steels (the third steel containing no cerium was the comparison standard).

b. Materials and Experimental Work

The three 200-pound heats of 18Ni(250) maraging steel were induction-vacuum-melted in the normal manner, except that the titanium addition was withheld in making each of the two cerium-bearing heats until the cerium addition was made and the heat was allowed to stand for 30 minutes to promote mixing and reaction of the cerium; finally, the titanium addition was made and the heat was poured into two 4- by 4-inch 100-pound ingots. The compositions of the three steels are given in Table 39. It was surprising to find that very little of the cerium added to heats W-8199 and W-8200 remained in the solid steel, despite precautions taken to prevent its loss by oxidation during steelmaking; presumably, some of the cerium may have reacted with sulfur (e.g., W-8200) and the sulfides floated out of the molten steel, and some may have been lost by vaporization (the boiling point of cerium at atmospheric pressure is 2550°F).

Nevertheless, the plan was to roll the ingots to 1/2-inch-thick plate according to the same rolling schedule used for the previously discussed experimental steels. However, the ingots of heat W-8200 (0.04% cerium) broke up in the early rolling passes, and the ingots of heat W-8199 (<0.01% cerium) cracked during rolling. Therefore, a short investigation was made to determine whether cerium actually was the cause of the hot-shortness.

46

c. Results and Discussion

The cerium used in making steels W-8199 and W-8200 was
analyzed and found to be 99.85+ percent pure—the principal
impurities found by spectographic analysis were manganese
(<0.01%), iron (0.016%), magnesium (0.11%), and silicon and
copper (each <0.01%). These impurities would not be expected
to result in hot-shortness, and consequently the small amounts
of cerium remaining in the steels appeared to be the cause.

Low-magnification examination of the fragments of the
rolled ingot of steel W-8200 showed that the fractures were
completely intergranular, as shown in Figure 73. Examination
of a metallographically prepared section of one of these fragments
revealed a "picture-frame" border completely surrounding the prior
austenite grains (Figure 74). This appearance strongly suggested
that gross, grain-boundary segregation of some element, very
probably cerium, had occurred, and so electron-microprobe scanning
analyses were made across these grain boundary regions. Definite
evidence was obtained of such segregation; the cerium contents
within the dark borders ranged from 4 to 11 percent. Similar
scans for other alloying and residual elements that were known
to be present in the steel, particularly for sulfur, did not show
a concomitant segregation of another element. In view of the
very limited solid solubility of cerium in iron at low tempera-
tures, it is quite likely that the segregated cerium was present
at the boundaries in the form of a low-melting (1200°F) eutectic
with iron.

Since these results indicated that cerium, even in very
small amounts, causes extreme hot-shortness in these steels, no
further attempt was made to pursue this approach to the problem
of eliminating titanium sulfide formation.

d. Summary

An experiment in which small amounts of cerium were added
to an 18Ni(250) maraging steel of normal alloy composition and
low-residual element content for the purpose of preferentially
combining with the residual sulfur to form stable sulfides that
would not impair toughness (especially during embrittling thermal
treatments) was not successful. Most of the intended cerium
additions were lost during steelmaking, possibly by vaporization,
and the small amounts of cerium remaining in the steels caused
such severe hot-shortness that the ingots could not be satisfac-
torily rolled to plate.

47

IV.   CONCLUSIONS

(1)   Severe embrittlement, in both the unaged and aged conditions, was induced in commercially produced 18Ni(250) maraging steel plate by heating at temperatures above 2000°F, followed by slow cooling, or interrupted cooling and holding, in the temperature range of 1500 to 1800°F. The degree of embrittlement increased with (1) the temperature of the high-temperature anneal, (2) the temperature of the intermediate anneal, and (3) the holding time at the intermediate temperature. The most severe embrittlement (CVN energy of about 5 ft-lb) resulted from annealing for 1 hour at temperatures in the range 2200 to 2400°F, cooling to an intermediate temperature in the range 1500 to 1800°F and holding for 4 hours, air cooling to room temperature, and aging at 900°F for 3 hours.

(2)   The source of the embrittlement has been found to be the copious solid-state precipitation of minute, platelike particles of the intermetallic compound Ti(C,N) preferentially along austenite grain boundaries at the intermediate annealing temperatures. The marked austenite grain growth that occurred during heating at 2200 to 2400°F is believed to have been an important contributing factor. A mechanism of thermal embrittlement has been postulated that is based on these findings. Small amounts of τ-Ti$_2$S also were found occasionally in the fracture surfaces of embrittled CVN specimens, but they are not considered to be an important factor in the embrittlement.

(3)   Reduction of the residual carbon content of the 18Ni(250) maraging steel to a very low level (about 0.004%) considerably improved the notch toughness of the steel in the conventionally annealed condition (1500°F for 1 hour) and in the annealed-and-aged condition. Nevertheless, the degree of embrittlement (CVN energy of 6 ft-lb), that resulted from heating at 2200°F for 1 hour, cooling to 1500°F and holding for 4 hours, air cooling to room temperature, and aging at 900°F for 3 hours, was just as severe as for a low-residual, companion, experimental heat of higher carbon content (0.027%) or a commercial plate steel (0.015% carbon). Many particles of Ti(C,N) also were found in the fracture surfaces of thermally embrittled CVN specimens of the low-carbon steel although in somewhat lower concentration than for the higher carbon steels. Evidently a carbon content as low as 0.004 percent is still sufficient to cause severe embrittlement through precipitation of Ti(C,N).

48

at austenite grain boundaries when the austenite grain size
of the steel has grown as large as ASTM No. -3.

(4) The substitution of aluminum for titanium, as the supple-
mental strengthening element in 18Ni(250) maraging steel of
low-residual element content (0.001 to 0.003% carbon)
considerably improved the resistance of the steel to thermal
embrittlement. This reduced susceptibility was observed for
steels of different strength levels (yield strengths of 225
to 283 ksi) that contained 0.2, 0.4, or 1.0 percent aluminum
and was particularly notable in the unaged condition. How-
ever, the substitution of aluminum for titanium in a steel
having a higher carbon content (0.018%) did not result in
improved resistance to thermal embrittlement. In the
embrittled steels of low-carbon content, a precipitate of
AlN particles was found in the fracture surfaces of CVN
specimens; thus, the mechanism of embrittlement appeared to
be analogous to that operative in the titanium-bearing
steels, although the degree of embrittlement was less. For
the steel of higher carbon content, greater amounts of pre-
cipitate were observed in the fracture surfaces of embrittled
CVN specimens; two types of particles were identified—
AlN and Mo_2C. The more severe embrittlement of the higher
carbon steel is attributed to the presence of the additional
Mo_2C precipitate on austenite grain boundaries.

(5) The addition of 0.1, 0.2, or 0.3 percent manganese to a
low-residual steel containing 0.4 percent aluminum did not
alter the resistance of the steel to thermal embrittlement.
The objective was to promote combination of the residual
sulfur in the steel with manganese to form innocuous manga-
nese sulfide particles in place of iron or titanium sulfides
that might have a deleterious effect on notch toughness and
resistance to thermal embrittlement. The absence of an
effect of the manganese addition indicated that the small
amounts of residual sulfur in these steels did not have an
important influence on embrittlement.

(6) A subsidiary investigation of the effects of different
aging treatments on the strength and toughness of two of
the aluminum-substituted steels revealed that superior
combinations of properties could be obtained by utilizing
shorter aging times (1 to 3 hours) at 900°F after conven-
tional annealing at 1500°F for 1 hour than the aging time
(6 hours) employed in the thermal embrittlement experiments.
The selection of the 6-hour aging time was based on pre-
liminary aging experiments, with hardness as the sole

49

criterion. A CVN energy level of 50 ft-lb (at a yield strength of 237 ksi) was obtained in one of the steels by aging at 900°F for 3 hours. The influence of the shorter aging times on the thermal embrittlement results was not determined.

(7) The substitution of 1.0 or 1.6 percent vanadium for titanium, as a supplemental strengthening element, was not effective in reducing the susceptibility of the 18Ni(250) maraging steel to thermal embrittlement. The embrittlement was associated with an intergranular type of fracture and with the presence of small particles of V(C,N) in the fracture surfaces of CVN specimens. Evidently, these particles precipitated on austenite grain boundaries upon cooling from 2200 or 2300°F and holding at 1500°F. Thus, the mechanism of embrittlement appears to be essentially the same as that for the titanium-bearing steels.

(8) The addition of a small amount (0.2%) of columbium or tantalum to a low-residual 18Ni(250) maraging steel of otherwise conventional composition did not effect a major improvement in the resistance of the steel to thermal embrittlement. The columbium addition, however, did significantly reduce the degree of embrittlement, and was nearly as effective as the substitution of 0.4 percent aluminum for titanium. The embrittlement was associated with an intergranular type of fracture, and the presence of Ti(C,N) particles in the fracture surfaces. It is speculated that the columbium formed massive, stable carbides and/or nitrides which reduced the amounts of carbon and/or nitrogen available for Ti(C,N) precipitation during the thermal embrittling treatments.

(9) Reduction of the silicon content (from 0.11 to 0.017%) of an 18Ni(250) maraging steel of low-residual element content but of conventional alloy composition did not significantly change the strength or toughness of the steel in the rolled-and-aged condition, or in the annealed-and-aged condition, nor did it provide a major increase in the resistance of the steel to thermal embrittlement. The lowest silicon steel (0.017% silicon) exhibited somewhat better toughness after the embrittling treatments than did the two higher silicon steels (0.056 and 0.11% silicon), and fewer particles of the embrittling constituent Ti(C,N) were found in the fracture surfaces of the CVN specimens of this steel.

50

(10) An experiment in which small additions of cerium were added to an 18Ni(250) maraging steel of normal alloy composition and low-residual element content for the purpose of perferentially combining with the residual sulfur (0.004 to 0.010%) to form stable sulfides that would not impair toughness, especially during embrittling thermal treatments, was not successful. Most of the intended cerium additions were lost during steelmaking, possibly by vaporization, and the small amounts of cerium remaining in the steels caused such severe hot-shortness that the ingots could not be satisfactorily rolled to plate.

(11) The beneficial influence on toughness and resistance to thermal embrittlement obtained by substituting aluminum (0.2 to 1.0%) for titanium in 18Ni(250) maraging steel of low-carbon content, and similar improvements effected by adding 0.2 percent columbium to 18Ni(250) maraging steel of conventional alloy composition and low-carbon content may be additive, judging from the results of the metallographic investigations performed on the embrittled specimens. This attractive possibility should be explored by evaluating the mechanical properties and resistance to thermal embrittlement of experimental 18Ni(250) maraging steels of low-carbon content that would contain aluminum in place of titanium and small amounts of columbium; still further improvements might be expected by utilizing shorter-than-normal aging times (1 to 3 hours) at 900°F for these steels.

REFERENCES

1. C. J. Novak, "Isothermal Embrittlement of Maraging Steel,"
    Fourth Maraging Steel Project Review, Dayton, Ohio,
    sponsored by U. S. Air Force Materials Laboratory, June 9-11,
    1964.

2. G. E. Pellissier, "The Physical Metallurgy and Properties
    of Maraging Steels," DMIC Report 210 entitled, "Problems
    in the Load Carrying Application of High-Strength Steels,"
    October 26-28, 1964.

3. B. G. Reisdorf, A. J. Birkle, and P. H. Salmon Cox, "An
    Investigation of the Mechanical Properties and Microstruc-
    tures of 18Ni(250) Maraging Steel Weldments," Technical
    Report AFML-TR-64-364, November 1965.

4. C. J. Novak and L. M. Diran, "Influence of Residual Elements
    in Maraging Steels," Proceedings of the Electric Furnace
    Conference 20, 1962, p. 294.

5. W. F. Brown, Jr., and J. E. Srawley, "Current Status of
    Plane Crack Toughness Testing," (Rough Draft) Presented to
    Subcommittee I of ASTM Committee E-24, February 1, 1966,
    Report No. NASA-TM-X-52209.

6. W. B. Pearson, "A Handbook of Lattice Spacings and Structures
    of Metals, Pergamon Press, New York, 1958, p. 960.

7. C. J. Barton, J. M. Chilton, and B. G. Reisdorf, "Investiga-
    tion of Thermal Embrittlement in 18Ni(250) Maraging Steel,"
    U. S. Steel Applied Research Laboratory Second Quarterly
    Progress Report No. 89.025-029(2) dated March 31, 1966,
    Contract Nr. AF 33(615)-2780.
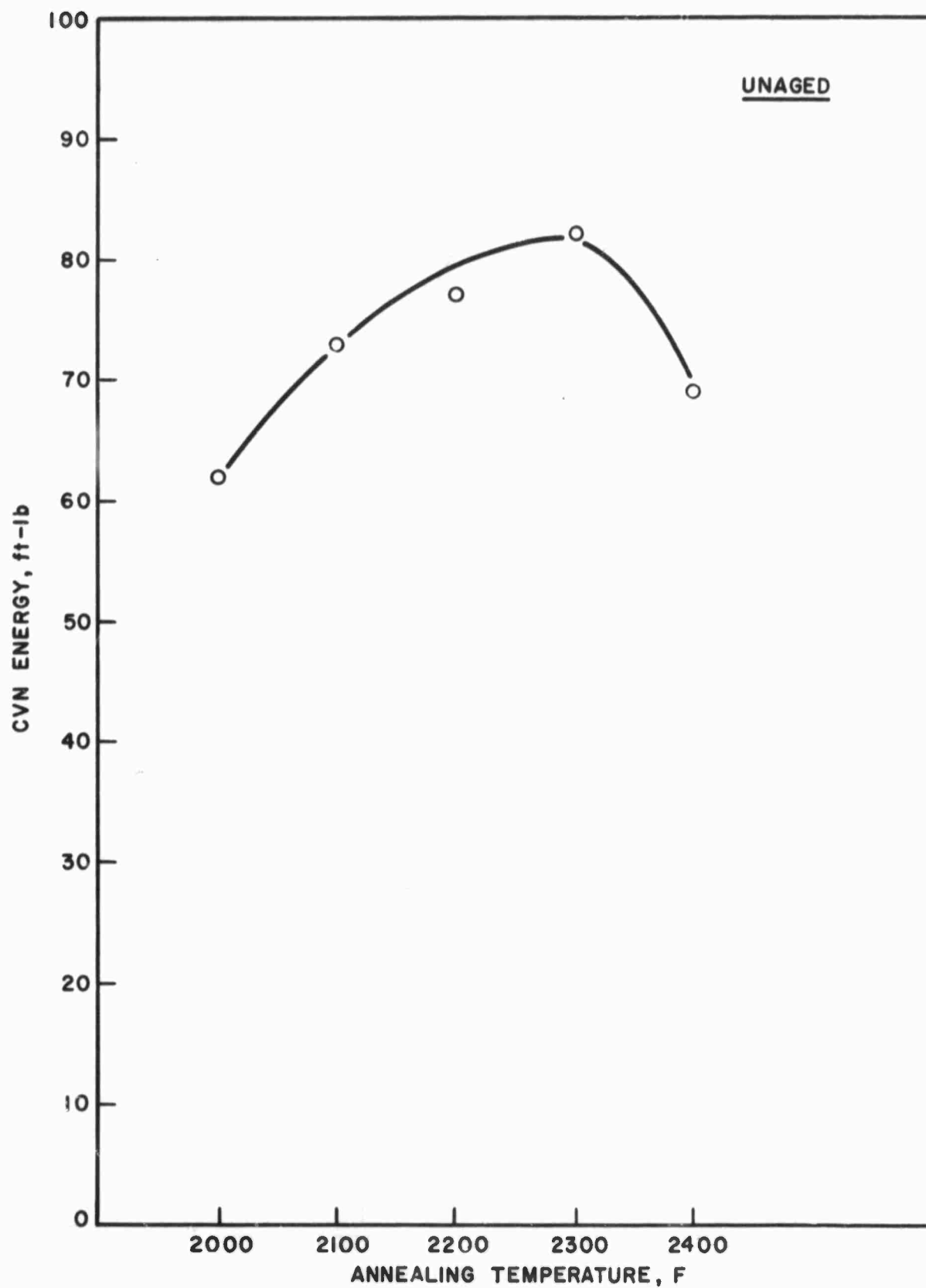
Figure 1. Effect of High-Temperature Annealing on
Notch Toughness of Unaged Specimens;
CVN Energy as a Function of Temperature.

53
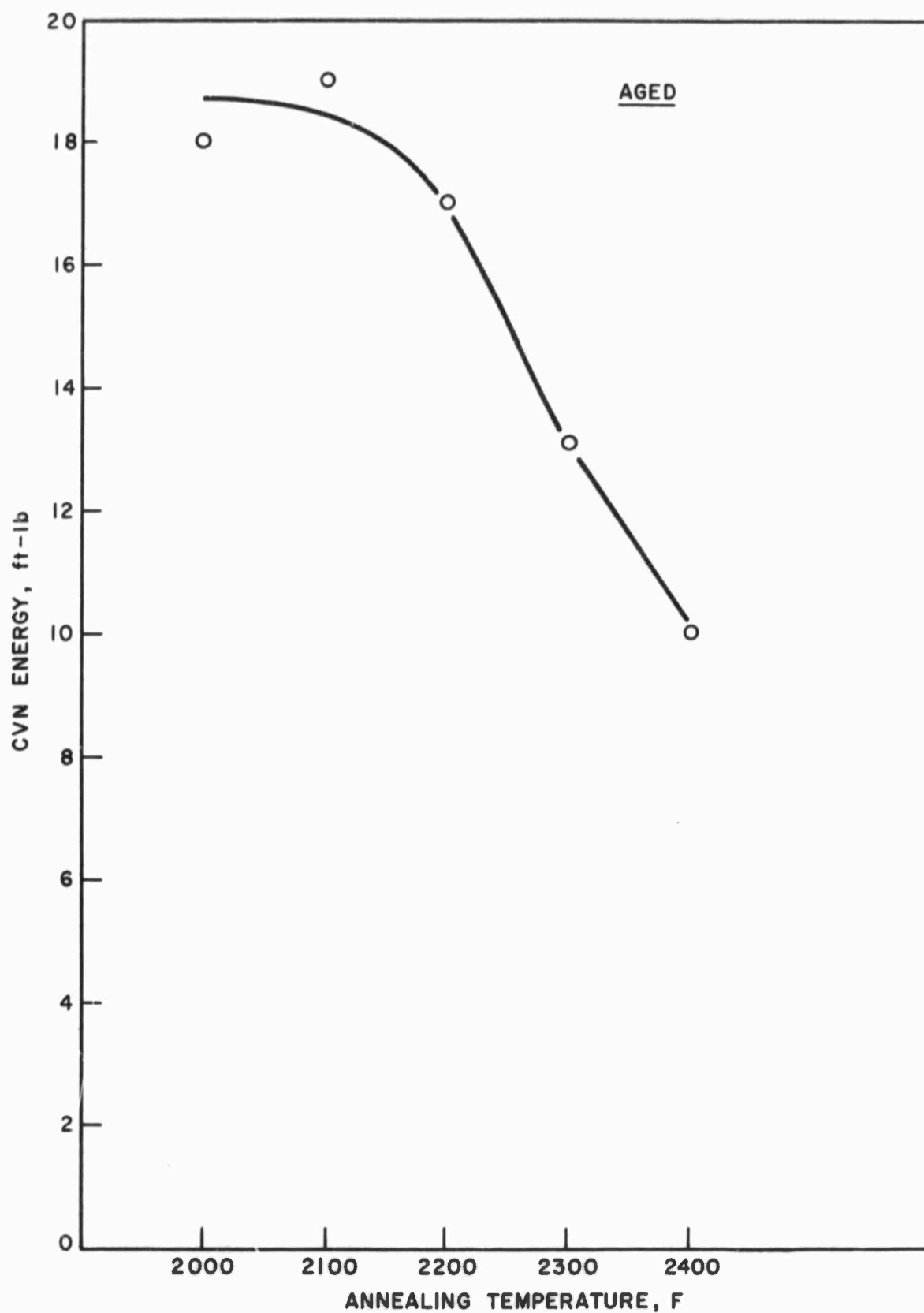
Figure 2. Effect of High-Temperature Annealing
on Notch Toughness of Aged Specimens;
CVN Energy as a Function of Temperature.

54
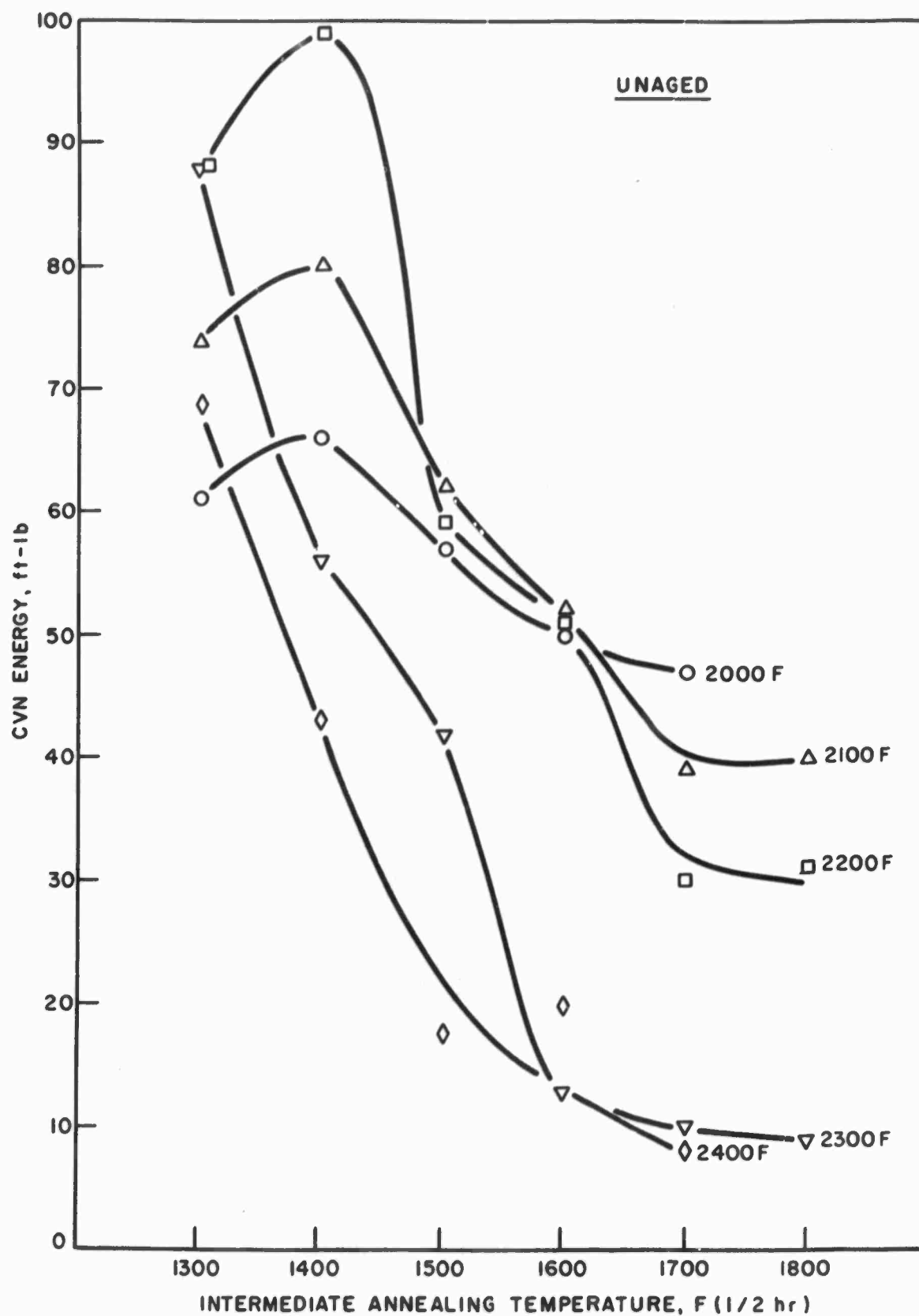
Figure 3. Effects of Combined Annealing Treatments on Notch Toughness of Unaged Specimens; CVN Energy as a Function of Intermediate Annealing Temperature (1/2 hour).
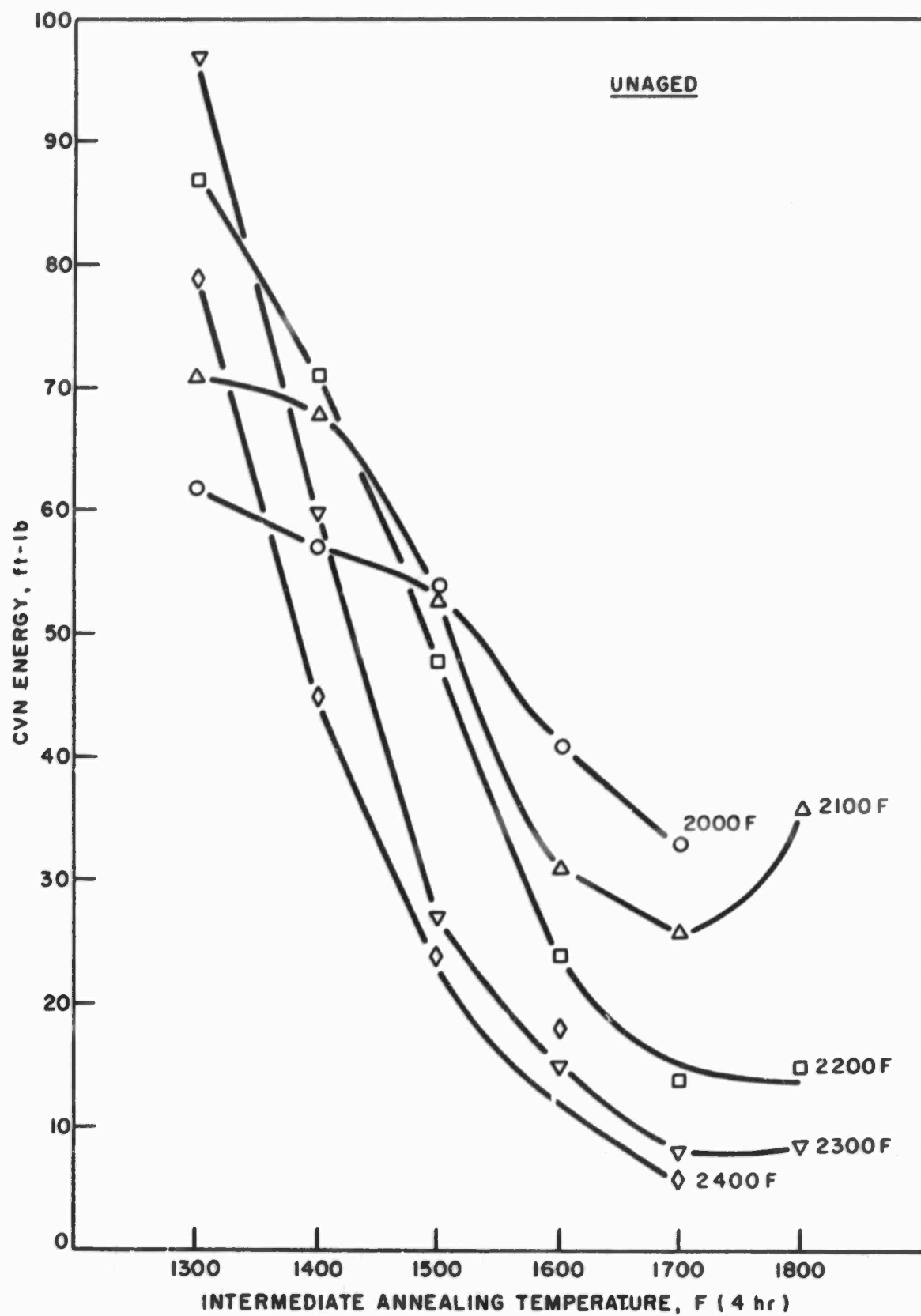
Figure 4. Effects of Combined Annealing Treatments on Notch Toughness of Unaged Specimens; CVN Energy as a Function of Intermediate Annealing Temperature (4 hours).

56
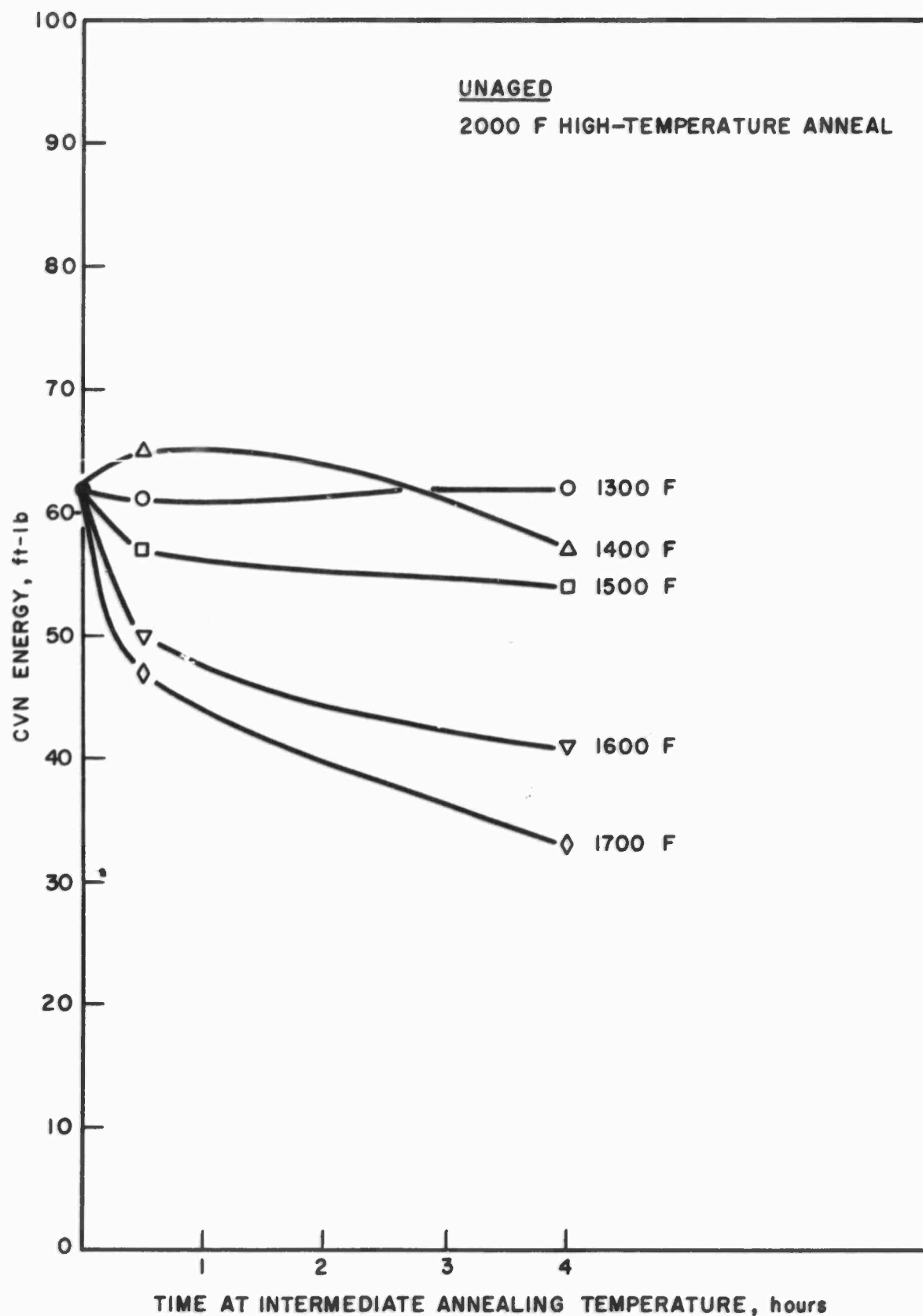
Figure 5. Effect of Time at Intermediate Annealing Temperatures on Notch Toughness of Unaged Specimens After a High-Temperature Treatment of 1 Hour at 2000°F.
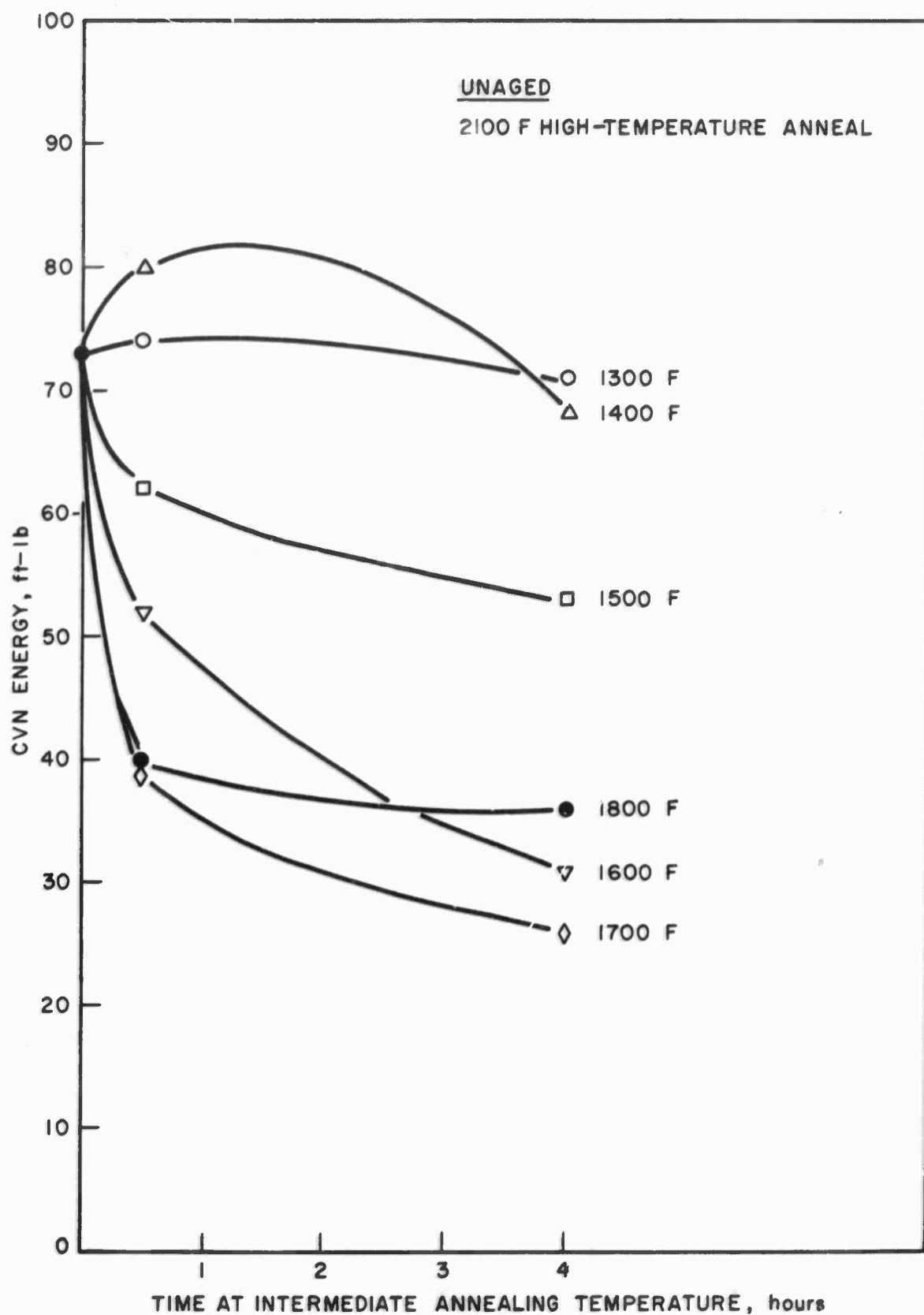
Figure 6. Effect of Time at Intermediate Annealing Temperatures on Notch Toughness of Unaged Specimens After a High-Temperature Treatment of 1 Hour at 2100°F.

58
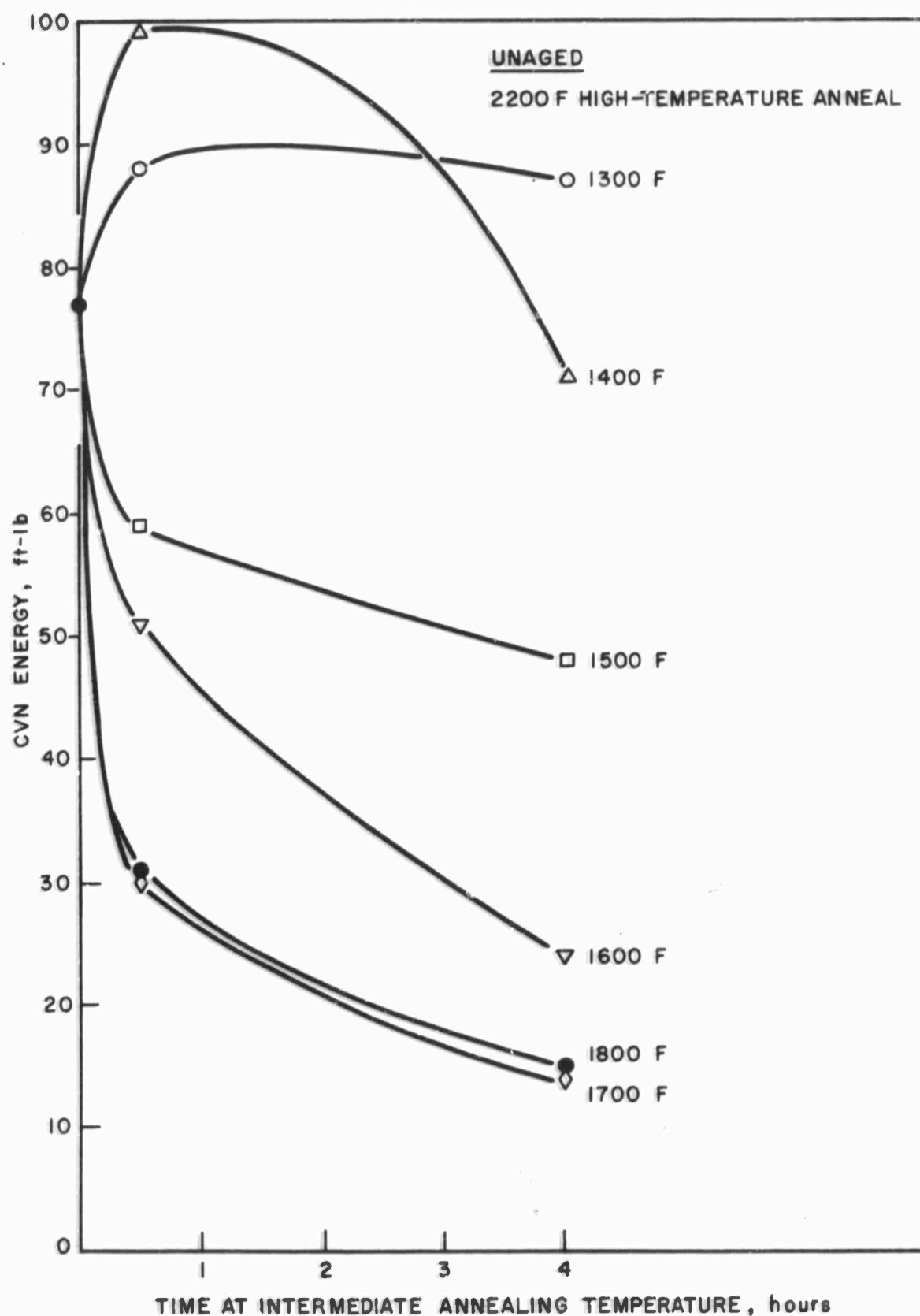
Figure 7. Effect of Time at Intermediate Annealing Temperatures on Notch Toughness of Unaged Specimens After a High-Temperature Treatment of 1 Hour at 2200°F.

59
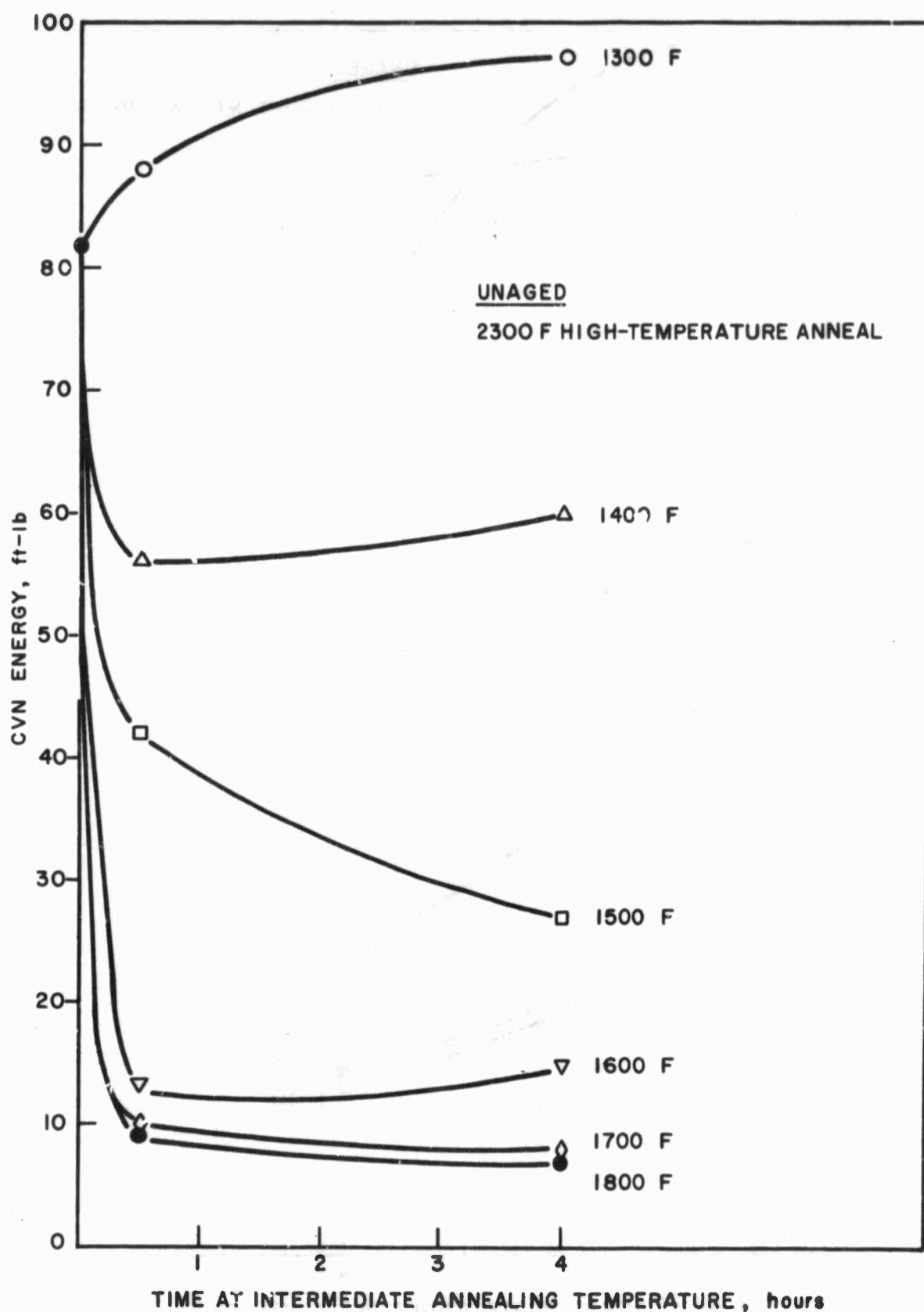
Figure 8. Effect of Time at Intermediate Annealing Temperatures on Notch Toughness of Unaged Specimens After a High-Temperature Treatment of 1 Hour at 2300°F.

60
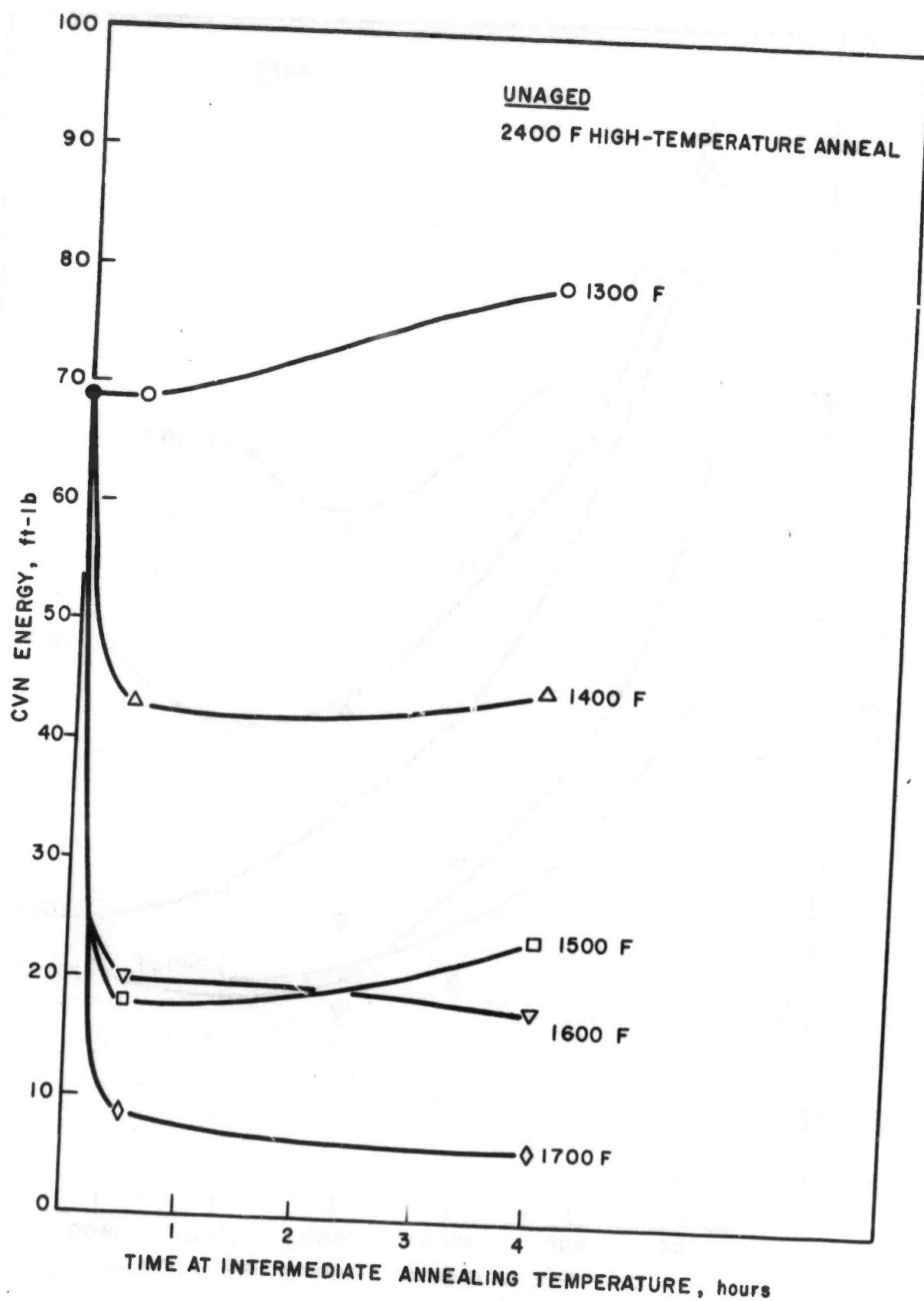
Figure 9. Effect of Time at Intermediate Annealing Temperatures on Notch Toughness of Unaged Specimens After a High-Temperature Treatment of 1 Hour at 2400°F.

61
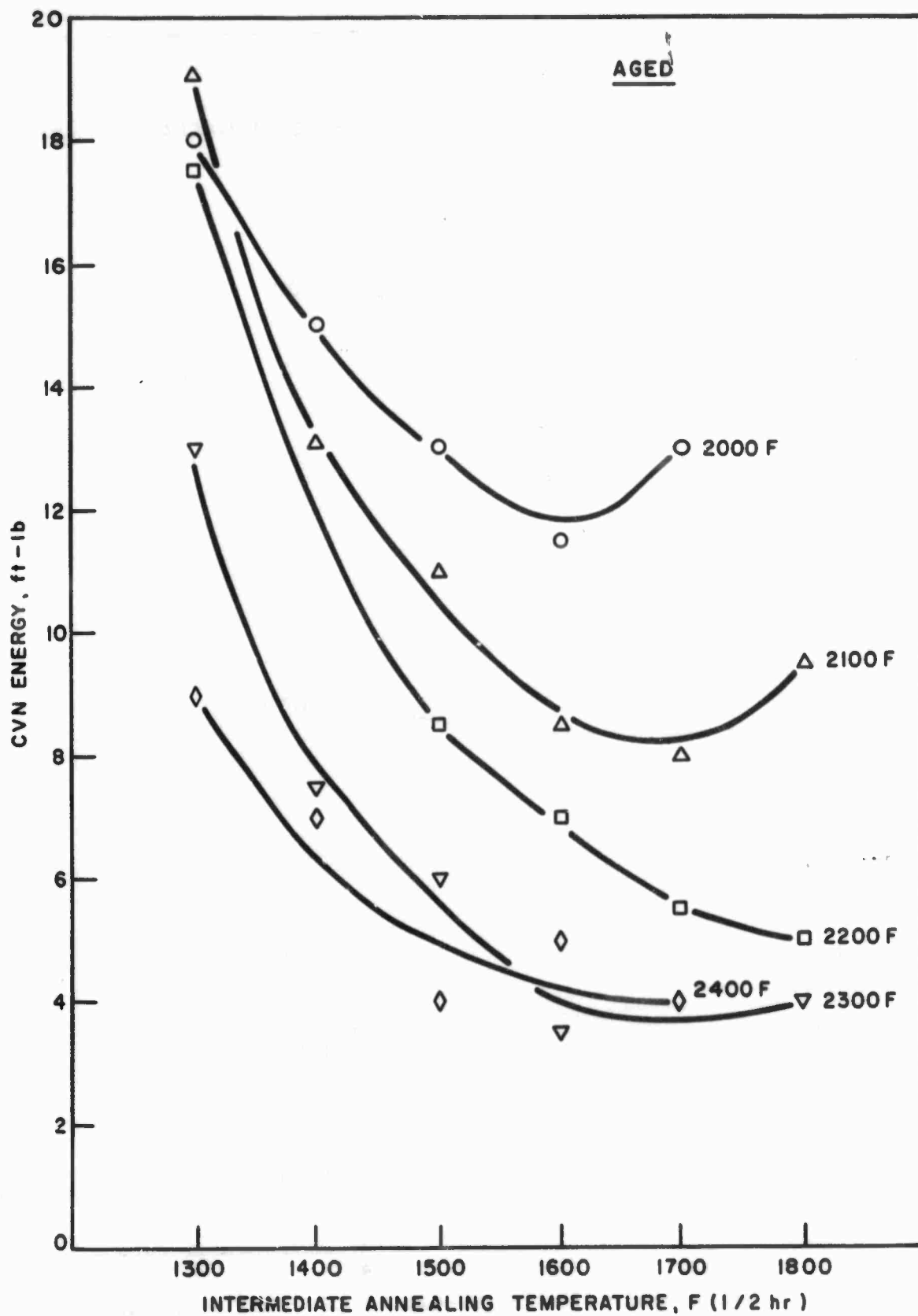
Figure 10.   Effects of Combined Annealing Treatments
on Notch Toughness of Aged Specimens;
CVN Energy as a Function of Intermediate
Annealing Temperature (1/2 hour).
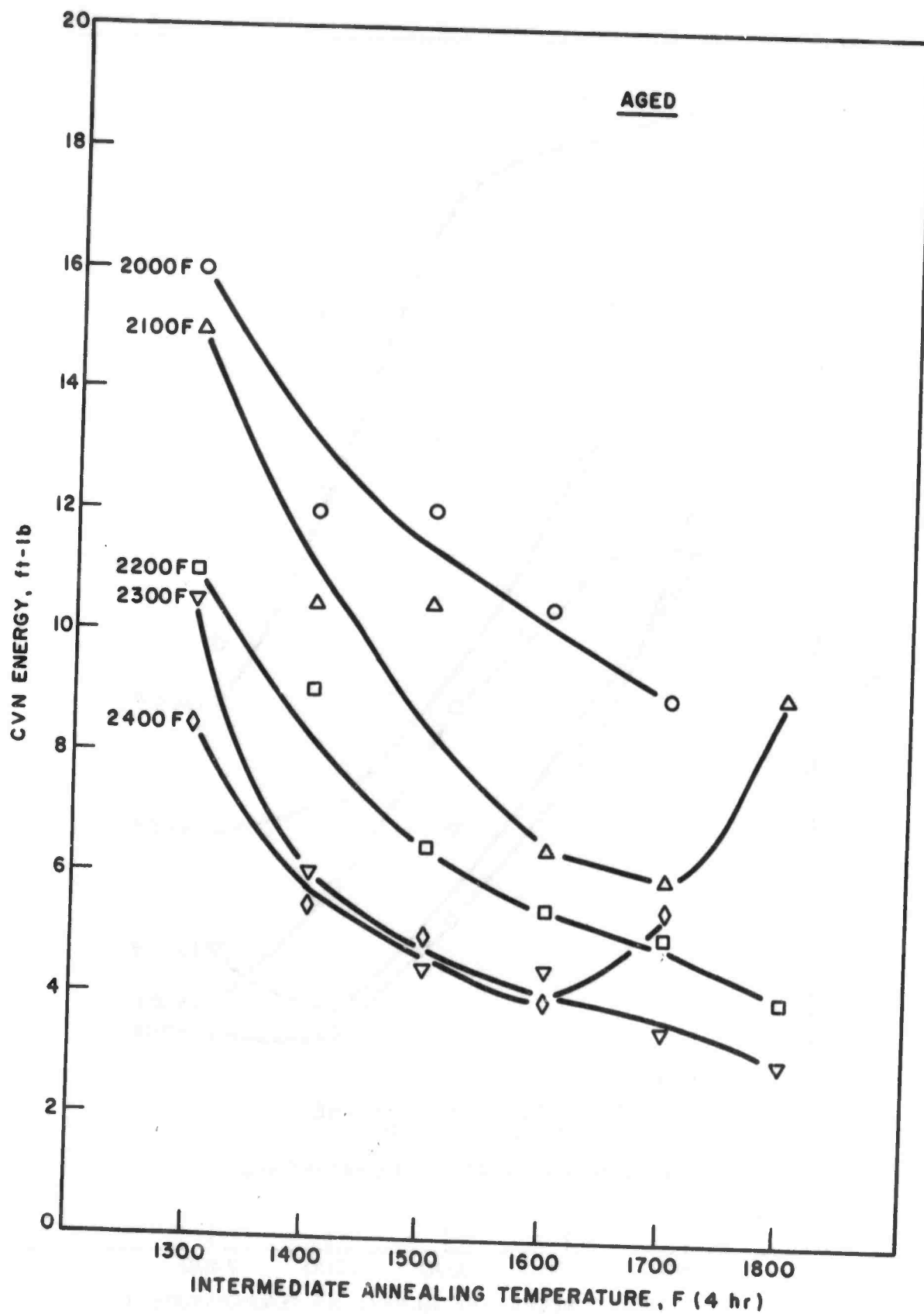
Figure 11. Effects of Combined Annealing Treatments on Notch Toughness of Aged Specimens; CVN Energy as a Function of Intermediate Annealing Temperature (4 hours).

63
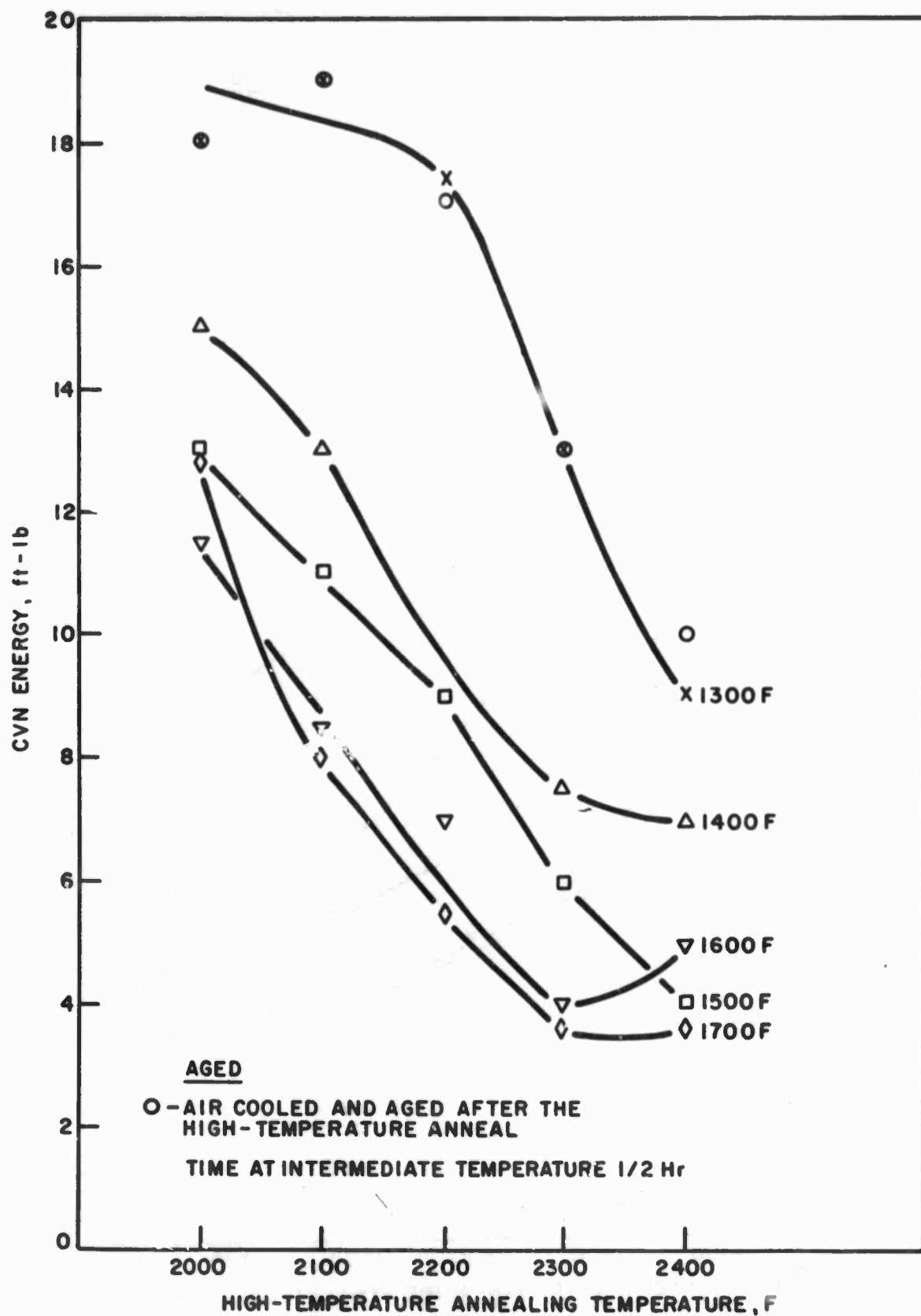
Figure 12. Effects of Combined Annealing Treatments on Notch Toughness of Aged Specimens; CVN Energy as a Function of High-Temperature Annealing Temperature.

64
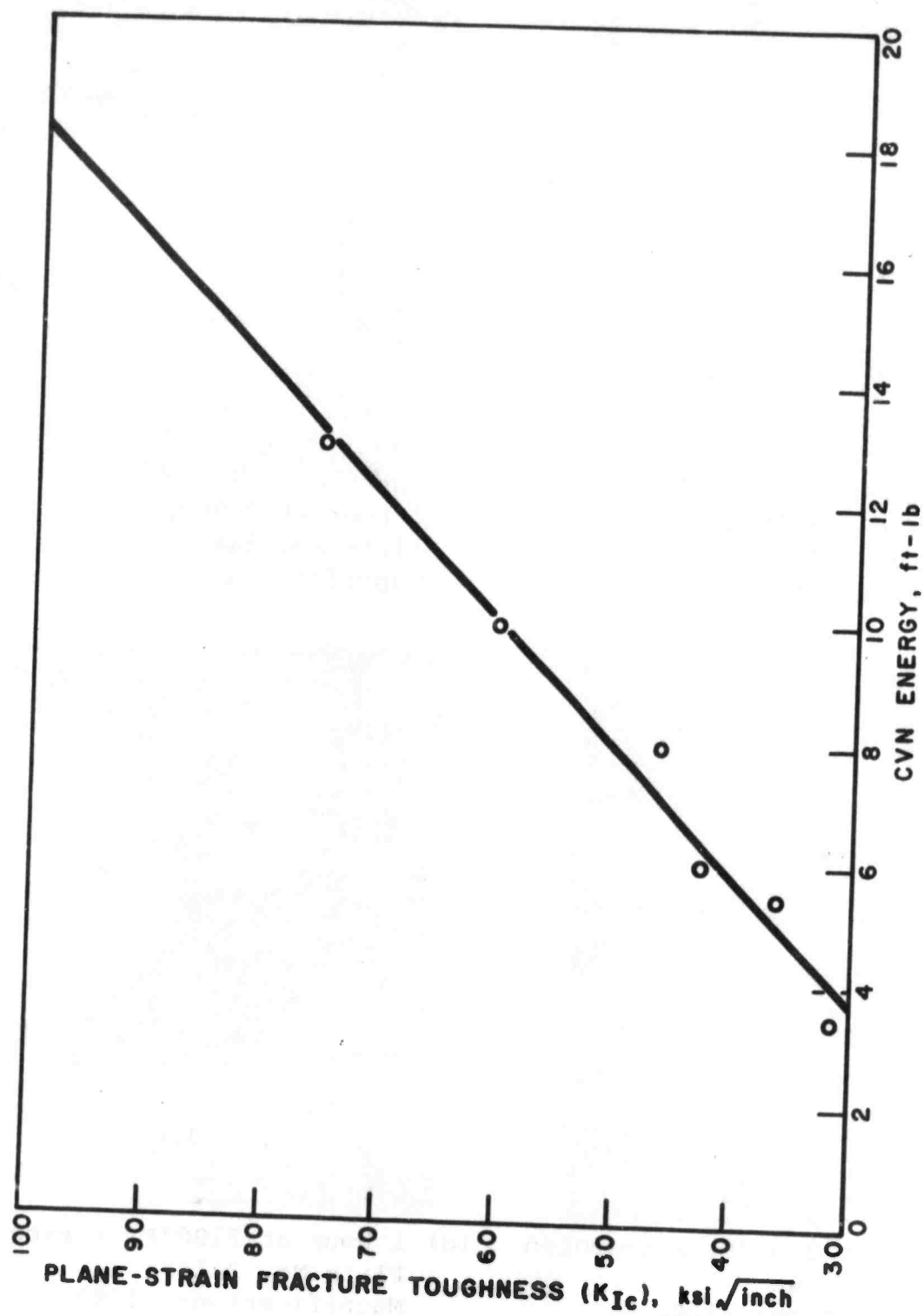
Figure 13. Correlation of Plane-Strain Fracture Toughness and CVN Toughness.

65
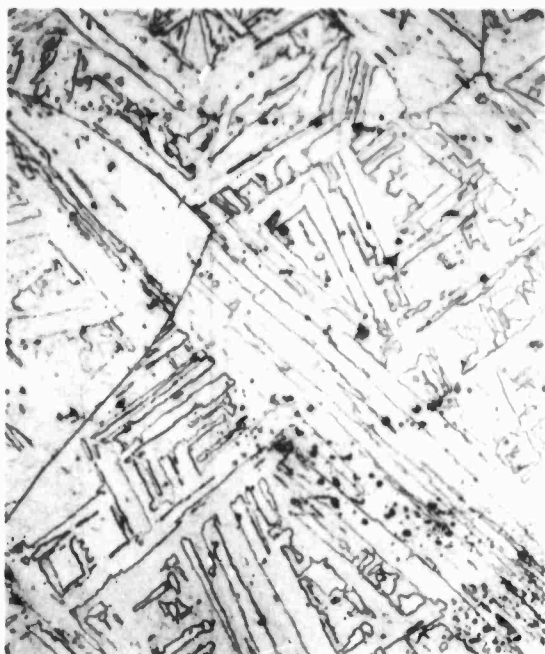
(a) 1 hour at 2400°F, air-cooled
Plate No. 245
Magnification: 100X

(b) 1 hour at 2300°F, air-cooled
Plate No. 244
Magnification: 100X

(c) 1 hour at 2200°F, air-cooled
Plate No. 240
Magnification: 100X

(d) 1 hour at 2100°F, air-cooled
Plate No. 241
Magnification: 100X

Figure 14(a-d). Light Micrographs of Heat No. X-53541
Annealed at Various Temperatures.

(e) 1 hour at 2000°F, air-cooled
    Plate No. 238
    Magnification: 100X

(f) 1 hour at 1900°F, air-cooled
    Plate No. 293
    Magnification: 246X

(g) 1 hour at 1800°F, air-cooled
    Plate No. 295
    Magnification: 246X

(h) 1 hour at 1700°F, air-cooled
    Plate No. 297
    Magnification: 500X

Figure 14(e-h). Light Micrographs of Heat No. X-53541
                Annealed at Various Temperatures.

(i) 1 hour at 1600°F, air-cooled
    Plate No. 300B
    Magnification: 750X

(j) 1 hour at 1500°F, air-cooled
    Plate No. 235
    Magnification: 100X

Figure 14(i,j). Light Micrographs of Heat No. X-53541
                Annealed at 1600°F and at 1500°F.

Plate No. 6957E   Magnification: 8000X

Figure 15.   Electron Micrograph of Heat No. X-53541
             (Annealed 1 hour at 1500°F, air-cooled—
             aged 1 hour at 950°F, air-cooled).
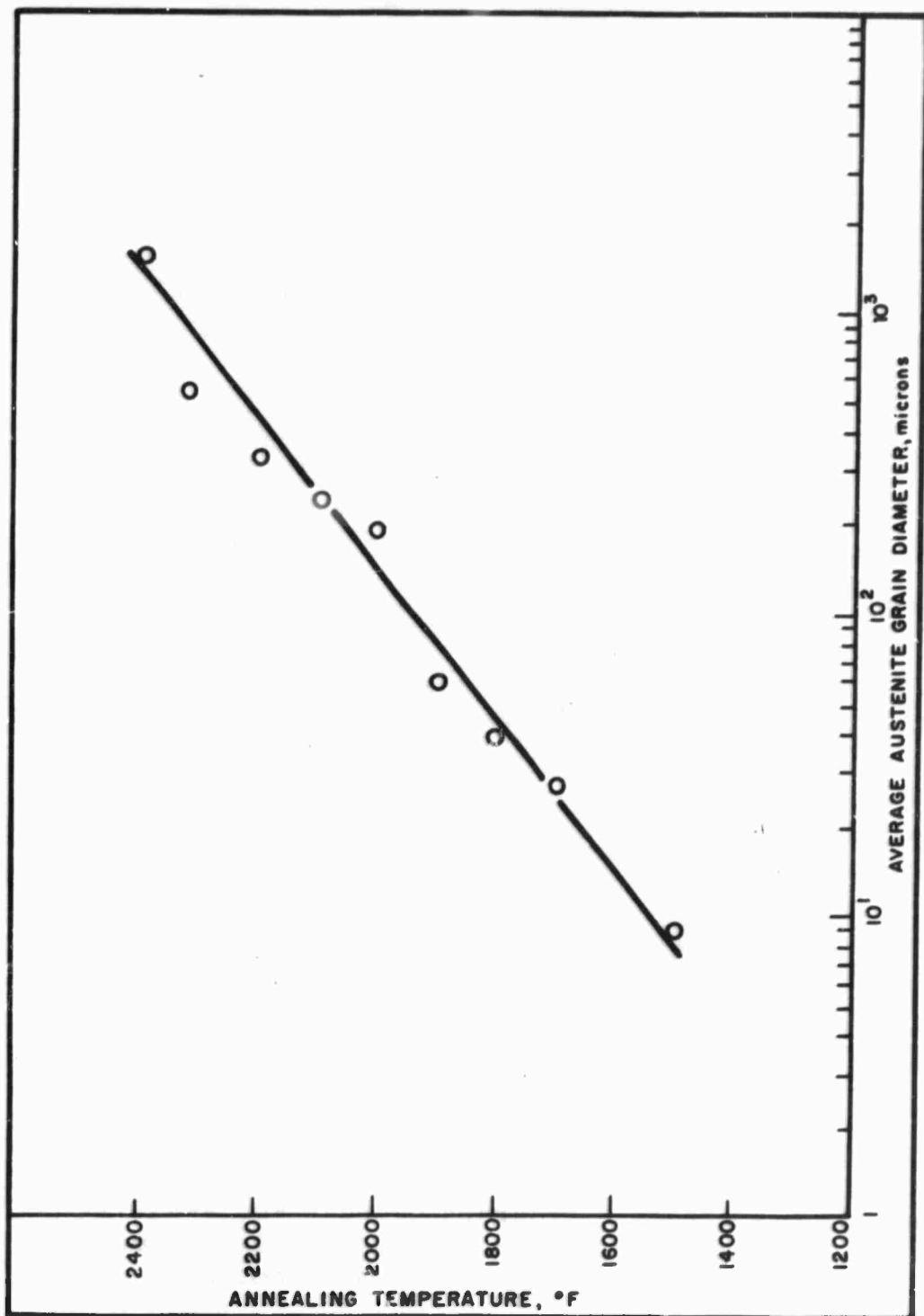
Figure 16. Effect of Annealing Temperature (1 hour) on Austenite Grain Size.

70

Plate No. 6896B

Magnification: 10,000X

Figure 17.   Extraction Replica of the Fracture
             Surface of Heat No. X-53541
             (1 hour at 1500°F, air-cooled—
             3 hours at 900°F, air-cooled).

Plate No. 6896E   Magnification: 10,000X

Figure 18. Extraction Replica ot the Fracture
            Surface of Heat No. X-53541
            (1 hour at 1500°F, air-cooled—
            3 hours at 900°F, air-cooled).

Plate No. 6917A   Magnification: 10,000X

Figure 19. Extraction Replica of the Fracture
            Surface of Heat No. X-53541 (1 hour
            at 2000°F → 4 hours at 1600°F, air-
            cooled).

73
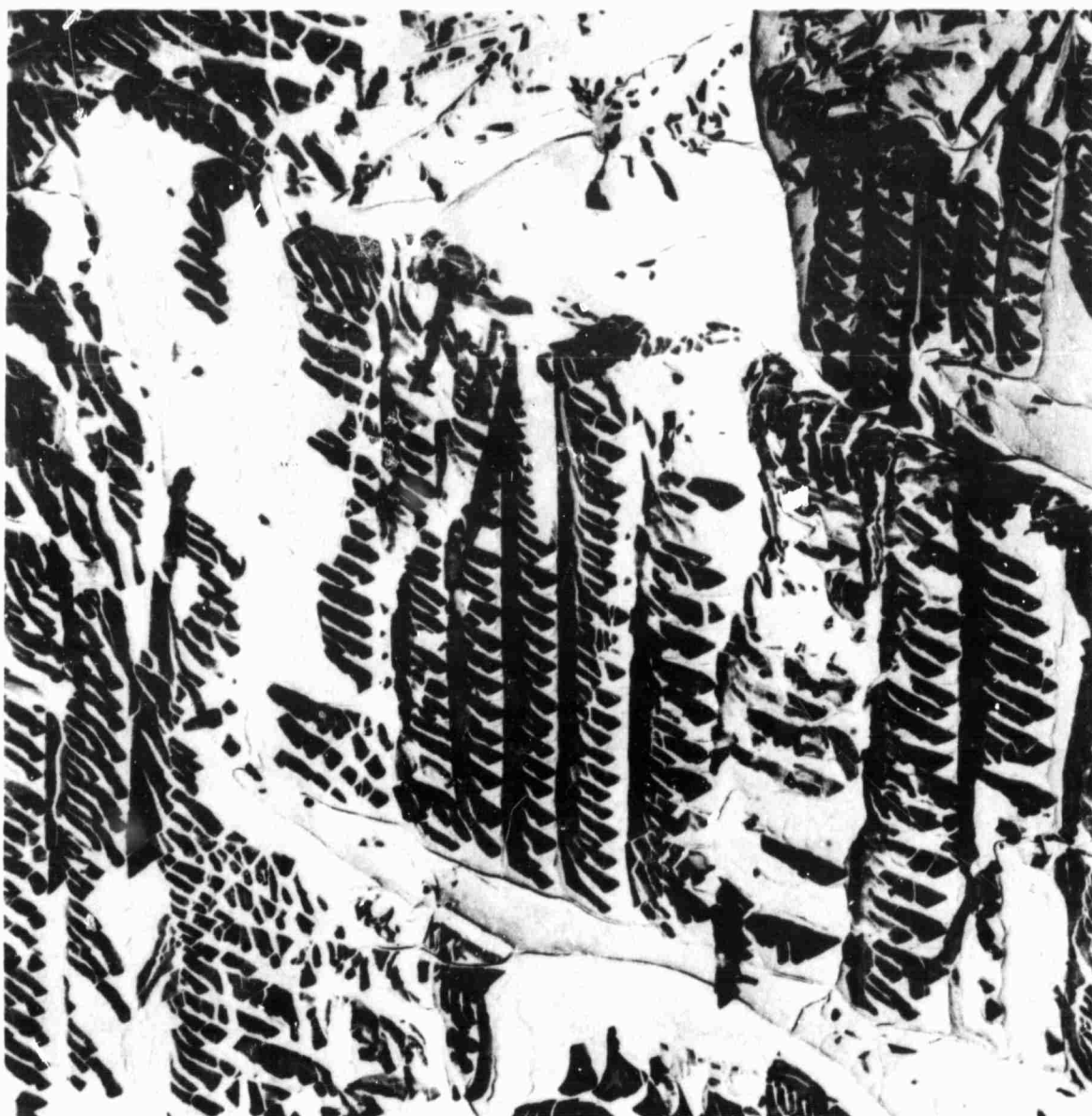
Plate No. 6895A   Magnification: 10,000X

Figure 20. Extraction Replica of the Fracture
            Surface of Heat No. X-53541 (1 hour
            at 2100°F → 4 hours at 1600°F, air-
            cooled).

74

Plate No. 6894B   Magnification: 10,000X

Figure 21.   Extraction Replica of the Fracture
             Surface of Heat No. X-53541 (1 hour
             at 2200°F → 4 hours at 1600°F, air-
             cooled).

Plate No. 6898C

Magnification: 10,000X

Figure 22. Extraction Replica of the Fracture
Surface of Heat No. X-53541 (1 hour
at 2200°F → 1/2 hour at 1600°F, air-
cooled).

Plate No. 6936D   Magnification: 10,000X

Figure 23.   Extraction Replica of the Fracture
             Surface of Heat No. X-53541 (1 hour
             at 2300°F → 4 hours at 1700°F, air-
             cooled).

77

Plate No. 6899D   Magnification: 10,000X

Figure 24. Extraction Replica of the Fracture Surface
            of Heat No. X-53541 (1 hour at 2200°F →
            4 hours at 1600°F, air-cooled, aged 3 hours
            at 900°F, air-cooled).
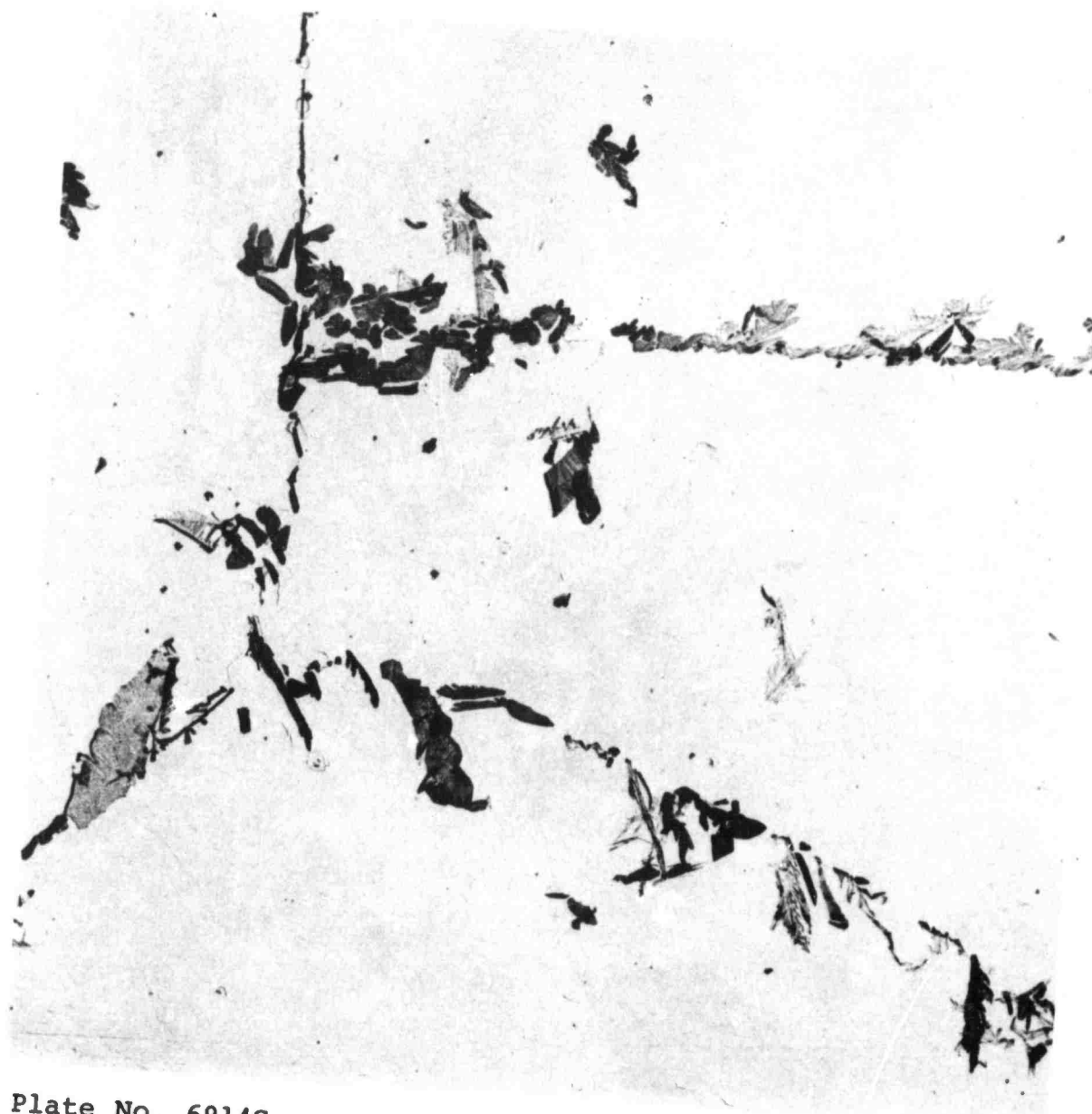
Plate No. 6914C

Magnification: 10,000X

Figure 25. Extraction Replica of a Polished and
Etched Surface of Heat No. X-53541
(1 hour at 2200°F → 1/2 hour at 1600°F,
air-cooled).
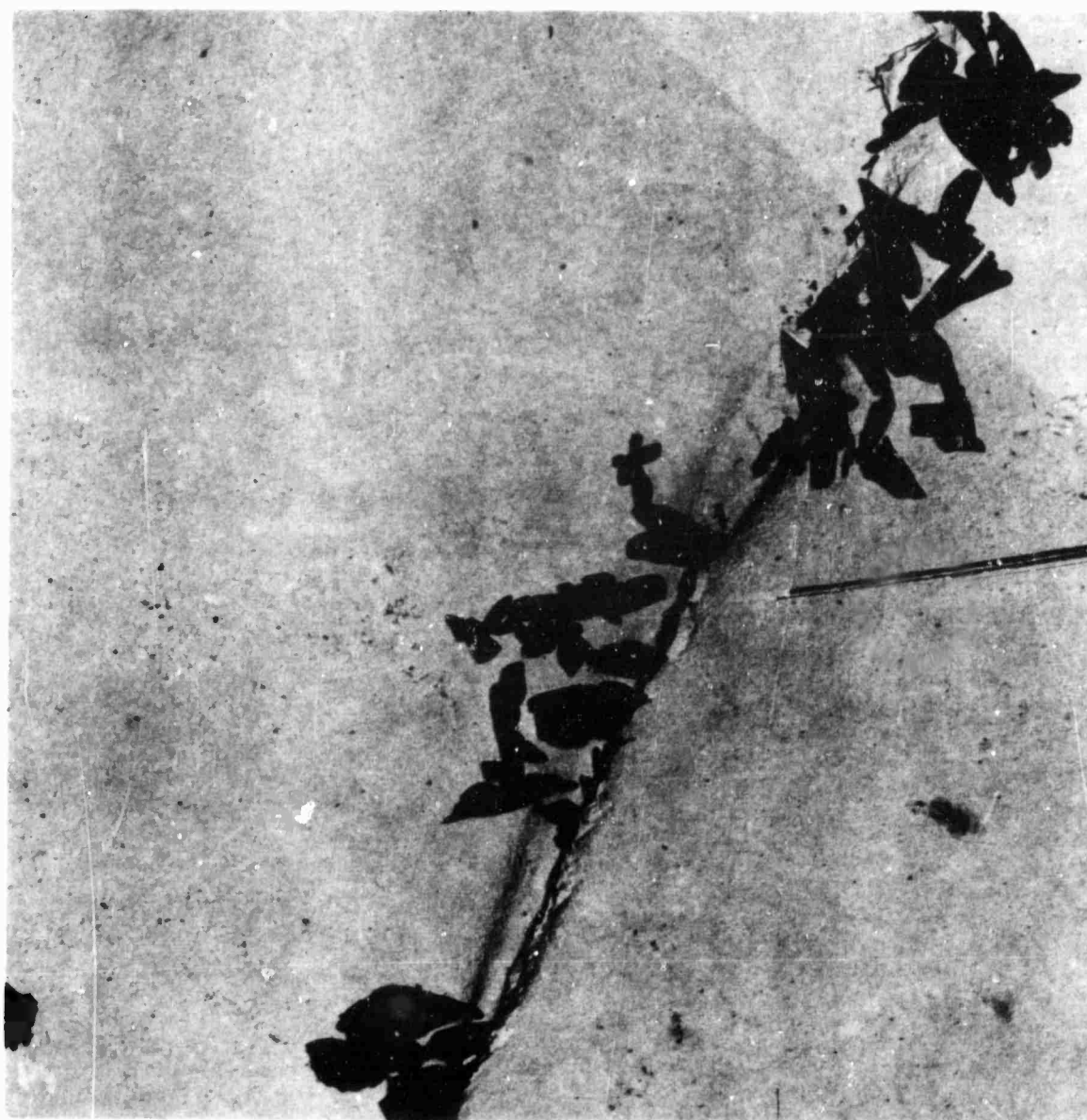
Plate No. 6910B   Magnification: 10,000X

Figure 26.   Extraction Replica of a Polished and
             Etched Surface of Heat No. X-53541
             (1 hour at 2200°F → 4 hours at 1600°F,
             air-cooled).

80
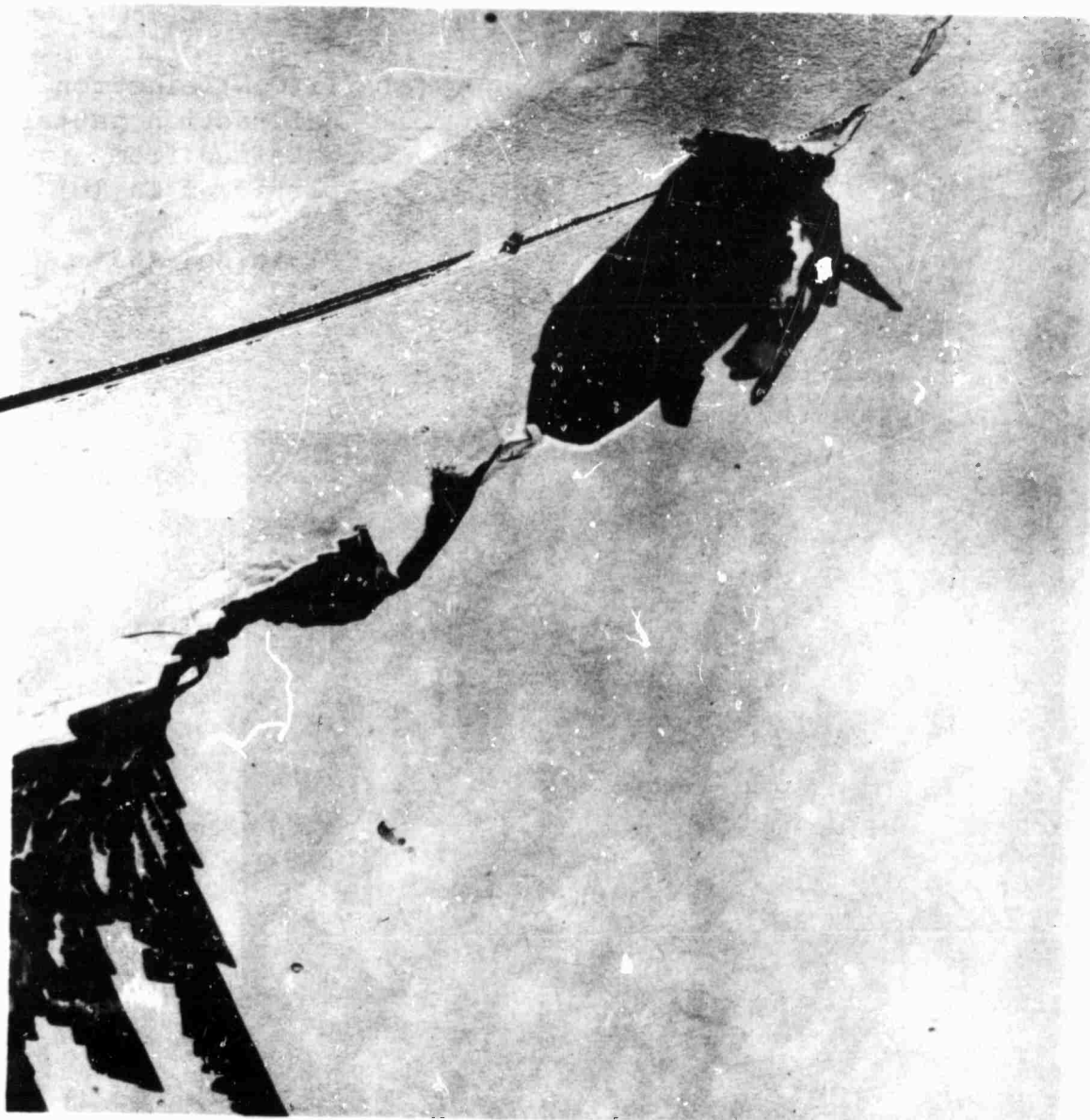
Plate No. 7015E   Magnification: 10,000X

Figure 27.   Extraction Replica of a Polished and
             Etched Surface of Heat No. X-53541
             (1 hour at 2300°F → 4 hours at 1700°F,
             air-cooled).

(a) Ti(C,N) electron
diffraction pattern
obtained from
particles in (b)

Plate No. 463

(b) Electron micrograph of the particles
Plate No. 462, Magnification: 25,000X

Figure 28(a,b). Particles Extracted from the Fracture
Surface of Heat No. X-53541 (1 hour at
2100°F → 4 hours at 1600°F, air-cooled).

(a) Ti(C,N) electron diffraction pattern obtained from particles in (b)

Plate No. 435
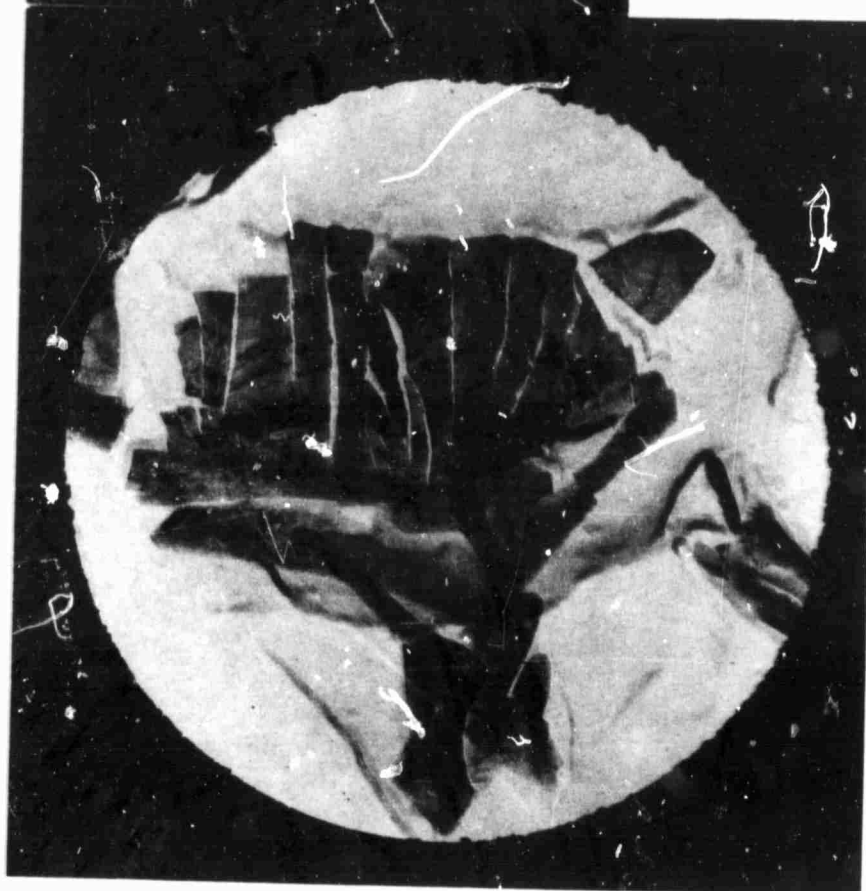
(b) Electron micrograph of the particles
Plate No. 433, Magnification: 42,000X

Figure 29(a,b). Particles Extracted from the Fracture
Surface of Heat No. X-53541 (1 hour at
2200°F → 4 hours at 1600°F, air-cooled).

(a) Ti$_2$S electron diffraction pattern obtained from largest particle in (b)

Plate No. 430

(b) Electron micrograph of the particles
Plate No. 428, Magnification: 42,000X

Figure 30(a,b). Particles Extracted from the Fracture Surface of Heat No. X-53541 (1 hour at 2200°F → 4 hours at 1600°F, air-cooled).
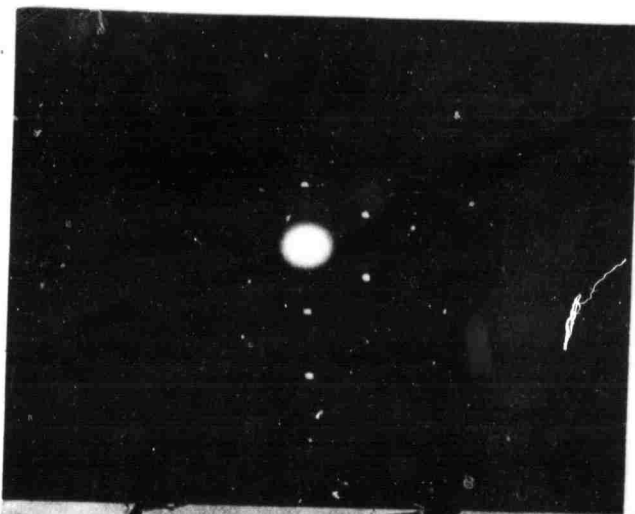
(a) Ti$_2$S electron diffraction pattern obtained from circled particle in (b)

Plate No. 426

(b) Electron micrograph of the particles
Plate No. 427, Magnification: 42,000X

Figure 31(a,b). Particles Extracted from the Fracture Surface of Heat No. X-53541 (1 hour at 2200°F → 4 hours at 1600°F, air-cooled).

85

(a)

Plate No. 59   Magnification: 100X

(b)

Plate No. 134   Magnification: 100X

Figure 32.   Photomicrographs of As-Rolled Micro-
             structure of (a) V-8858 and (b) V-8497.
             Nital Etch.

(a)
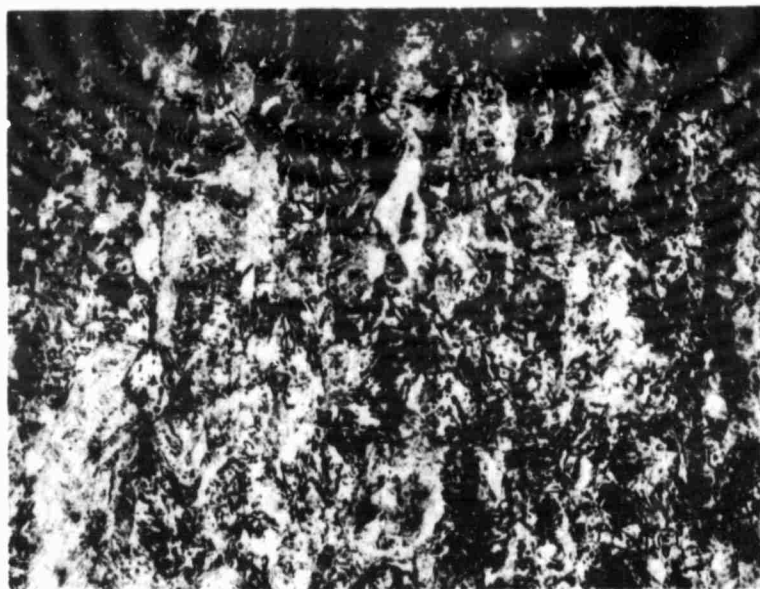
Plate No. 73   Magnification: 100X

(b)
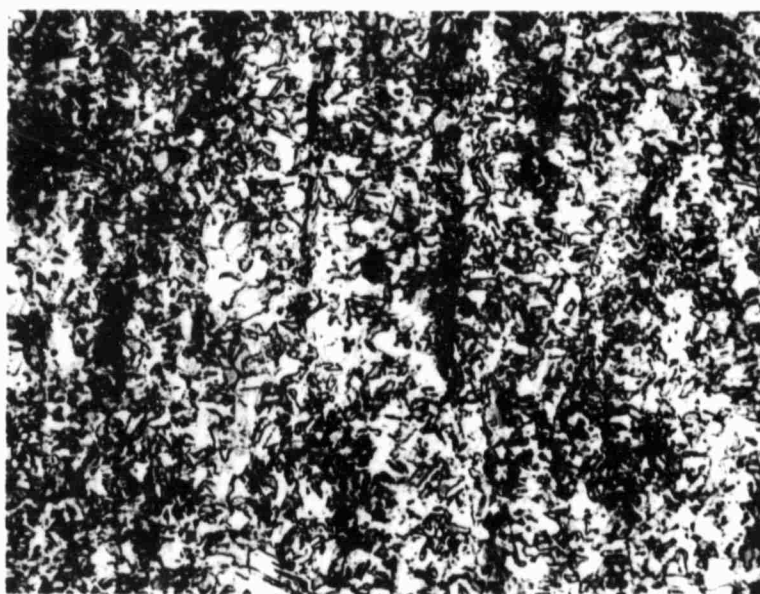
Plate No. 69   Magnification: 100X

Figure 33.   Photomicrographs of Microstructure of
             (a) V-8858 and (b) V-8497 after 1 Hour
             at 1500°F, Air-Cooled. Nital Etch.

87

(a)
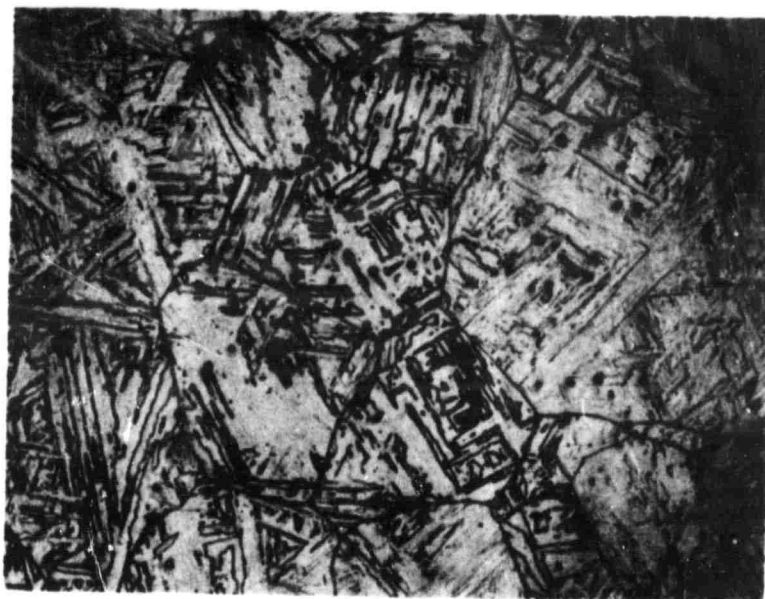
Plate No. 86   Magnification: 100X

(b)

Plate No. 68   Magnification: 100X

Figure 34. Photomicrographs of Microstructure of
            (a) V-8858 and (b) V-8497 after 1 Hour
            at 2200°F, Air-Cooled. Nital Etch.

88

(a)

Plate No. 94   Magnification: 100X

(b)

Plate No. 88   Magnification: 100X

Figure 35.   Photomicrographs of Microstructure of
             (a) V-8858 and (b) V-8497 after 1 Hour
             at 2200°F, Cooled to 1500°F for 4 Hours,
             Air-Cooled. Nital Etch.

89
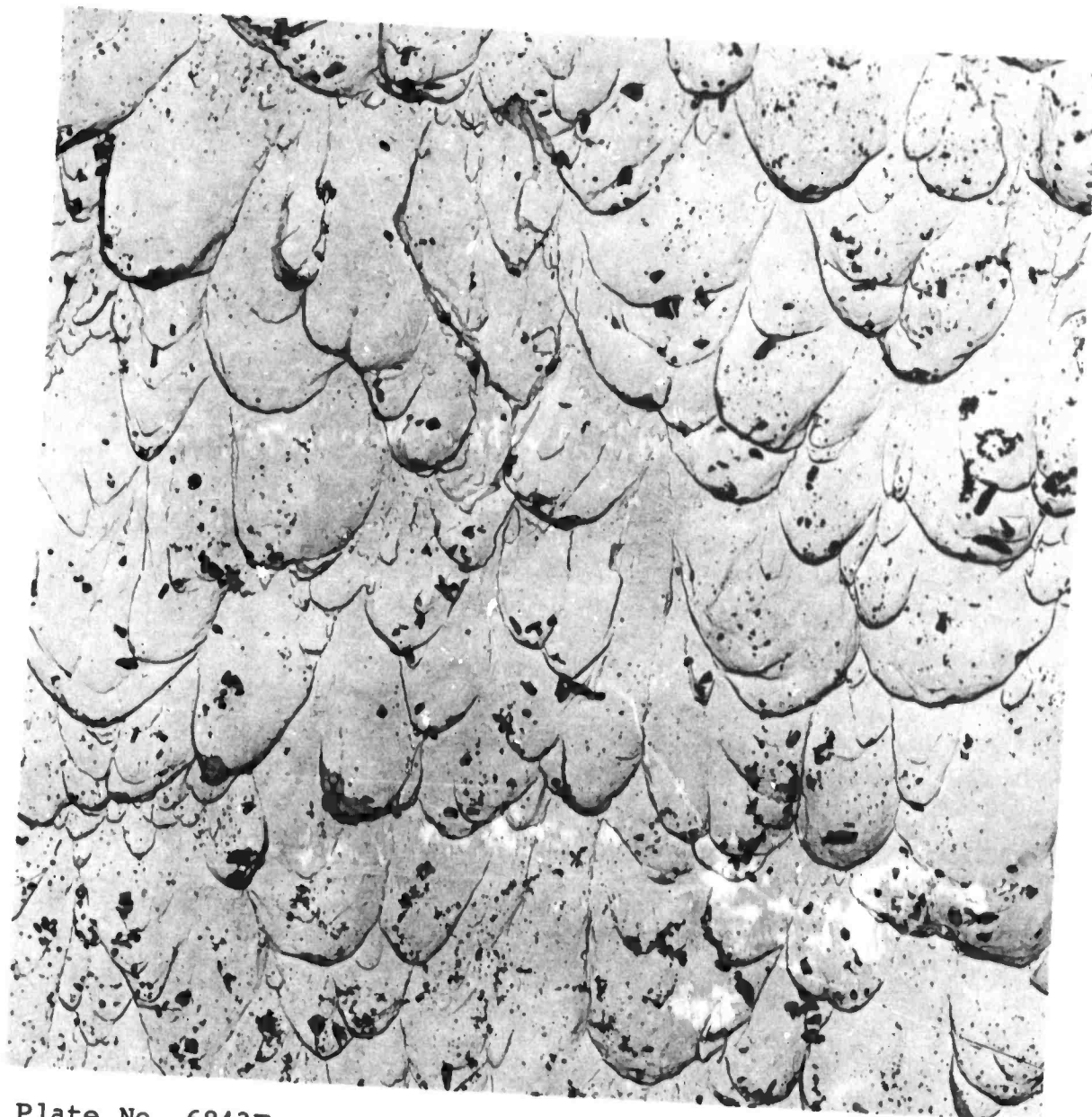
Plate No. 6843F

Magnification: 10,000X

Figure 36. Extraction Replica of Fracture
Surface of V-8858 after 1 Hour
at 1500°F, Air-Cooled.

Plate No. 6841D   Magnification: 10,000X

Figure 37.   Extraction Replica of Fracture
             Surface of V-6858 after 1 Hour
             at 2200°F, Air-Cooled.

91

Plate No. 6839C   Magnification: 10,000X

Figure 38.   Extraction Replica of Fracture
             Surface of V-8858 after 1 Hour
             at 2200°F → 4 Hours at 1500°F,
             Air-Cooled.

92

Plate No. 6840A   Magnification: 10,000X

Figure 39. Extraction Replica of Fracture Surface
            of V-8858 after 1 Hour at 2200°F →
            4 Hours at 1500°F, Air-Cooled, 3 Hours
            at 900°F.

93

Plate No. 213   Magnification: 80,000X

Figure 40. Extraction Replica of Fracture Surface
            of V-8858 after 1 Hour at 2200°F →
            4 Hours at 1500°F, Air-Cooled, 3 Hours
            at 900°F. Details of Extracted Particles.
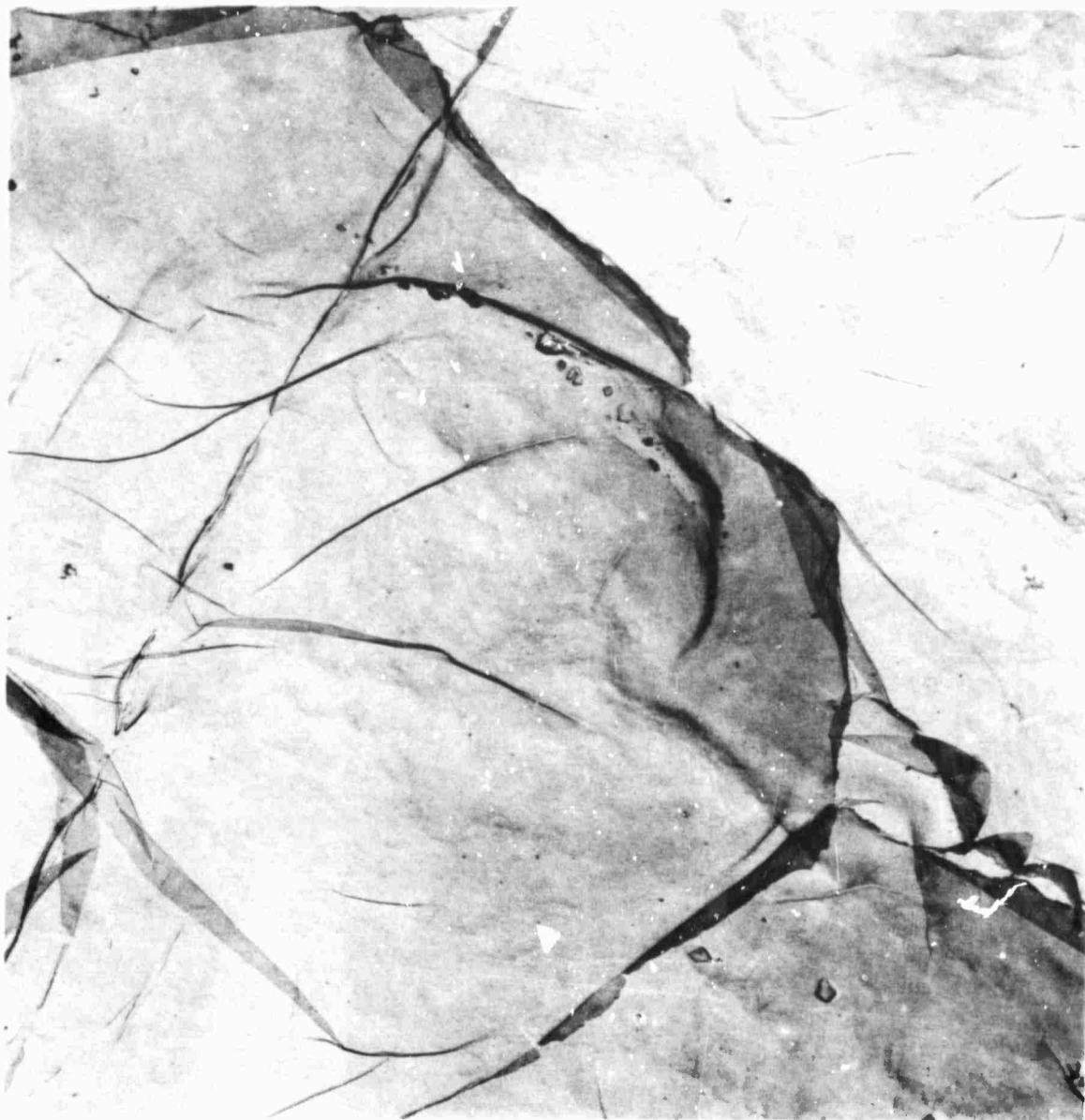
Plate No. 6852D   Magnification: 10,000X

Figure 41.   Extraction Replica of Fracture
             Surface of V-8497 after 1 Hour
             at 2200°F, Air-Cooled.

Plate No. 6846C   Magnification: 10,000X

Figure 42.   Extraction Replica of V-8497 after
             1 Hour at 2200°F → 4 Hours at 1500°F,
             Air-Cooled.

96
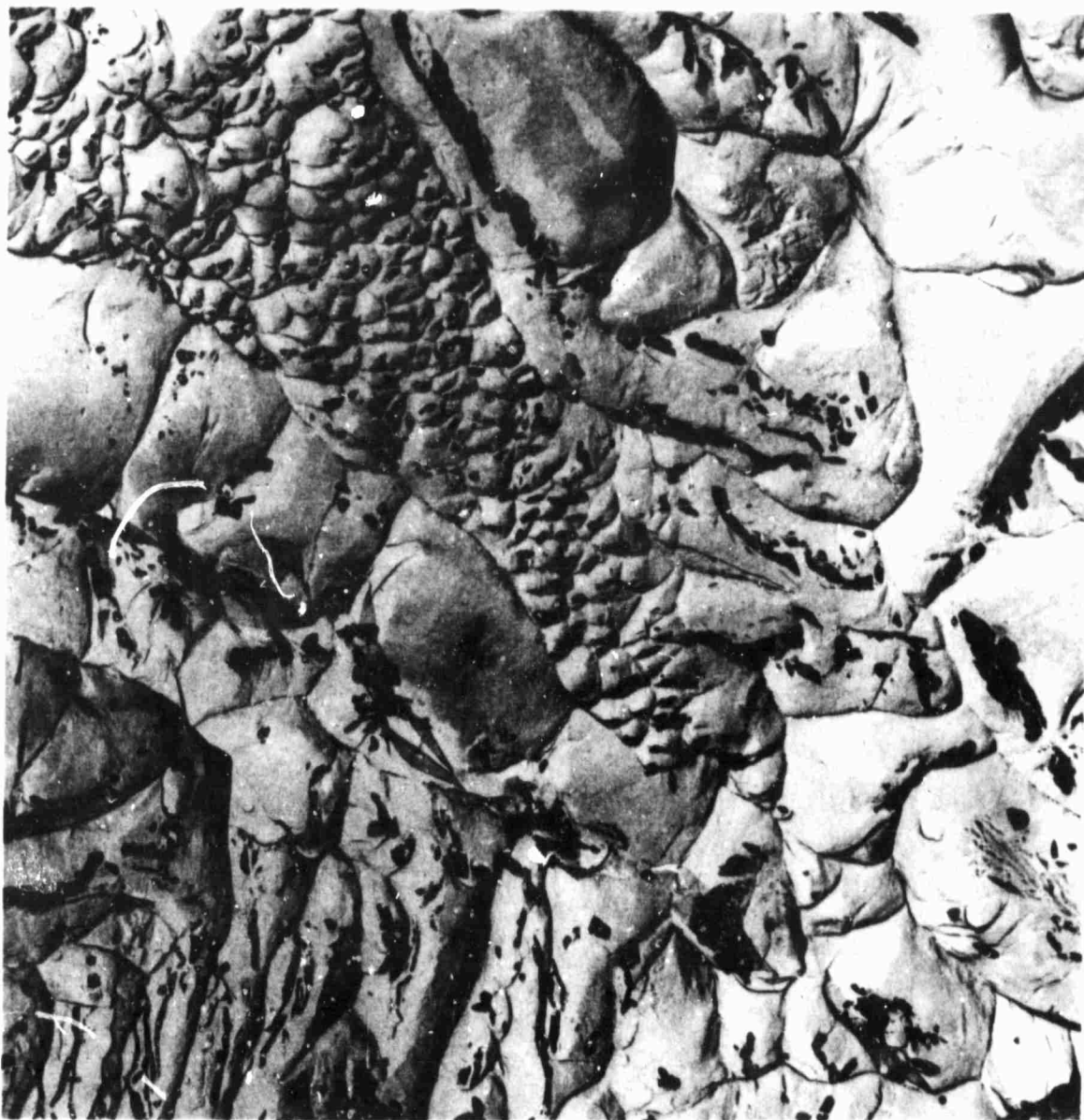
Plate No. 6854E   Magnification: 10,000X

Figure 43. Extraction Replica of V-8497 after
            1 Hour at 2200°F → 4 Hours at 1500°F,
            Air-Cooled, 3 Hours at 900°F.

97
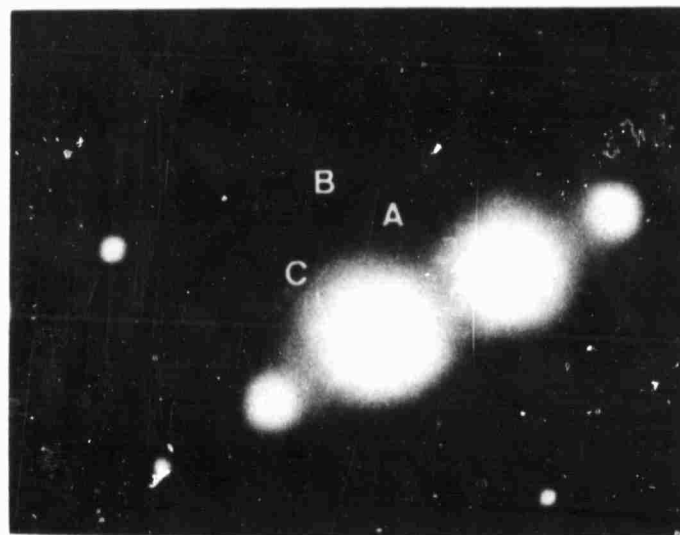
(a) Electron diffraction pattern of
T-6110 after 1 hour 2200°F →
4 hours at 1400°F

Plate No. 8463

$< 022, 111 = 35.26°$

$< 111, \bar{1}11 = 70.53°$

SPOT	d_{calc}	TiC PLANE	d_{lit}
A	2.49	(111)	2.51
B	1.50	(022)	1.54
C	2.49	($\bar{1}$11)	2.51
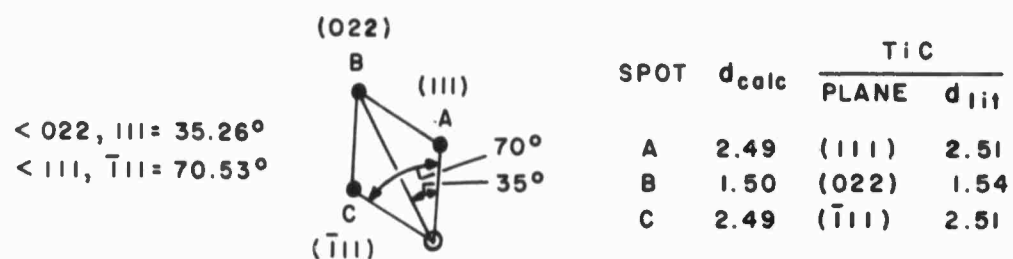
(b) Solution of electron diffraction
pattern as a <110> zone of Ti(C,N)

Figure 44. Selected-Area Diffraction
Analysis of Ti(C,N).

98
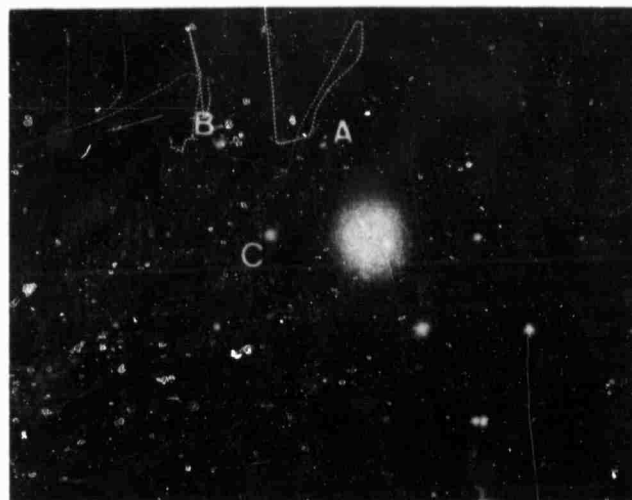
(a) Electron diffraction pattern of
     V-8858 after 1 hour at 2200°F

     Plate No. 367

$< 10\bar{1}0, 11\bar{2}0 = 30°$
$< 10\bar{1}0, 01\bar{1}0 = 60°$

SPOT	d_{calc}	τ - Ti$_2$S PLANE	d_{lit}
A	2.79	(10$\bar{1}$0)	2.78
B	1.61	(11$\bar{2}$0)	1.60
C	2.79	(01$\bar{1}$0)	2.78
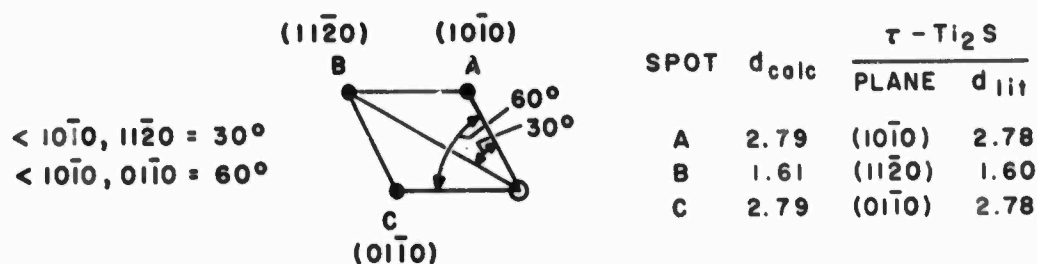
(b) Solution of electron diffraction
     pattern as a <0001> zone of τ-Ti$_2$S

Figure 45.   Selected-Area Diffraction
             Analysis of τ-Ti$_2$S.

99
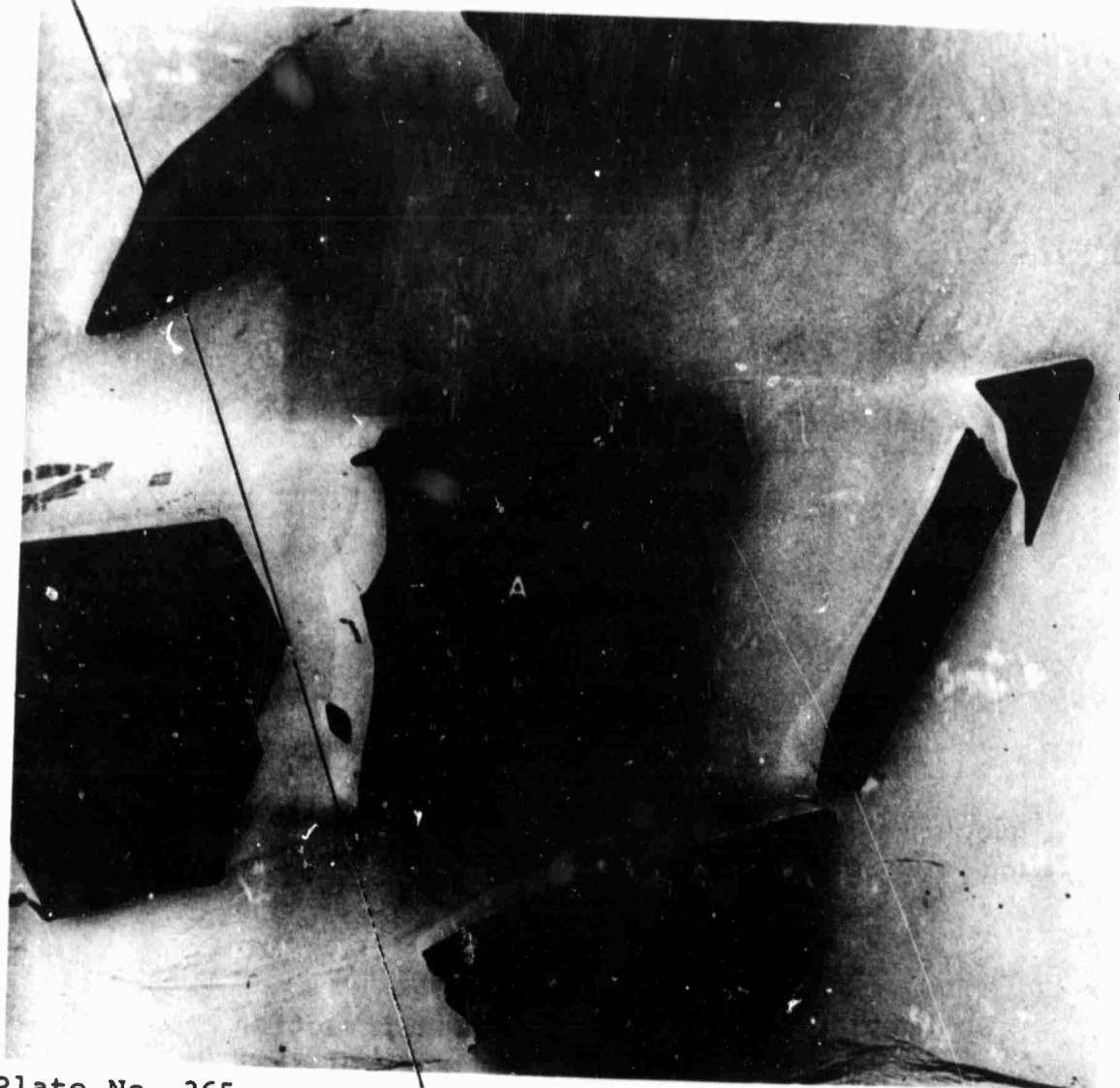
Plate No. 365   Magnification: 25,000X

Figure 46. Electron Micrograph of τ-Ti_2S
            Particles from V-8858 after
            Heating at 2200°F for 1 Hour.
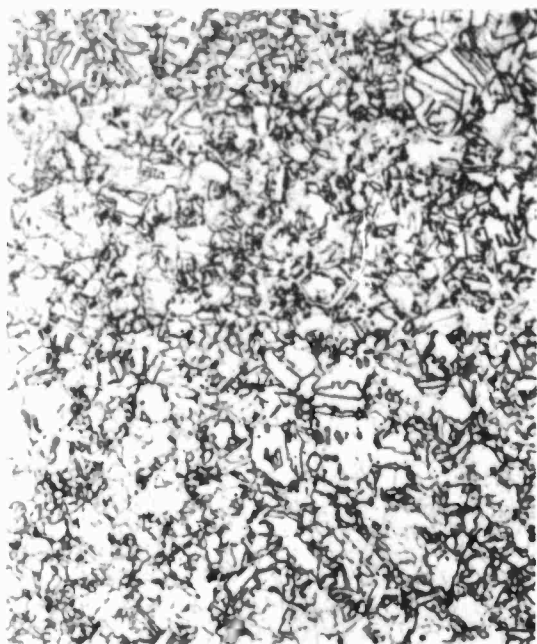
(a) 1 hour at 1700°F, air-cooled   (b) 1 hour at 1800°F, air-cooled
    Negative No. 284   Negative No. 289
    Magnification: 100X   Magnification: 100X

(c) 1 hour at 1900°F, air-cooled   (d) 1 hour at 2000°F, air-cooled
    Negative No. 279   Negative No. 276
    Magnification: 100X   Magnification: 100X

Figure 47(a-d).   Light Micrographs of Heat No. T-6109
                  Annealed at Temperatures of 1700 to
                  2000°F.

101

(e) 1 hour at 2100°F, air-cooled
    Negative No. 271
    Magnification: 100X

(f) 1 hour at 2200°F, air-cooled
    Negative No. 267
    Magnification: 100X
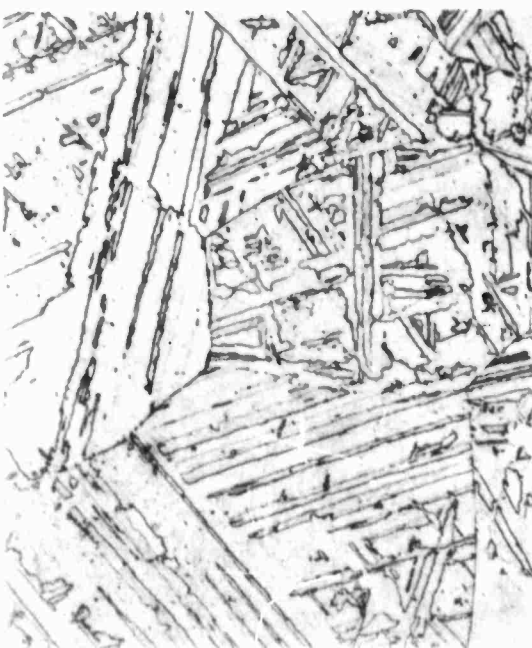
(g) 1 hour at 2300°F, air-cooled
    Negative No. 263
    Magnification: 100X

(h) 1 hour at 2400°F, air-cooled
    Negative No. 259
    Magnification: 100X

Figure 47(e-h). Light Micrographs of Heat No. T-6109
                Annealed at Temperatures of 2100 to
                2400°F.

102
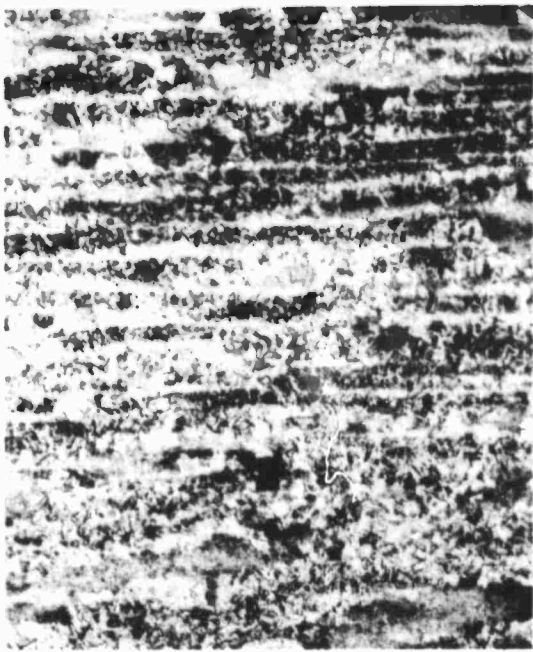
(a) 1 hour at 1500°F, air-cooled
Negative No. 569
Magnification: 100X

(b) 1 hour at 2200°F, quenched
into salt at 1500°F for 4
hours, air-cooled
Negative No. 573
Magnification: 100X

(c) 1 hour at 2400°F, quenched into salt
at 1500°F for 4 hours, air-cooled
Negative No. 571, Magnification: 100X

Figure 48. Light Micrographs of Heat No. W-8068.

(a) 1 hour at 1500°F, air-cooled
    Negative No. 575
    Magnification: 100X

(b) 1 hour at 2200°F, quenched
    into salt at 1500°F for 4
    hours, air-cooled
    Negative No. 568
    Magnification: 100X

(c) 1 hour at 2400°F, quenched into salt
    at 1500°F for 4 hours, air-cooled
    Negative No. 566, Magnification: 100X

Figure 49.   Light Micrographs of Heat No. W-8135-2.

Plate No. 7002C   Magnification: 10,000X

Figure 50.   Extraction Replica of the Fracture Surface
             of Heat No. W-8135-2 (1 hour at 2200°F,
             air-cooled, 6 hours at 900°F, air-cooled).
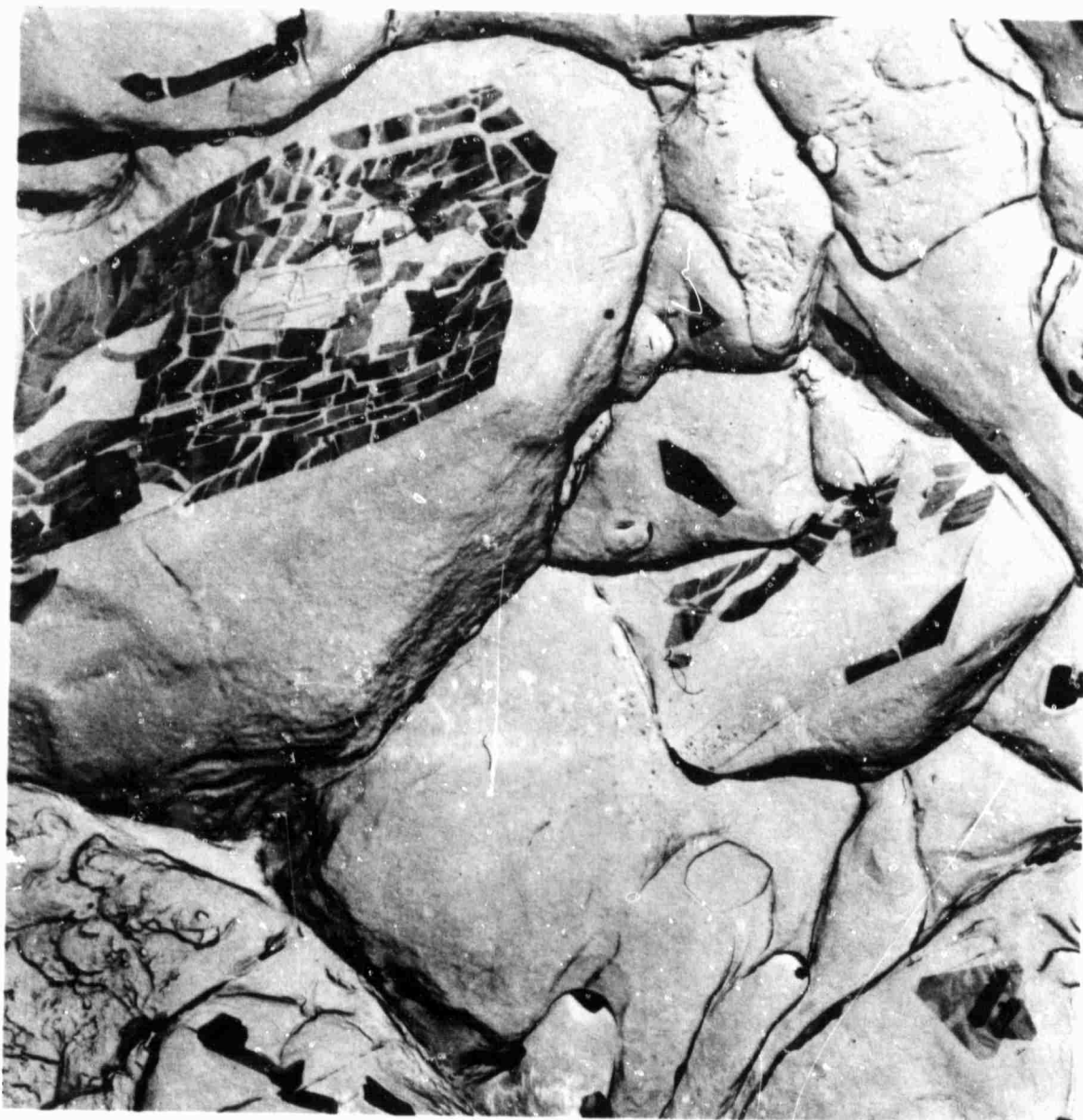
Plate No. 6997B   Magnification: 10,000X

Figure 51. Extraction Replica of Fracture Surface of
            Heat No. W-8068 (1 hour at 2200°F → 4 hours
            at 1500°F, air-cooled, 6 hours at 900°F,
            air-cooled).

106
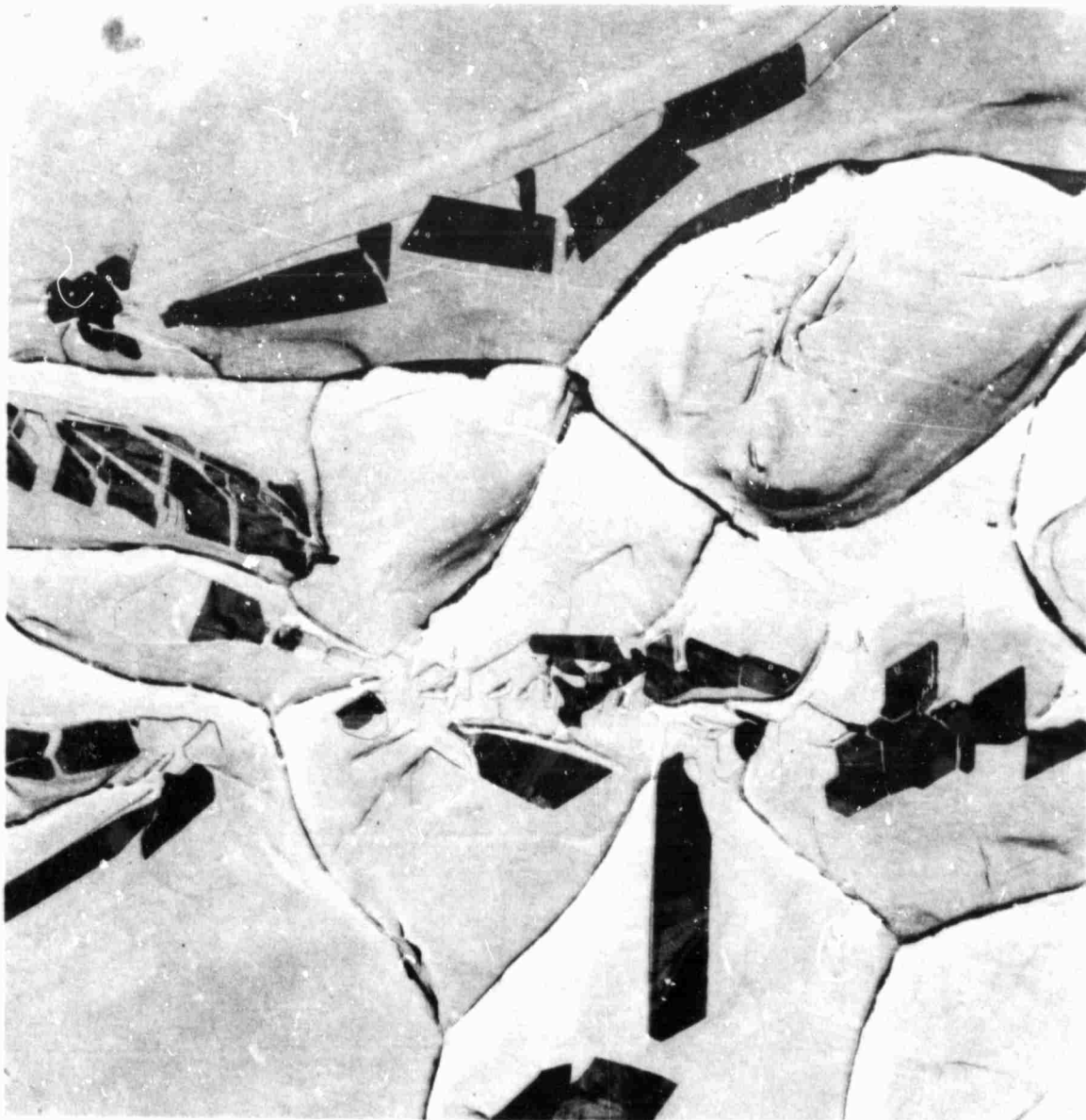
Plate No. 7035D   Magnification: 10,000X

Figure 52.   Extraction Replica of Fracture Surface of
             Heat No. W-8068 (1 hour at 2400°F → 4 hours
             at 1500°F, air-cooled, 6 hours at 900°F,
             air-cooled).

107
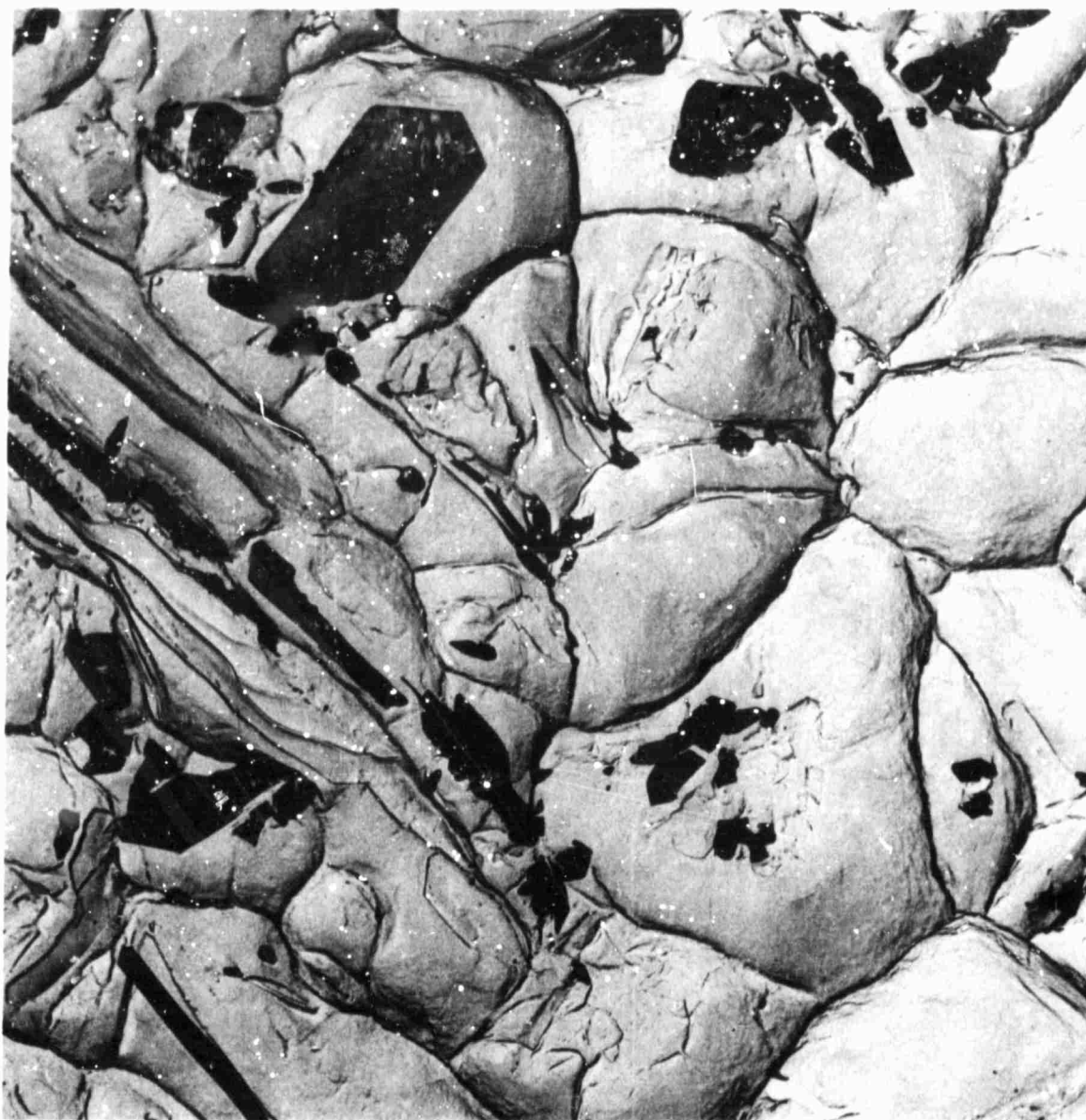
Plate No. 7034D   Magnification: 10,000X

Figure 53.   Extraction Replica of the Fracture Surface of
             Heat No. W-8135-2 (1 hour at 2200°F → 4 hours
             at 1500°F, air-cooled, 6 hours at 900°F, air-
             cooled).

108

Plate No. 7000D

Magnification: 10,000X

Figure 54. Extraction Replica of the Fracture Surface
of Heat No. W-8135-2 (1 hour at 2400°F →
4 hours at 1500°F, air-cooled, 6 hours at
900°F).
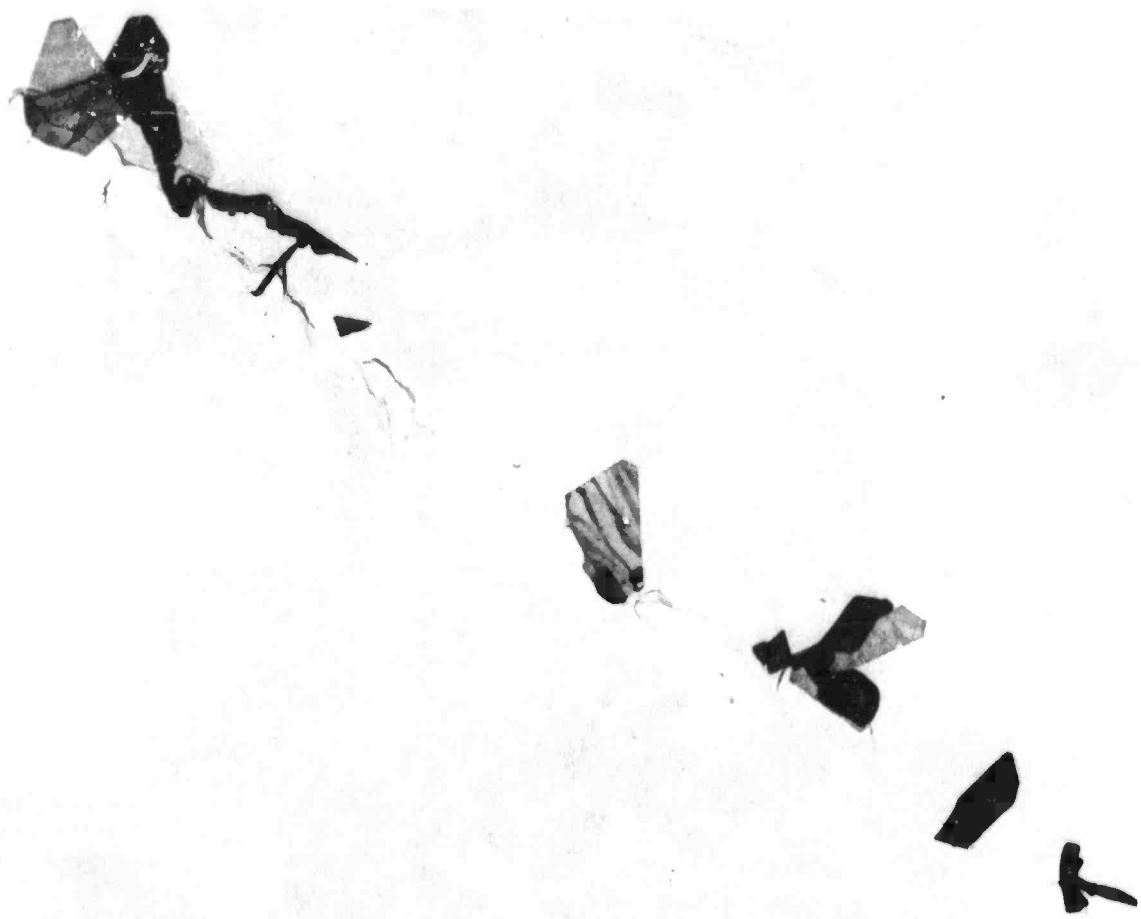
Plate No. 7031-C   Magnification: 10,000X

Figure 55. Extraction Replica of a Polished and Etched
            Surface of Heat No. W-8135-2 (1 hour at
            2200°F → 4 hours at 1500°F, air-cooled).

110

(a) 1 hour at 1500°F, air-cooled   (b) 1 hour at 2200°F, quenched
    Negative No. 578   into salt at 1500°F for 4
    Magnification: 100X   hours, air-cooled
                                          Negative No. 579
                                          Magnification: 100X
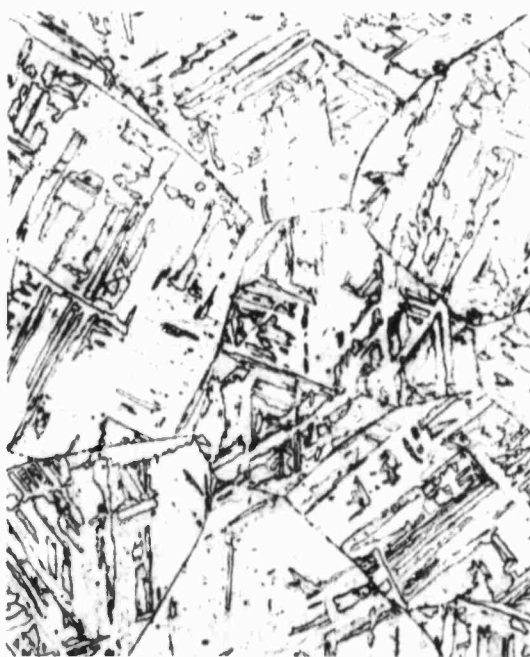
(c) 1 hour at 2300°F, quenched into salt
    at 1500°F for 4 hours, air-cooled
    Negative No. 581, Magnification: 100X

Figure 56. Light Micrographs of Heat No. W-8133-1A

111
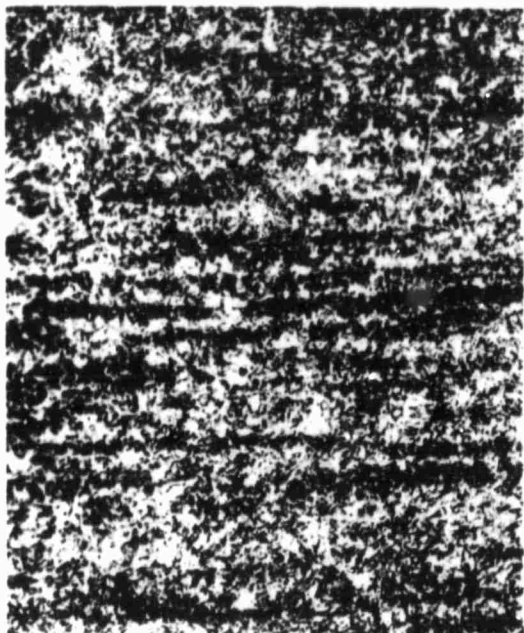
(a) 1 hour at 1500°F, air-cooled
Negative No. 589
Magnification: 100X

(b) 1 hour at 2200°F, quenched
into salt at 1500°F for 4
hours, air-cooled
Negative No. 588
Magnification: 100X
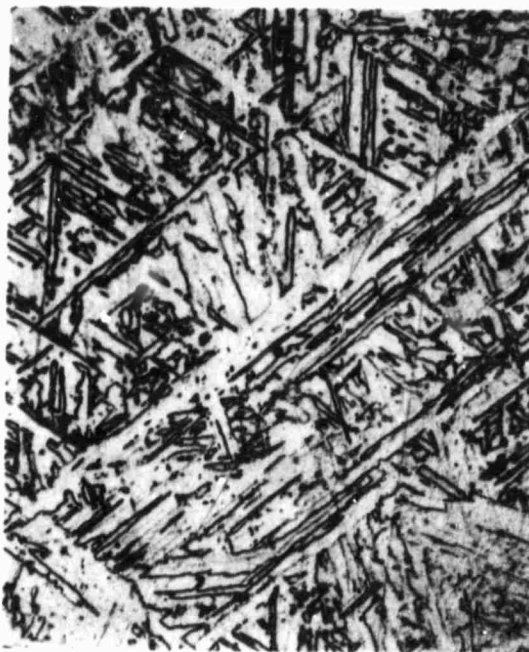
(c) 1 hour at 2300°F, quenched into salt
at 1500°F for 4 hours, air-cooled
Negative No. 585, Magnification: 100X

Figure 57. Light Micrographs of Heat No. W-8134-1A

Plate No. 7084E

Magnification: 10,000X

Figure 58. Extraction Fractograph of Fracture Surface
of Heat No. W-8133-1A (1 hour at 2200°F,
air-cooled, 3 hours at 900°F, air-cooled).

Plate No. 7081-A   Magnification: 10,000A

Figure 59. Extraction Fractograph of Fracture Surface
            of Heat No. W-8133-1A (1 hour at 2200°F →
            4 hours at 1500°F, air-cooled, 3 hours at
            900°F, air-cooled).

Plate No. 7081-B

Magnification: 10,000X

Figure 60. Extraction Fractograph of Fracture Surface
of Heat No. W-8133-1A (1 hour at 2200°F →
4 hours at 1500°F, air-cooled, 3 hours at
900°F, air-cooled).
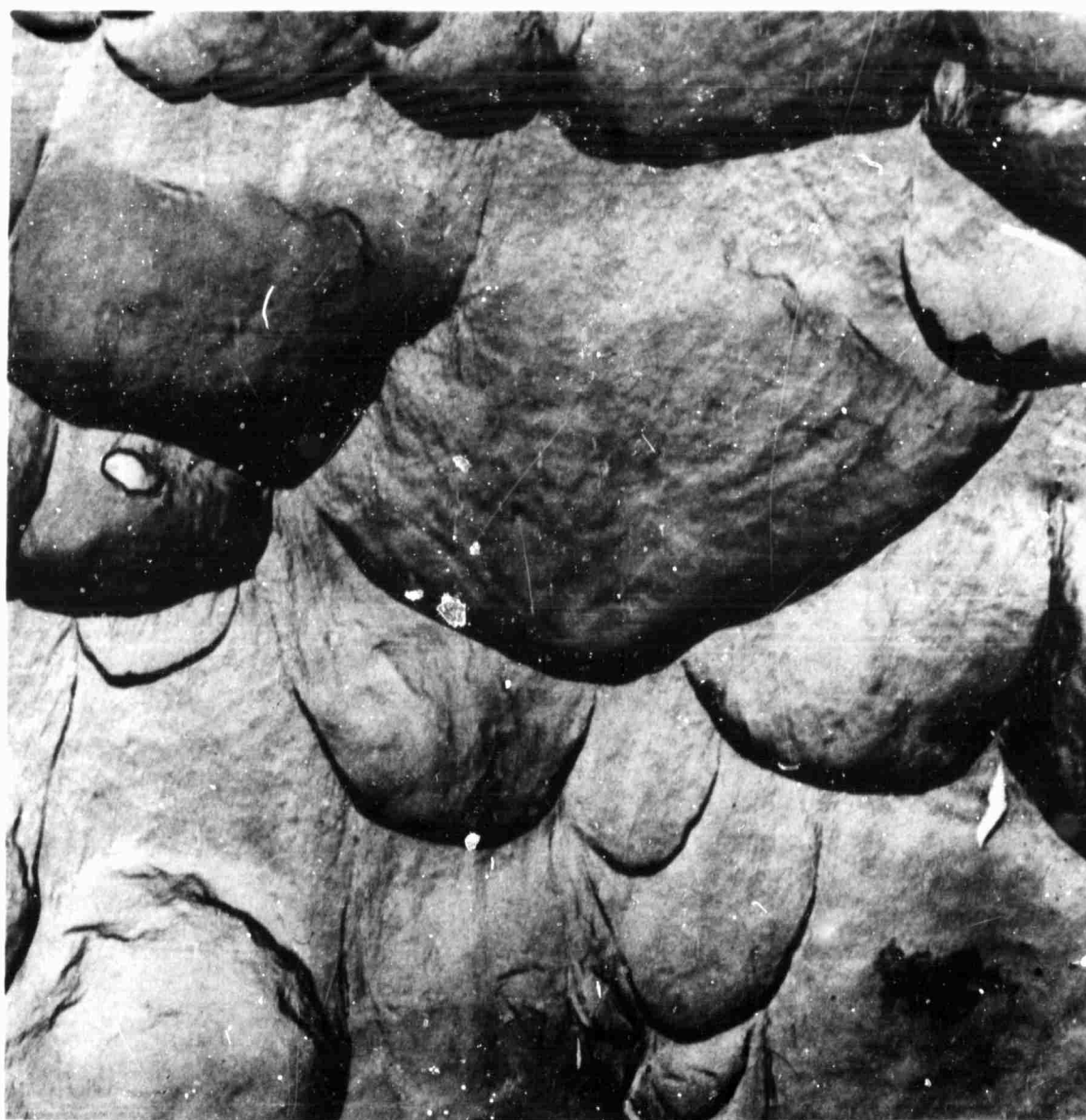
Plate No. 7127-E   Magnification: 10,000X

Figure 61. Extraction Replica of Fracture Surface
            of Steel W-8196 (1 hour at 2200°F, air-
            cooled, 3 hours at 900°F, air-cooled).

116

Plate No. 7132-F

Magnification: 10,000X

Figure 62. Extraction Replica of Fracture Surface of
Steel W-8196 (1 hour at 2200°F → 1/2 hour
at 1500°F, air-cooled, 3 hours at 900°F,
air-cooled).

117

Plate No. 7130-D   Magnification: 10,000X

Figure 63.   Extraction Replica of Fracture Surface of
             Steel W-8196 (1 hour at 2200°F → 4 hours
             at 1500°F, air-cooled, 3 hours at 900°F,
             air-cooled).

118
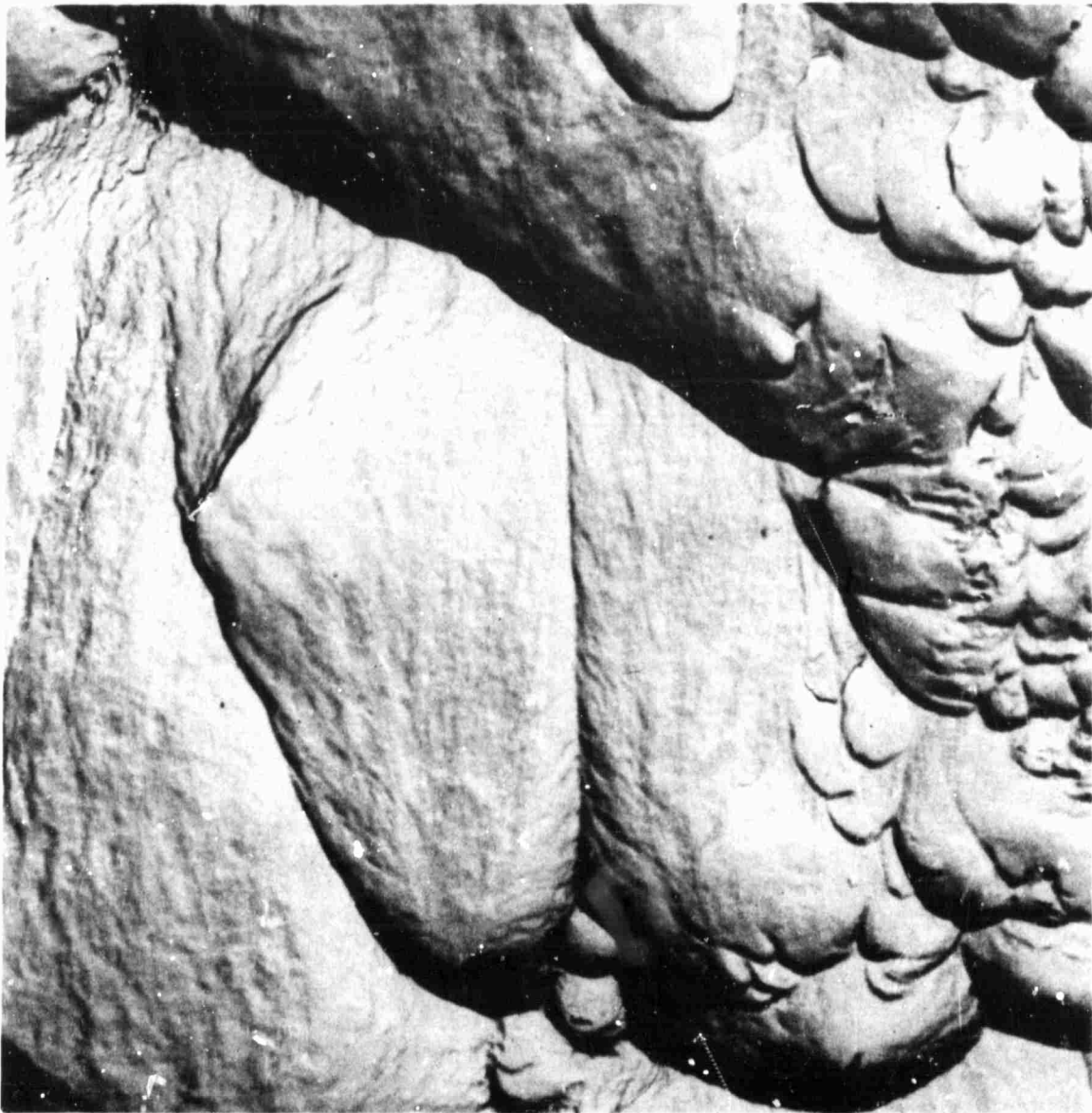
Plate No. 7106-B   Magnification: 10,000X

Figure 64. Extraction Replica of Fracture Surface of
            Steel W-8197 (1 hour at 2200°F, air-cooled,
            3 hours at 900°F, air-cooled).

119

Plate No. 7125-E

Magnification: 10,000X

Figure 65.   Extraction Replica of Fracture Surface of
             Steel W-8197 (1 hour at 2200°F → 1/2 hour
             at 1500°F, air-cooled, 3 hours at 900°F,
             air-cooled).

120

Plate No. 7135-A   Magnification: 10,000X

Figure 66.   Extraction Replica of Fracture Surface of
             Steel W-8197 (1 hour at 2200°F → 4 hours
             at 1500°F, air-cooled, 3 hours at 900°F,
             air-cooled).
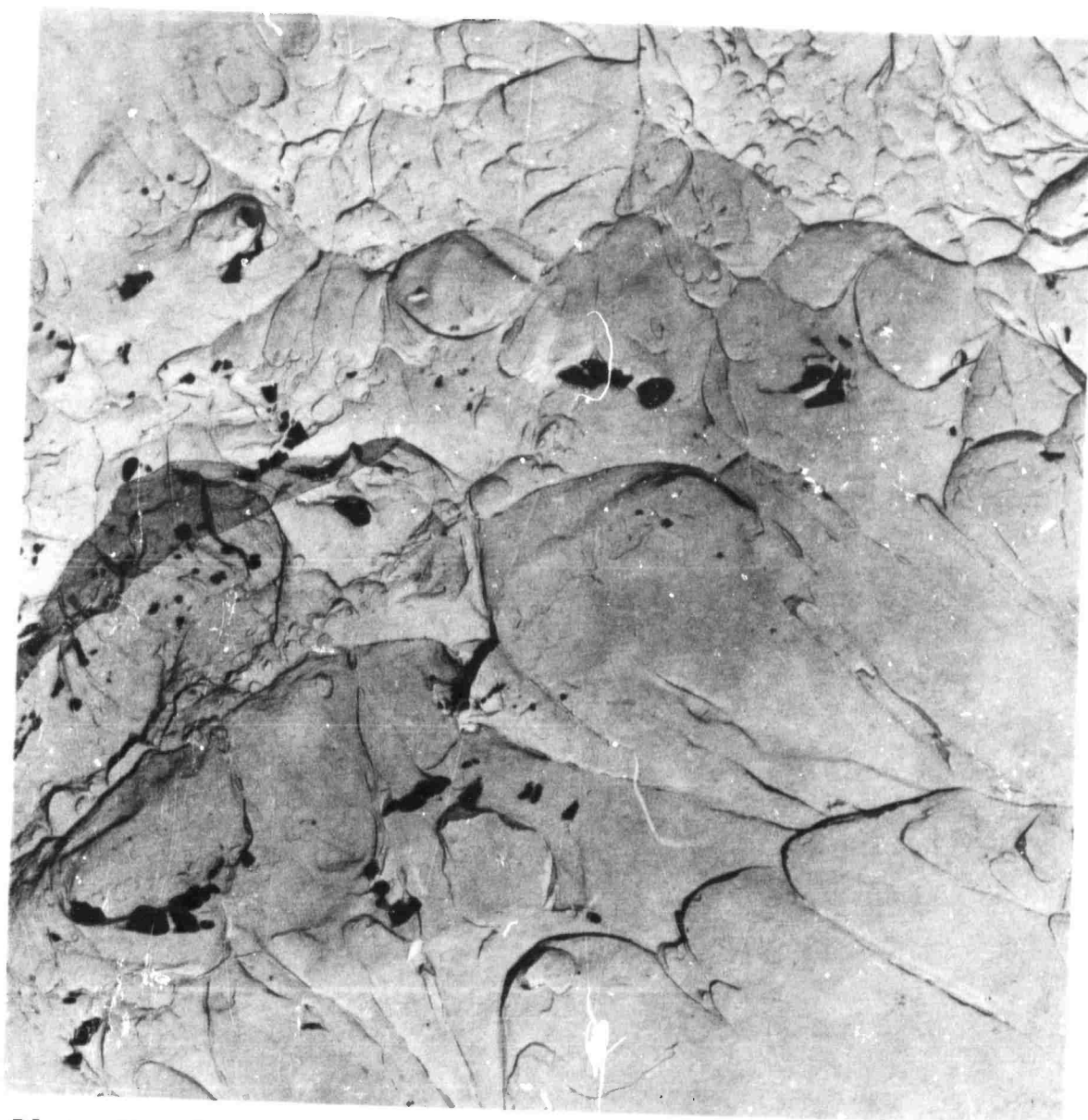

121

Plate No. 7103-E   Magnification: 10,000X

Figure 67. Extraction Replica of Fracture Surface of
            Steel W-8198 (1 hour at 2200°F, air-cooled,
            3 hours at 900°F, air-cooled).

122

Plate No. 7111-A   Magnification: 10,000X

Figure 68.   Extraction Replica of Fracture Surface of
             Steel W-8198 (1 hour at 2200°F → 1/2 hour
             at 1500°F, air-cooled, 3 hours at 900°F,
             air-cooled).

123

Plate No. 7128-B   Magnification: 10,000X

Figure 69.   Extraction Replica of Fracture Surface of
             Steel W-8198 (1 hour at 2200°F → 4 hours
   at 1500°F, air-cooled, 3 hours at 900°F,
             air-cooled).

124
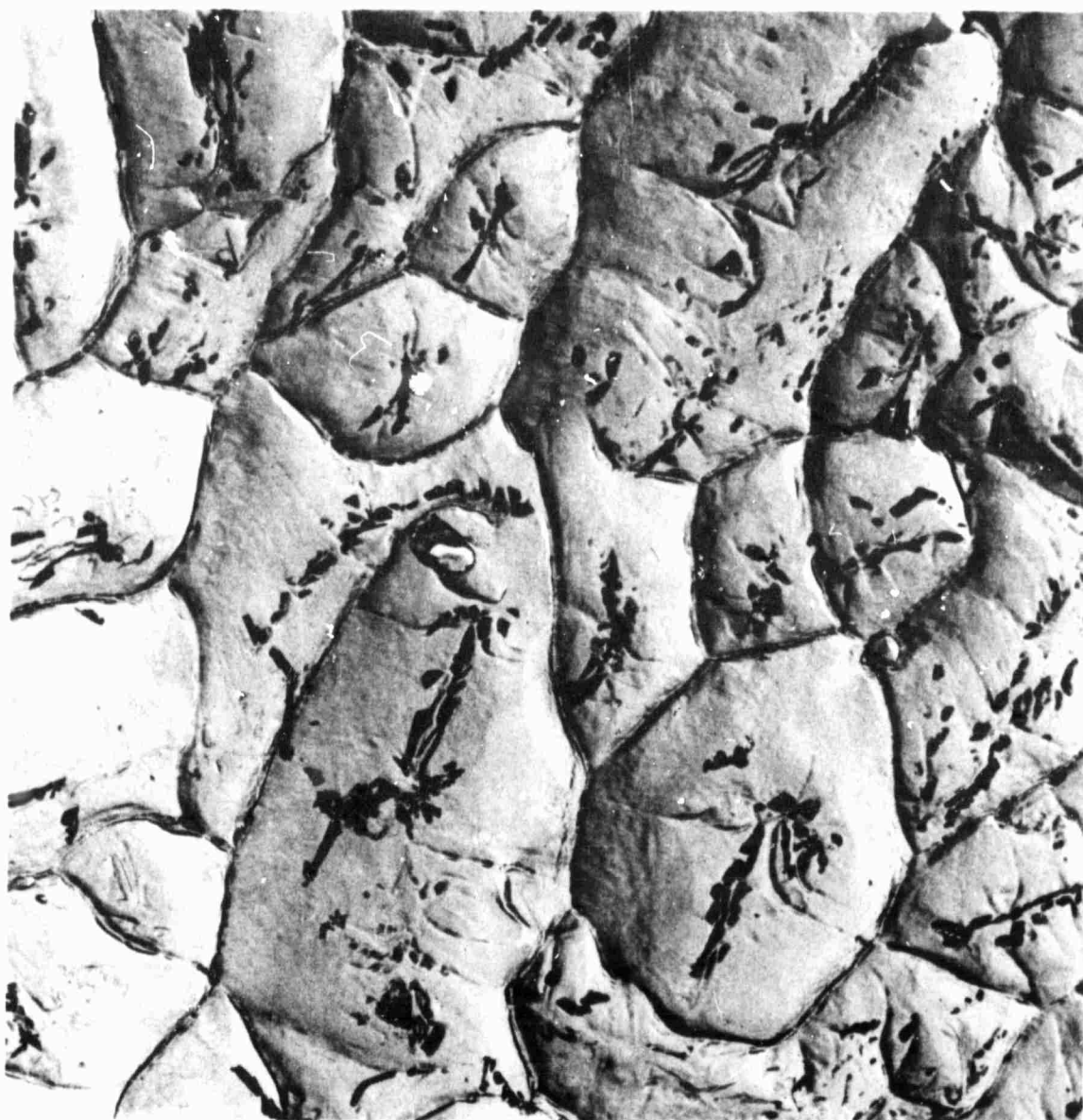
Plate No. 7183-E   Magnification: 10,000X

Figure 70.   Extraction Replica of Fracture Surface of
             Steel W-8202-A (1 hour at 2200°F → 4 hours
             at 1500°F, air-cooled, 3 hours at 900°F,
             air-cooled).

125

Plate No. 7182-D   Magnification: 10,000X

Figure 71. Extraction Replica of Fracture Surface of
            Steel W-8202-B (1 hour at 2200°F → 4 hours
            at 1500°F, air-cooled, 3 hours at 900°F,
            air-cooled).

126

Plate No. 7180-E   Magnification: 10,000X

Figure 72.   Extraction Replica of Fracture Surface of
             Steel W-8202-C (1 hour at 2200°F → 4 hours
   at 1500°F, air-cooled, 3 hours at 900°F,
             air-cooled).

127

(a)
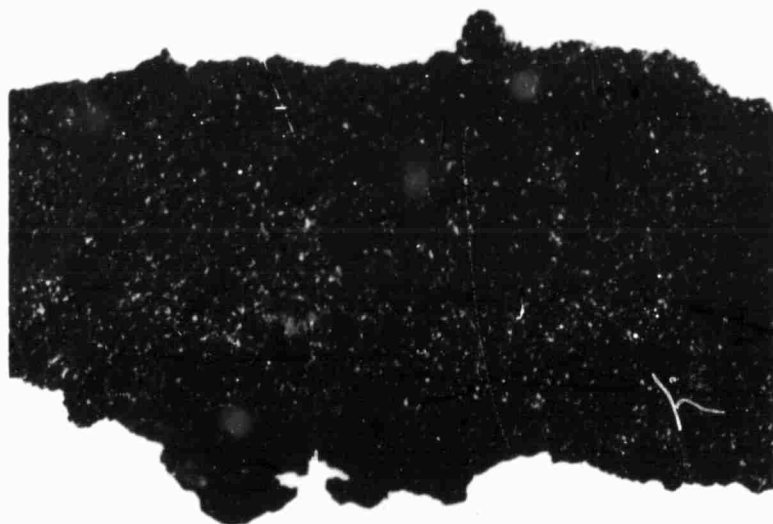
Negative No. P-6746A-1
Magnification: 3X

(b)
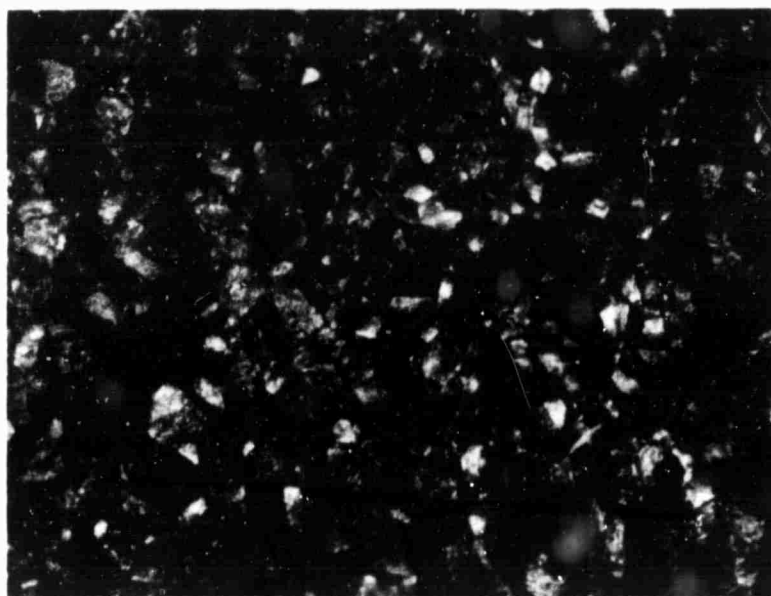
Negative No. P-6746A-2
Magnification: 30X

Figure 73. Photomacrographs of Cerium Heat W-8200
Exhibiting Hot-Shortness.
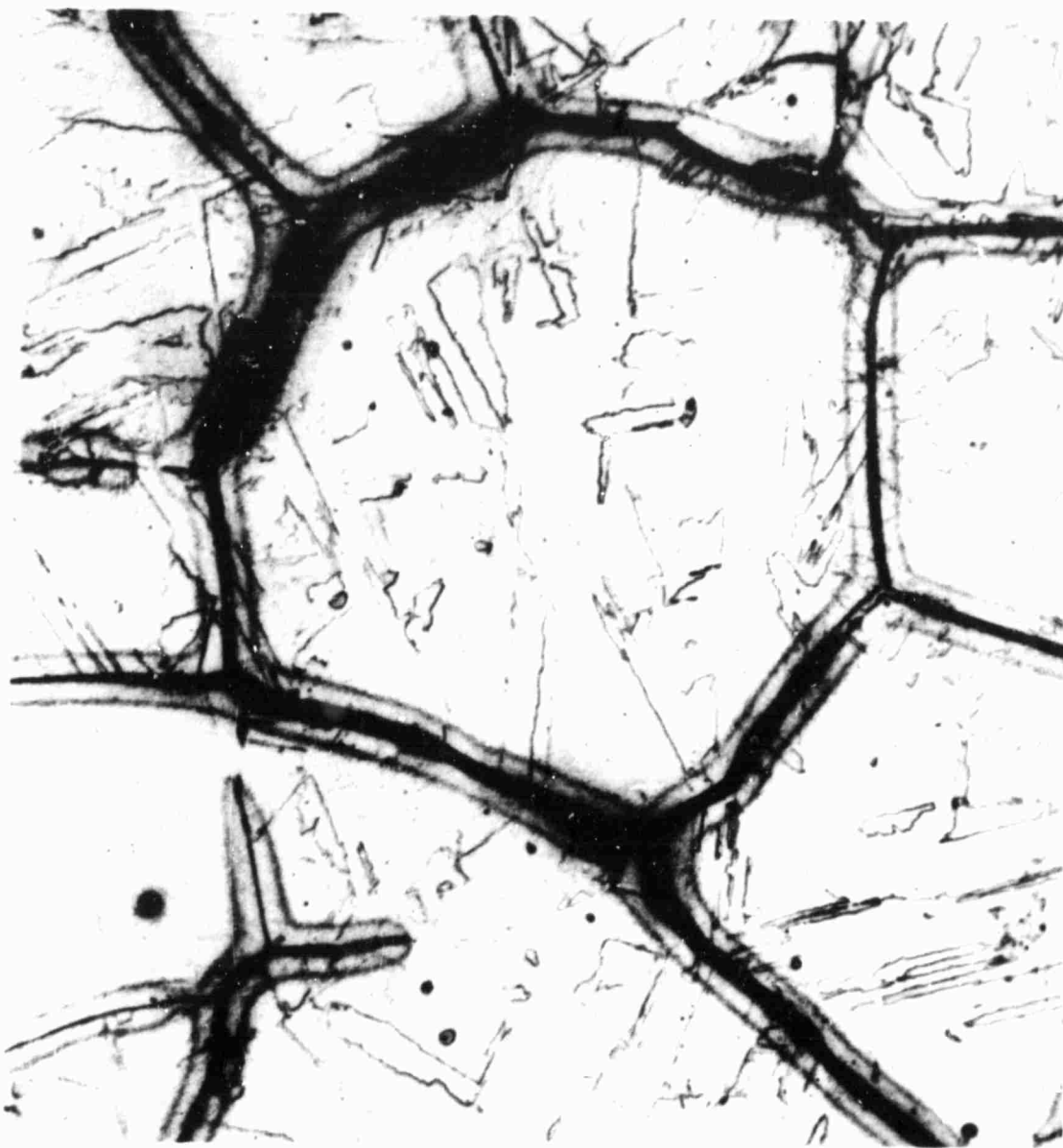
Plate No. 393   Magnification: 200X

Figure 74. Photomicrograph of Grain-Boundary
            Condition of Cerium Heat W-8200.

TABLE 1

Chemical Analysis of the Commercial Plate (Heat No. X-53541), percent*

C	Mn	P	S	Si	Ni	Mo	Ti	Al	Co	N
0.015	0.05	0.001	0.009	0.032	17.3	4.88	0.42	0.114	8.27	0.005

*In this table, and all subsequent chemical analyses, compositions are given in terms of weight percent.

130

TABLE 2 (sheet 1 of 3 sheets)

Thermal Treatment and Mechanical Properties of the Commercial Plate (Heat Number x-53541)
(High-Temperature Annealing Atmosphere—Cracked Ammonia)

Code No.	Thermal Treatment	Unaged CVN Energy Absorbed at +80°F, ft-lb	Unaged Yield Strength (0.2% Offset), ksi	Unaged Tensile Strength, ksi	Unaged Elongation in 1.4 Inch, %	Unaged Reduction of Area, %	Aged Code No.	Aged CVN Energy Absorbed at +80°F, ft-lb	Aged Yield Strength (0.2% Offset), ksi	Aged Tensile Strength, ksi	Aged Elongation in 1.4 Inch, %	Aged Reduction of Area, %
1	Mill-Annealed*	61	133	148	17.1	69.7	1A	19	247	256	9.6	43.8
2	1 hr at 1500°F, AC**	62	114	144	17.4	69.3	2A	18	246	257	10.4	45.0
3	1 hr at 2000°F, AC	62	115	151	14.6	58.0	3A	18	244	257	11.0	42.2
4	1 hr at 2100°F, AC	73	110	153	14.3	54.0	4A	19	239	253	10.0	43.4
5	1 hr at 2200°F, AC	77	106	146	5.4	23.2	5A	17	240	254	6.8	21.6
6	1 hr at 2300°F, AC	82	108	141	4.3	16.6	6A	13	238	255	5.4	14.8
7	1 hr at 2400°F, AC	69	108	131	2.9	13.3	7A	10	239	252	2.5	3.0
8	1 hr at 2000°F, AC, 1 hr at 1500°F, AC	68	113	150	15.0	61.4	8A	19	249	259	10.4	43.1
9	1 hr at 2100°F, AC, 1 hr at 1500°F, AC	69	112	151	15.7	64.1	9A	17	244	250	8.2	34.3
10	1 hr at 2200°F, AC, 1 hr at 1500°F, AC	73	117	151	15.1	58.7	10A	16	247	256	7.5	27.9
11	1 hr at 2300°F, AC, 1 hr at 1500°F, AC	62	120	150	14.6	60.2	11A	13	248	258	4.6	11.1
12	1 hr at 2400°F, AC, 1 hr at 1500°F, AC	55	117	150	14.3	57.6	12A	11	244	255	2.1	4.2
13	1 hr at 2000°F + 1/2 hr at 1300°F, AC	61	120	150	15.4	60.6	13A	18	240	255	11.4	46.2
14	1 hr at 2000°F + 4 hr at 1300°F, AC	62	118	148	16.4	64.0	14A	16	239	253	8.6	33.4
15	1 hr at 2000°F + 1/2 hr at 1400°F, AC	66	115	151	15.7	58.2	15A	15	237	251	7.5	28.0
16	1 hr at 2000°F + 4 hr at 1400°F, AC	57	116	146	16.0	60.4	16A	12	235	248	6.8	22.2
17	1 hr at 2000°F + 1/2 hr at 1500°F, AC	57	112	147	15.4	58.8	17A	13	235	249	8.0	28.1
18	1 hr at 2000°F + 4 hr at 1500°F, AC	54	104	140	16.4	53.7	18A	12	230	244	8.0	29.6
19	1 hr at 2000°F + 1/2 hr at 1600°F, AC	50	108	147	14.3	62.4	19A	11.5	236	250	6.0	18.8
20	1 hr at 2000°F + 4 hr at 1600°F, AC	41	103	140	14.6	54.4	20A	10.5	231	243	6.0	20.6
21	1 hr at 2000°F + 1/2 hr at 1700°F, AC	47	113	143	14.3	55.6	21A	13	229	250	9.6	37.4
22	1 hr at 2000°F + 4 hr at 1700°F, AC	33	103	140	14.3	56.5	22A	9	227	250	5.4	20.4

*Double Annealed: 1-1/2 hr at 1650°F, Air-Cooled; 1-1/2 hr at 1530°F, Air-Cooled.
**Air-Cooled.

131

TABLE 2 (sheet 2 of 3 sheets)

Code No.	Thermal Treatment	Unaged CVN Energy Absorbed at +80°F, ft-lb	Unaged Yield Strength (0.2% Offset), ksi	Unaged Tensile Strength, ksi	Unaged Elongation in 1.4 Inch, %	Unaged Reduction of Area, %	Code No.	Aged CVN Energy Absorbed at +80°F, ft-lb	Aged Yield Strength (0.2% Offset), ksi	Aged Tensile Strength, ksi	Aged Elongation in 1.4 Inch, %	Aged Reduction of Area, %
23	1 hr at 2100°F + 1/2 hr at 1300°F, AC	74	109	150	14.6	60.8	23A	19	242	256	8.5	32.2
24	1 hr at 2100°F + 4 hr at 1300°F, AC	71	108	149	15.0	58.1	24A	15	239	253	6.8	20.4
25	1 hr at 2100°F + 1/2 hr at 1400°F, AC	80	108	150	15.0	61.2	25A	13	242	255	5.2	15.3
26	1 hr at 2100°F + 4 hr at 1400°F, AC	68	109	148	15.4	58.7	26A	10.5	238	252	4.8	14.0
27	1 hr at 2100°F + 1/2 hr at 1500°F, AC	62	121	150	14.3	52.2	27A	11	238	252	5.7	18.6
28	1 hr at 2100°F + 4 hr at 1500°F, AC	53	118	144	15.4	57.6	28A	10.5	235	248	5.9	19.2
29	1 hr at 2100°F + 1/2 hr at 1600°F, AC	52	119	150	13.6	49.3	29A	8.5	240	254	3.8	11.4
30	1 hr at 2100°F + 4 hr at 1600°F, AC	31	120	144	14.0	50.8	30A	6.5	234	248	3.6	7.4
31	1 hr at 2100°F + 1/2 hr at 1700°F, AC	39	113	148	14.6	52.7	31A	8	221	252	5.4	16.6
32	1 hr at 2100°F + 4 hr at 1700°F, AC	26	98	140	14.3	53.0	32A	6	+	+	+	+
33	1 hr at 2200°F + 1/2 hr at 1300°F, AC	88	114	129	9.8	++	33A	17.5	230	246	4.8	13.8
34	1 hr at 2200°F + 4 hr at 1300°F, AC	87	117	150	17.1	61.6	34A	11	229	247	5.0	17.5
35	1 hr at 2200°F + 1/2 hr at 1400°F, AC	99	117	150	14.3	51.6	35A	15	235	254	6.1	21.4
36	1 hr at 2200°F + 4 hr at 1400°F, AC	71	117	149	15.7	58.3	36A	10	+	+	+	+
37	1 hr at 2200°F + 1/2 hr at 1500°F, AC	59	119	151	15.7	52.9	37A	8.5	237	255	3.6	7.4
38	1 hr at 2200°F + 4 hr at 1500°F, AC	48	116	143	15.7	53.4	38A	6.5	234	248	4.3	10.0
39	1 hr at 2200°F + 1/2 hr at 1600°F, AC	51	119	150	15.4	49.8	39A	7	246	249	4.3	7.6
40	1 hr at 2200°F + 4 hr at 1600°F, AC	24	115	142	14.3	52.6	40A	5.5	228	244	4.3	10.0
41	1 hr at 2200°F + 1/2 hr at 1700°F, AC	30	114	150	14.3	50.3	41A	5.5	230	251	2.5	8.8
42	1 hr at 2200°F + 4 hr at 1700°F, AC	14	110	143	12.1	45.6	42A	5	222	247	1.4	3.4
43	1 hr at 2300°F + 1/2 hr at 1300°F, AC	88	113	148	13.6	48.9	43A	13	229	248	4.0	6.6
44	1 hr at 2300°F + 4 hr at 1300°F, AC	97	114	149	17.1	63.9	44A	10.5	235	253	4.3	9.4
45	1 hr at 2300°F + 1/2 hr at 1400°F, AC	56	109	150	11.8	60.4	45A	7.5	234	249	4.0	8.2
46	1 hr at 2300°F + 4 hr at 1400°F, AC	60	104	148	15.0	57.0	46A	6	225	251	1.4	5.6

+Not Determined.
++Broke Outside Gage Marks.

132

TABLE 2 (sheet 3 of 3 sheets)

Code No.	Thermal Treatment	Unaged CVN Energy Absorbed at +80°F, ft-lb	Unaged Yield Strength (0.2% Offset), ksi	Unaged Tensile Strength, ksi	Unaged Elongation in 1.4 Inch, %	Unaged Reduction of Area, %	Aged Code No.	Aged CVN Energy Absorbed at +80°F, ft-lb	Aged Yield Strength (0.2% Offset), ksi	Aged Tensile Strength, ksi	Aged Elongation in 1.4 Inch, %	Aged Reduction of Area, %
47	1 hr at 2300°F → 1/2 hr at 1500°F, AC	42	117	150	13.2	43.4	47A	6	239	250	1.4	2.6
48	1 hr at 2300°F → 4 hr at 1500°F, AC	27	114	143	12.8	47.3	48A	4.5	235	246	2.1	2.2
49	1 hr at 2300°F → 1/2 hr at 1600°F, AC	13	117	151	11.4	37.4	49A	3.5	241	253	1.4	2.8
50	1 hr at 2300°F → 4 hr at 1600°F, AC	15	115	142	12.1	42.5	50A	4.5	230	242	1.8	3.4
51	1 hr at 2300°F → 1/2 hr at 1700°F, AC	10	118	151	12.2	33.2	51A	4	236	249	1.4	2.0
52	1 hr at 2300°F → 4 hr at 1700°F, AC	8	115	144	9.3	27.8	52A	3.5	232	236	1.4	0.9
53	1 hr at 2400°F → 1/2 hr at 1300°F, AC	69	110	149	14.6	57.6	53A	9	237	253	2.9	7.1
54	1 hr at 2400°F → 4 hr at 1300°F, AC	79	109	149	16.4	63.3	54A	8.5	237	254	1.4	4.4
55	1 hr at 2400°F → 1/2 hr at 1400°F, AC	43	113	150	16.4	58.8	55A	7	231	247	0.5	2.0
56	1 hr at 2400°F → 4 hr at 1400°F, AC	45	116	148	15.4	58.3	56A	5.5	235	245	0.7	2.2
57	1 hr at 2400°F → 1/2 hr at 1500°F, AC	18	117	151	13.2	43.7	57A	4	*	222	1.4	1.4
58	1 hr at 2400°F → 4 hr at 1500°F, AC	24	113	142	13.6	49.8	58A	5	236	244	1.4	2.2
59	1 hr at 2400°F → 1/2 hr at 1600°F, AC	20	115	151	11.9	40.0	59A	5	232	246	1.4	1.1
60	1 hr at 2400°F → 4 hr at 1600°F, AC	18	107	142	12.1	44.1	60A	4	220	237	1.4	1.7
61	1 hr at 2400°F → 1/2 hr at 1700°F, AC	8.5	115	149	8.2	26.2	61A	4	221	235	4.3	6.0
62	1 hr at 2400°F → 4 hr at 1700°F, AC	19	110	142	12.9	52.8	62A	5.5	237	256	1.4	2.3
63	1 hr at 2100°F → 1/2 hr at 1800°F, AC	40	112	149	15.7	59.8	63A	9.5	241	257	4.0	12.2
64	1 hr at 2100°F → 4 hr at 1800°F, AC	36	107	144	15.0	59.2	64A	9	240	254	5.4	16.6
65	16 hr at 2200°F, AC	97	115	145	16.0	66.6	65A	16	231	253	6.4	23.6
66	16 hr at 2200°F → 1/2 hr at 1500°F, AC	61	103	148	15.7	60.8	66A	7.5	237	253	2.2	2.8
67	16 hr at 2200°F → 4 hr at 1500°F, AC	40	110	145	14.3	56.6	67A	5.5	240	255	2.8	4.5

*Fractured Before 0.2% Yield.

133

TABLE 3

Thermal Treatments and Mechanical Properties of the Commercial Plate (Heat No. X-53541) (High-Temperature Annealing Atmosphere—Argon)

Code	Heat Treatment	Unaged CVN Energy Absorbed at +80°F, ft-lb	Unaged Yield Strength (0.2% Offset), ksi	Unaged Tensile Strength, ksi	Unaged Elongation in 1.4 Inch, %	Unaged Reduction of Area, %	Aged CVN Energy Absorbed at +80°F, ft-lb	Aged Yield Strength (0.2% Offset), ksi	Aged Tensile Strength, ksi	Aged Elongation in 1.4 Inch, %	Aged Reduction of Area, %
101	1 hr at 1500°F, AC*	67	100	142	16.4	67.4	19	252	261	11.5	42.7
102	1 hr at 2000°F, AC	72	110	150	16.4	64.3	17	234	252	11.4	44.8
103	1 hr at 2100°F, AC	83	111	150	16.7	65.8	18	231	250	10.7	46.8
104	1 hr at 2200°F, AC	81	106	149	13.9	64.8	16	233	250	9.3	36.9
105	1 hr at 2300°F, AC	75	115	150	16.4	63.0	13	223	246	6.8	24.4
106	1 hr at 2400°F, AC	81	108	149	10.6	68.6	11	234	252	2.1	3.0
107	1 hr at 2300°F, AC, 1 hr at 1500°F, AC	78	105	149	16.7	67.9	11	241	258	4.3	12.3
108	1 hr at 2000°F + 4 hr at 1500°F, AC	54	107	141	14.6	55.4	8	235	250	5.3	17.6
109	1 hr at 2100°F + 4 hr at 1500°F, AC	51	110	149	15.0	58.2	11	234	253	6.2	21.2
110	1 hr at 2200°F + 1/2 hr at 1400°F, AC	94	112	148	16.4	64.0	13	230	249	4.5	15.5
111	1 hr at 2200°F + 4 hr at 1400°F, AC	83	110	148	15.0	56.3	10	234	250	4.3	7.2
112	1 hr at 2200°F + 1/2 hr at 1500°F, AC	66	111	147	15.7	58.5	8.5	232	249	4.3	6.0
113	1 hr at 2200°F + 4 hr at 1500°F, AC	59	112	141	15.3	58.7	7	227	242	3.2	8.1
114	1 hr at 2200°F + 1/2 hr at 1800°F, AC	31	110	148	15.0	53.1	5	224	245	2.9	4.5
115	1 hr at 2200°F + 4 hr at 1800°F, AC	15	109	142	12.1	42.7	4	234	251	1.4	2.2
116	1 hr at 2300°F + 1/2 hr at 1400°F, AC	60	106	152	14.4	56.3	7	230	251	3.9	6.5
117	1 hr at 2300°F + 1/2 hr at 1500°F, AC	48	112	149	15.7	58.3	7	230	248	2.9	2.5
118	1 hr at 2300°F + 4 hr at 1500°F, AC	40	108	140	15.3	56.3	5.5	232	248	1.7	3.5
119	1 hr at 2300°F + 1/2 hr at 1600°F, AC	18	111	147	12.4	44.0	4	231	249	1.8	3.0
120	1 hr at 2300°F + 1/2 hr at 1700°F, AC	16	113	149	11.6	37.3	5	234	248	1.4	2.5
121	1 hr at 2300°F + 1/2 hr at 1800°F, AC	9	100	148	10.7	35.3	4	228	242	0.7	2.8
122	1 hr at 2300°F + 4 hr at 1800°F, AC	7	110	144	9.3	33.5	3	232	247	1.4	1.0
123	1 hr at 2400°F + 4 hr at 1500°F, AC	28	108	151	13.1	52.2	5	229	249	1.3	2.0

*Air-Cooled.

134

TABLE 4

Effect of Annealing Atmosphere on Impact Toughness and Tensile Ductility

Treatment Number	Heat Treatment	Unaged				Aged			
		CVN** Energy Absorbed at +80°F, ft-lb	CVN+ Energy Absorbed at +80°F, ft-lb	Reduction of Area,** %	Reduction of Area,+ %	CVN** Energy Absorbed at +80°F, ft-lb	CVN+ Energy Absorbed at +80°F, ft-lb	Reduction of Area,** %	Reduction of Area,+ %
1	1 hr at 1500°F, AC*	62	67	69.3	67.4	18	19	45.0	42.7
2	1 hr at 2000°F, AC	62	72	58.0	64.3	18	17	42.2	44.8
3	1 hr at 2100°F, AC	73	83	54.0	65.8	19	18	43.4	46.8
4	1 hr at 2200°F, AC	77	81	23.2	64.8	17	16	21.6	36.9
5	1 hr at 2300°F, AC	82	79	16.6	64.8	13	13	14.8	24.4
6	1 hr at 2400°F, AC	69	81	13.3	68.6	10	11	3.0	3.0
7	1 hr at 2300°F, AC, 1 hr at 1500°F, AC	62	78	60.2	67.9	13	11	11.1	12.3
8	1 hr at 2000°F + 4 hr at 1500°F, AC	54	54	53.7	55.4	12	8	29.6	17.6
9	1 hr at 2100°F + 4 hr at 1500°F, AC	53	51	57.6	58.2	10.5	11	19.2	21.2
10	1 hr at 2200°F + 1/2 hr at 1400°F, AC	99	94	51.6	64.0	15	13	21.4	15.5
11	1 hr at 2200°F + 4 hr at 1400°F, AC	71	83	58.3	56.3	10	10		7.2
12	1 hr at 2200°F + 1/2 hr at 1500°F, AC	59	66	52.9	58.5	8.5	8.5	7.4	6.0
13	1 hr at 2200°F + 4 hr at 1500°F, AC	48	59	53.4	58.7	6.5	7	10.0	8.1
14	1 hr at 2300°F + 1/2 hr at 1400°F, AC	56	60	40.4	46.3	7.5	7	8.2	6.5
15	1 hr at 2300°F + 1/2 hr at 1500°F, AC	42	48	43.4	58.3	6	7	2.6	2.5
16	1 hr at 2300°F + 4 hr at 1500°F, AC	27	40	47.3	56.3	4.5	5.5	2.2	3.5
17	1 hr at 2300°F + 1/2 hr at 1600°F, AC	13	15	37.4	44.0	3.5	4	2.8	3.0
18	1 hr at 2300°F + 1/2 hr at 1700°F, AC	10	13	33.2	37.3	4	5	2.0	2.5
19	1 hr at 2400°F + 4 hr at 1500°F	24	28	49.8	52.2	5	5	2.2	2.0

*Air-Cooled.
**Cracked-Ammonia Annealing Atmosphere.
+Argon Annealing Atmosphere.

TABLE 5

Hydrogen and Nitrogen Analyses of the Commercial Plate

Annealing Atmosphere	Thermal Treatment	Hydrogen, ppm	Nitrogen, %
Air	1-1/2 hr at 1650°F, AC, 1-1/2 hr at 1530°F, AC*[+]	0.49	0.005
Cracked Ammonia	1 hr at 2300°F, WQ**	4.72	0.007
Cracked Ammonia	1 hr at 2300°F, WQ, 3 hr at 900°F, AC	0.34	0.007
Cracked Ammonia	1 hr at 2300°F, AC	3.89	0.007
Cracked Ammonia	1 hr at 2300°F, AC, 1 hr at 1500°F, AC	2.53	0.007
Cracked Ammonia	1 hr at 1500°F, AC	2.14	0.004
Cracked Ammonia	1 hr at 1500°F, AC, 3 hr at 900°F, AC	0.28	0.005
Cracked Ammonia	1 hr at 2300°F → 4 hr at 1500°F, AC	0.78	0.005
Argon	1 hr at 2300°F, AC	0.42	0.003

*Air-Cooled.
**Water-Quenched.
[+]Mill-Annealed.

TABLE 6

Effect of Thermal Embrittlement on Plane-Strain Fracture Toughness

Heat Treatment	Plane-Strain Fracture Toughness K_{Ic}, ksi√inch		CVN Energy, ft-lb
1 hr at 2300°F, AC, 3 hr at 900°F, AC*	77.5, 73.4	Av 75.4	13
1 hr at 2300°F → 4 hr at 1700°F, AC	46.2, 46.5	Av 46.3	8
1 hr at 2300°F → 4 hr at 1700°F, AC, 3 hr at 900°F, AC	29.4, 33.6	Av 31.5	3.5
1 hr at 2400°F, AC, 3 hr at 900°F, AC	56.4, 61.8, 62.3	Av 60.2	10
1 hr at 2400°F → 4 hr at 1700°F, AC	45.4, 39.6	Av 42.5	6
1 hr at 2400°F → 4 hr at 1700°F, AC, 3 hr at 900°F, AC	36.8, 35.6	Av 36.2	5.5

*Air-Cooled.

137

TABLE 7

Electron Diffraction Pattern from Extraction Replica
of Fracture Surface of Commercial Plate*

Replica		TiC**		TiN+		τ-Ti$_2$S++	
I/I$_O$	d(Å)	I/I$_O$	d(Å)	I/I$_O$	d(Å)	I/I$_O$	d(Å)
W	2.77					50	2.77
						20	2.69
S	2.48	80	2.51	77	2.44		
VW	2.22					100	2.22
S	2.14	100	2.18	100	2.12		
						20	1.96
						30	1.86
						10	1.74
W	1.60					70	1.60
VS	1.52	50	1.54	56	1.50	50	1.54
VW	1.42					60	1.38
S	1.31	30	1.31	26	1.28	50	1.30
W	1.25	10	1.26	16	1.22		
						50	1.21
VVW	1.12					30	1.13
VW	1.08	5	1.09	7	1.06	20	1.11
						10	1.05
VVW	1.04					20	1.04
VW	1.00					70	1.01
W	0.99	5	1.00	11	0.97		
M	0.97	30	0.97	22	0.95	20	0.95

*Annealed 1 Hour at 2300°F → 4 Hours at 1700°F and Air-Cooled.

**ASTM X-Ray Powder Data File, Card No. 6-0614.

+ASTM X-Ray Powder Data File, Card No. 6-0642.

++ASTM X-Ray Powder Data File, Card No. 11-664.

138

TABLE 8

Chemical Composition of Heats Investigated

Heat No.	C	Mn	P	S	Si	Ni	Mo	Co	Ti	Al	N	O (ppm)
V-8497	0.004	0.004	0.0006	0.002	<0.01	18.0	4.67	7.99	0.30	0.004	0.003	20
V-8858	0.027	0.004	<0.001	0.0025	0.004	18.1	4.78	8.04	0.35	0.019	0.001	10

139

TABLE 9

Mechanical Properties of Heats V-8497 and V-8858

Heat Treatment No.	Heat Treatment	Yield Strength (0.2% Offset), ksi	Tensile Strength, ksi	Elongation in 1 Inch, %	Reduction of Area, %	CVN Energy Absorbed at +80°F, ft-lb
	Heat V-8497					
1	As-rolled	104	137	19.0	81.8	158
2	As-rolled, 3 hr at 900°F, AC*	233	242	12.5	62.2	31
3	1 hr at 1500°F, AC	109	137	18.0	82.3	173
4	1 hr at 1500°F, AC, 3 hr at 900°F, AC	230	240	12.5	65.0	39
5	1 hr at 2200°F, AC	111	135	18.5	79.1	139
6	1 hr at 2200°F, AC, 3 hr at 900°F, AC	222	228	11.0	49.4	21
7	1 hr at 2200°F + 4 hr at 1500°F, AC	101	133	18.5	78.0	38
8	1 hr at 2200°F + 4 hr at 1500°F, AC, 3 hr at 900°F, AC	218	231	4.5	10.0	6
9	1 hr at 2200°F, AC, 1 hr at 1500°F, AC	113	144	18.0	77.8	148
10	1 hr at 2200°F, AC, 1 hr at 1500°F, AC, 3 hr at 900°F, AC	239	247	10.8	55.4	32
	Heat V-8858					
1	As-rolled	119	156	15.5	69.0	47
2	As-rolled, 3 hr at 900°F, AC	238	248	10.5	53.0	16
3	1 hr at 1500°F, AC	107	144	17.0	73.5	78
4	1 hr at 1500°F, AC, 3 hr at 900°F; AC	239	245	11.0	53.0	20
5	1 hr at 2200°F, AC	105	153	16.0	65.4	60
6	1 hr at 2200°F, AC, 3 hr at 900°F, AC	226	240	8.0	30.5	16
7	1 hr at 2200°F + 4 hr at 1500°F, AC	114	142	14.5	59.5	38
8	1 hr at 2200°F + 4 hr at 1500°F, AC, 3 hr at 900°F, AC	225	239	3.5	8.5	7
9	1 hr at 2200°F, AC, 1 hr at 1500°F, AC	117	149	16.5	71.8	88
10	1 hr at 2200°F, AC, 1 hr at 1500°F, AC, 3 hr at 900°F, AC	244	246	9.8	48.8	20

*Air-Cooled.

TABLE 10

Typical Ring Diffraction Patterns from Fracture Surface Extraction Replicas of Thermally Embrittled Specimens

Heat No. V-8858 (0.027% Carbon)

Heat Treatment No. 8			Heat Treatment No. 5		
I/I_o	d(Å)	Ti(C,N)*	I/I_o	d(Å)	τ-Ti$_2$S**
VW	2.76		S	2.82	X
VS	2.46	X	M	2.72	X
S	2.13	X	M	2.51	
VW	1.60		M	2.24	X
VS	1.51	X	VVW	2.19	
S	1.29	X	S	1.61	X
W	1.23	X	W	1.54	X
VW	1.06	X	VW	1.39	X
M	0.99	X	VW	1.35	
M	0.96	X	M	1.31	X
M	0.87	X	W	1.05	X
			VVW	1.03	X
			M	1.01	X

Heat No. V-8497 (0.004% Carbon)

Heat Treatment No. 9			
I/I_o	d(Å)	Ti(C,N)*	τ-Ti$_2$S**
W	2.79		X
S	2.51	X	
W	2.25		X
S	2.19	X	
M	1.61	X	X
S	1.54		X
VW	1.49		
W	1.39	X	X
S	1.30	X	X
W	1.25	X	X
VVW	1.22	X	X
VVW	1.075		
VW	1.045		X
W	1.015		X
W	0.99	X	
M	0.965	X	
VW	0.93		X
VVW	0.92		X
M	0.88	X	

*ASTM X-Ray Powder Data File, Cards No. 6-0642 and No. 6-0614.

**ASTM X-Ray Powder Data File, Card No. 11-664.

TABLE 11

Chemical Composition of Aluminum-Substituted Steels

Heat No.	C	Mn	P	S	Si	Ni	Mo	Ti	Al	Co	N	O (ppm)
					Composition, percent							
T-6109	0.001	0.003	0.0005	0.0018	0.015	17.7	4.97	-	0.19	9.00	0.001	9
W-8068	0.002	0.002	0.0009	0.0011	0.002	18.7	5.00	-	0.44	9.12	0.001	5
W-8135-2	0.018	0.002	0.0009	0.0011	0.003	18.4	4.93	-	0.38	9.08	0.001	5
W-8598	0.001	0.008	0.0003	0.0015	0.006	18.1	4.94	<0.02	0.40	8.97	0.001	14
W-8252-1A	0.003	0.098	0.0006	0.0017	0.015	18.0	5.04	<0.02	0.49	8.85	0.002	7
W-8252-1B	0.002	0.19	0.0005	0.0023	0.012	18.0	5.10	<0.02	0.49	8.86	0.001	8
W-8252-1C	0.002	0.29	0.0005	0.0022	0.012	18.0	4.96	<0.02	0.48	8.81	0.002	7
W-8236	0.002	0.002	0.0007	0.0008	0.001	18.4	4.93	-	1.06	9.05	0.001	11

142

TABLE 12

Thermal Treatment and Mechanical Properties of the Aluminum-Substituted Steel (Heat No. T-6109)

Thermal Treatment	Yield Strength (0.2% Offset), ksi	Tensile Strength, ksi	Elongation in 1 Inch, %	Reduction of Area, %	Charpy V-Notch Energy Absorbed at +80°F, ft-lb
1 hr at 1500°F, AC*	113	145	18.0	81.3	194
1 hr at 1500°F, AC, 3 hr at 900°F, AC	225	235	12.5	64.3	33
1 hr at 2100°F, AC	110	141	13.0	56.7	98
1 hr at 2100°F, AC, 3 hr at 900°F, AC	225	233	11.5	53.0	39
1 hr at 2100°F, AC**	108	144	20.5	81.5	191
1 hr at 2100°F, AC, 3 hr at 900°F, AC**	215	232	13.0	65.8	49
1 hr at 2100°F + 20 min at 1500°F, AC	114	146	17.0	79.6	168
1 hr at 2100°F + 20 min at 1500°F, AC, 3 hr at 900°F, AC	218	235	11.3	62.5	34
1 hr at 2100°F + 1 hr at 1500°F, AC	110	143	18.0	81.3	174
1 hr at 2100°F + 1 hr at 1500°F, AC, 3 hr at 900°F, AC	219	234	11.0	60.0	28
1 hr at 2100°F + 4 hr at 1500°F, AC	114	143	17.0	76.6	109
1 hr at 2100°F + 4 hr at 1500°F, AC, 3 hr at 900°F, AC	218	233	10.0	45.6	17
1 hr at 2100°F + 4 hr at 1500°F, AC**	112	143	17.8	77.3	131
1 hr at 2100°F + 4 hr at 1500°F, AC, 3 hr at 900°F, AC**	209	234	11.0	42.5	22
1 hr at 2200°F + 4 hr at 1500°F, AC	111	143	15.8	76.4	153
1 hr at 2200°F + 4 hr at 1500°F, AC, 3 hr at 900°F, AC	214	231	9.0	46.2	33
1 hr at 2300°F + 4 hr at 1500°F, AC	112	143	16.5	76.5	112
1 hr at 2300°F + 4 hr at 1500°F, AC, 3 hr at 900°F, AC	215	232	5.3	26.9	22
1 hr at 2300°F + 4 hr at 1500°F, AC**	111	140	18.3	79.8	113
1 hr at 2300°F + 4 hr at 1500°F, AC, 3 hr at 900°F, AC**	207	231	5.5	22.7	27

*Air-Cooled.
**Heat-Treated in Argon Atmosphere.

TABLE 13

Thermal Treatment and Mechanical Properties of an Aluminum-Substituted Steel (Heat No. W-8068)

Thermal Treatment	Yield Strength (0.2% Offset), ksi	Tensile Strength, ksi	Elongation in 1 Inch, %	Reduction of Area, %	Charpy V-Notch Energy Absorbed at +80°F, ft-lb
As-Rolled	98	139	17.0	86.2	206
As-Rolled, 6 hr at 900°F, AC*	235	258	12.0	67.5	38
1 hr at 1500°F, AC	108	147	18.0	80.2	181
1 hr at 1500°F, AC, 6 hr at 900°F, AC	248	262	12.5	62.6	29
1 hr at 2200°F, AC, 6 hr at 900°F, AC	236	252	8.8	38.0	22
1 hr at 2200°F + 1/2 hr at 1500°F, AC	113	139	19.0	83.5	167
1 hr at 2200°F + 1/2 hr at 1500°F, AC, 6 hr at 900°F, AC	237	252	7.2	37.8	20
1 hr at 2200°F + 4 hr at 1500°F, AC	112	138	14.8	66.2	39
1 hr at 2200°F + 4 hr at 1500°F, AC, 6 hr at 900°F, AC	235	252	5.8	22.3	12
1 hr at 2400°F, AC, 6 hr at 900°F, AC	235	249	7.0	28.7	24
1 hr at 2400°F + 1/2 hr at 1500°F, AC	113	137	19.2	81.5	149
1 hr at 2400°F + 1/2 hr at 1500°F, AC, 6 hr at 900°F, AC	235	251	6.8	27.2	17
1 hr at 2400°F + 4 hr at 1500°F, AC	114	137	16.0	68.0	25
1 hr at 2400°F + 4 hr at 1500°F, AC, 6 hr at 900°F, AC	237	249	3.3	9.0	9
1 hr at 2200°F, AC, 1/2 hr at 1500°F, AC	108	152	17.5	77.1	168
1 hr at 2200°F, AC, 1/2 hr at 1500°F, AC, 6 hr at 900°F, AC	243	256	10.0	46.4	21
1 hr at 2200°F, AC, 4 hr at 1500°F, AC	109	145	18.0	76.5	173
1 hr at 2200°F, AC, 4 hr at 1500°F, AC, 6 hr at 900°F, AC	240	254	9.2	45.2	20

*Air-Cooled.

144

TABLE 14

Thermal Treatment and Mechanical Properties of an Aluminum-Substituted Steel (Heat No. W-8135-2)

Thermal Treatment	Yield Strength (0.2% Offset), ksi	Tensile Strength, ksi	Elongation in 1 Inch, %	Reduction of Area, %	Charpy V-Notch Energy Absorbed at +80°F, ft-lb
As-Rolled	117	156	16.0	79.0	171
As-Rolled, 6 hr at 900°F, AC*	246	262	12.2	67.0	27
1 hr at 1500°F, AC	116	154	17.0	80.2	163
1 hr at 1500°F, AC, 6 hr at 900°F, AC	243	251	11.5	63.4	28
1 hr at 2200°F, AC, 6 hr at 900°F, AC	239	258	11.3	55.1	20
1 hr at 2200°F → 1/2 hr at 1500°F, AC	118	152	18.2	76.9	86
1 hr at 2200°F → 1/2 hr at 1500°F, AC, 6 hr at 900°F, AC	241	258	5.5	23.1	15
1 hr at 2200°F → 4 hr at 1500°F, AC	120	152	10.0	36.0	12
1 hr at 2200°F → 4 hr at 1500°F, AC, 6 hr at 900°F, AC	239	257	2.5	4.0	6
1 hr at 2400°F, AC, 6 hr at 900°F, AC	241	256	8.0	36.5	23
1 hr at 2400°F, 1/2 hr at 1500°F, AC	113	151	17.8	75.6	77
1 hr at 2400°F → 1/2 hr at 1500°F, AC, 6 hr at 900°F, AC	240	257	3.5	10.5	16
1 hr at 2400°F → 4 hr at 1500°F, AC	115	151	6.2	16.7	7
1 hr at 2400°F → 4 hr at 1500°F, AC, 6 hr at 900°F, AC	**	232			4
1 hr at 2200°F, AC, 1/2 hr at 1500°F, AC	120	155	17.5	76.7	163
1 hr at 2200°F, AC, 1/2 hr at 1500°F, AC, 6 hr at 900°F, AC	248	255	10.8	50.4	28
1 hr at 2200°F, AC, 4 hr at 1500°F, AC	115	150	18.0	77.0	162
1 hr at 2200°F, AC, 4 hr at 1500°F, AC, 6 hr at 900°F, AC	242	252	10.5	46.8	18

*Air-Cooled.

**Broke Outside Gage Length.

145

TABLE 15

Electron Diffraction Data Obtained from Fracture Surface Extraction Replica of Steel W-8068*

Replica			AlN**	
I/I_O	$d(\text{Å})$		I/I_O	$d(\text{Å})$
S	2.70		100	2.70
VW	2.49		60	2.49
			70	2.37
+	1.82		21	1.83
M	1.56		30	1.56
+	1.42		21	1.41
W	1.35		5	1.35
VW	1.32		17	1.32
VW	1.30		7	1.30
VW	1.19		4	1.19
W	1.04		6	1.05

*Heat Treatment of 1 Hour at 2200°F→ 4 Hours at 1500°F, Air-Cooled, 6 Hours at 900°F, Air-Cooled.

**ASTM X-Ray Powder Data File, Card No. 8-262.

+Diffraction rings not present, only occasional spots.

TABLE 16

Electron Diffraction Data Obtained from Fracture Surface Extraction Replica of Steel W-8135-2*

Replica		AlN**		Mo_2C^+	
I/I_O	d(Å)	I/I_O	d(Å)	I/I_O	d(Å)
S	2.70	100	2.70		
VW	2.60			20	2.60
W	2.51	60	2.49		
S	2.37	70	2.37	30	2.37
W	2.28			100	2.28
W	1.82	21	1.83		
W	1.76			16	1.75
S	1.56	30	1.56		
VW	1.51			12	1.50
VVW	1.42	21	1.41		
M	1.35	5	1.35	18	1.35
M	1.32	17	1.32		
W	1.30	7	1.30	2	1.30
W	1.28			16	1.27
W	1.26			2	1.255
VW	1.185	4	1.19	2	1.18
VVW	1.145			2	1.14
VVW	1.08			2	1.08
VW	1.05	6	1.05		
W	1.02				
W	1.00			2	1.00

*Heat Treatment of 1 Hour at 2200°F → 4 Hours at 1500°F, Air-Cooled, 6 Hours at 900°F, Air-Cooled.

**ASTM X-Ray Powder Data File, Card No. 8-262.

+ASTM X-Ray Powder Data File, Card No. 11-680.

147

TABLE 17

Thermal Treatment and Mechanical Properties of an Aluminum-Substituted Steel (Heat No. W-8598)

Thermal Treatment	Yield Strength (0.2% Offset), ksi	Tensile Strength, ksi	Elongation in 1 Inch, %	Reduction of Area, %	Charpy V-Notch Energy Absorbed at +80°F, ft-lb
As-Rolled	99	139	19.0	82.6	229
As-Rolled, 3 hr at 900°F, AC	222	236	13.5	69.5	70
1 hr at 1500°F, AC	101	144	17.0	80.0	202
1 hr at 1500°F, AC, 3 hr at 900°F, AC	229	240	13.0	65.5	37
1 hr at 2200°F, AC, 3 hr at 900°F, AC	214	227	12.0	58.2	40
1 hr at 2200°F + 1/2 hr at 1500°F, AC	102	136	16.5	78.2	190
1 hr at 2200°F + 1/2 hr at 1500°F, AC, 3 hr at 900°F, AC	215	229	11.0	56.8	40
1 hr at 2200°F + 4 hr at 1500°F, AC	109	136	16.0	73.5	72
1 hr at 2200°F + 4 hr at 1500°F, AC, 3 hr at 900°F, AC	214	229	10.0	45.9	23
1 hr at 2300°F, AC, 3 hr at 900°F, AC	216	228	12.0	59.8	38
1 hr at 2300°F + 1/2 hr at 1500°F, AC	110	136	16.5	76.6	184
1 hr at 2300°F + 1/2 hr at 1500°F, AC, 3 hr at 900°F, AC	216	229	11.5	56.4	37
1 hr at 2300°F + 4 hr at 1500°F, AC	102	136	16.5	74.4	116
1 hr at 2300°F + 4 hr at 1500°F, AC, 3 hr at 900°F, AC	214	229	10.5	50.4	26
1 hr at 2200°F, AC, 1 hr at 1500°F, AC	117	149	17.0	77.2	168
1 hr at 2200°F, AC, 1 hr at 1500°F, AC, 3 hr at 900°F, AC	235	245	11.0	53.4	35

*Air-Cooled.

TABLE 18

Effect of Different Aging Treatments on the Mechanical Properties of Steels W-8068 and W-8598

Thermal Treatment	Yield Strength (0.2% Offset), ksi	Tensile Strength, ksi	Elongation in 1 Inch, %	Reduction of Area, %	Charpy V-Notch Energy Absorbed at +80°F, ft-lb
Steel W-8068					
6 hr at 900°F, AC*	239	256	12.0	66.2	38
3 hr at 900°F, AC	237	253	13.5	68.2	50
1 hr at 900°F, AC	212	231	14.0	70.8	89
24 hr at 800°F, AC	250	267	11.0	56.0	16
3 hr at 800°F, AC	212	232	14.0	63.9	37
1 hr at 800°F, AC	186	209	14.0	64.9	81
24 hr at 700°F, AC	220	214	12.0	46.6	20
3 hr at 700°F, AC	172	195	16.0	69.5	93
1 hr at 700°F, AC	156	180	16.0	72.0	123
Steel W-8598					
3 hr at 900°F, AC	225	241	14.0	71.0	65
1 hr at 900°F, AC	195	213	15.0	74.1	122
24 hr at 800°F, AC	238	257	13.5	63.9	23
3 hr at 800°F, AC	199	219	14.0	67.0	71
1 hr at 800°F, AC	173	196	16.0	68.6	116
24 hr at 700°F, AC	209	230	14.0	60.4	30
3 hr at 700°F, AC	162	186	16.5	71.4	117
1 hr at 700°F, AC	147	172	18.0	77.8	139

*Air-Cooled.

149

TABLE 19

Thermal Treatment and Mechanical Properties of an Aluminum-Substituted Steel (Heat No. W-8252-1A)

Thermal Treatment	Yield Strength (0.2% Offset), ksi	Tensile Strength, ksi	Elongation in 1 Inch, %	Reduction of Area, %	Charpy V-Notch Energy Absorbed at +80°F, ft-lb
As-Rolled	111	143	17.0	81.7	180
As-Rolled, 6 hr at 900°F, AC*	241	262	10.5	57.0	25
1 hr at 1500°F, AC	119	152	17.3	79.3	170
1 hr at 1500°F, AC, 6 hr at 900°F, AC	253	266	10.0	49.3	26
1 hr at 2200°F, AC, 6 hr at 900°F, AC	239	257	7.0	34.3	16
1 hr at 2200°F + 1/2 hr at 1500°F, AC	98	139	16.3	78.7	147
1 hr at 2200°F + 1/2 hr at 1500°F, AC, 6 hr at 900°F, AC	241	258	5.8	26.5	15
1 hr at 2200°F + 4 hr at 1500°F, AC	102	139	16.5	78.2	133
1 hr at 2200°F + 4 hr at 1500°F, AC, 6 hr at 900°F, AC	240	255	6.0	23.3	12
1 hr at 2300°F, AC/ 6 hr at 900°F, AC	239	253	17.0	28.3	16
1 hr at 2300°F + 1/2 hr at 1500°F, AC	102	139	16.8	80.0	137
1 hr at 2300°F + 1/2 hr at 1500°F, AC, 6 hr at 900°F, AC	236	251	5.5	25.3	13
1 hr at 2300°F + 4 hr at 1500°F, AC	108	138	17.0	79.3	134
1 hr at 2300°F + 4 hr at 1500°F, AC, 6 hr at 900°F, AC	239	254	4.5	20.3	12
1 hr at 2200°F, AC, 1 hr at 1500°F, AC	109	153	17.0	78.5	161
1 hr at 2200°F, AC, 1 hr at 1500°F, AC, 6 hr at 900°F, AC	256	265	11.0	54.3	21

*Air-Cooled.

150

TABLE 20

Thermal Treatment and Mechanical Properties of an Aluminum-Substituted Steel (Heat No. W-8252-1B)

Thermal Treatment	Yield Strength (0.2% Offset), ksi	Tensile Strength, ksi	Elongation in 1 Inch, %	Reduction of Area, %	Charpy V-Notch Energy Absorbed at +80°F, ft-lb
As-Rolled	112	139	18.0	80.9	175
As-Rolled, 6 hr at 900°F, AC*	249	260	11.5	57.5	23
1 hr at 1500°F, AC	118	150	18.0	79.3	162
1 hr at 1500°F, AC, 6 hr at 900°F, AC	252	266	13.0	58.0	25
1 hr at 2200°F, AC, 6 hr at 900°F, AC	238	255	7.0	29.3	15
1 hr at 2200°F → 1/2 hr at 1500°F, AC	102	137	17.5	78.8	134
1 hr at 2200°F → 1/2 hr at 1500°F, AC, 6 hr at 900°F, AC	243	255	6.0	19.9	14
1 hr at 2200°F → 4 hr at 1500°F, AC	118	137	16.0	78.8	132
1 hr at 2200°F → 4 hr at 1500°F, AC, 6 hr at 900°F, AC	235	253	4.0	16.4	12
1 hr at 2300°F, AC, 6 hr at 900°F, AC	233	250	5.5	19.3	15
1 hr at 2300°F → 1/2 hr at 1500°F, AC	107	136	18.0	79.8	124
1 hr at 2300°F → 1/2 hr at 1500°F, AC, 6 hr at 900°F, AC	235	249	5.5	16.7	12
1 hr at 2300°F → 4 hr at 1500°F, AC	106	136	17.0	76.6	129
1 hr at 2300°F → 4 hr at 1500°F, AC, 6 hr at 900°F, AC	236	249	5.0	14.5	12
1 hr at 2200°F, AC, 1 hr at 1500°F, AC	107	149	18.0	76.5	158
1 hr at 2200°F, AC, 1 hr at 1500°F, AC, 6 hr at 900°F, AC	249	262	11.0	46.5	20

*Air-Cooled.

TABLE 21

Thermal Treatment and Mechanical Properties of an Aluminum-Substituted Steel (Heat No. W-8252-1C)

Thermal Treatment	Yield Strength (0.2% Offset), ksi	Tensile Strength, ksi	Elongation in 1 Inch, %	Reduction of Area, %	Charpy V-Notch Energy Absorbed at +80°F, ft-lb
As-Rolled	107	137	18.0	75.0	169
As-Rolled, 6 hr at 900°F, AC*	239	257	12.0	53.0	23
1 hr at 1500°F, AC	112	149	17.0	76.5	163
1 hr at 1500°F, AC, 6 hr at 900°F, AC	252	265	11.5	55.5	24
1 hr at 2200°F, AC, 6 hr at 900°F, AC	239	255	5.0	18.3	14
1 hr at 2200°F + 1/2 hr at 1500°F, AC	115	138	17.0	75.7	114
1 hr at 2200°F + 1/2 hr at 1500°F, AC, 6 hr at 900°F, AC	240	255	4.0	11.1	12
1 hr at 2200°F + 4 hr at 1500°F, AC	109	137	16.0	76.2	130
1 hr at 2200°F + 4 hr at 1500°F, AC, 6 hr at 900°F, AC	242	255	4.0	14.1	11
1 hr at 2300°F, AC, 6 hr at 900°F, AC	240	254	2.0	14.1	14
1 hr at 2300°F + 1/2 hr at 1500°F, AC	105	136	16.0	77.5	131
1 hr at 2300°F + 1/2 hr at 1500°F, AC, 6 hr at 900°F, AC	239	253	4.0	13.0	11
1 hr at 2300°F + 4 hr at 1500°F, AC	103	137	18.0	76.4	116
1 hr at 2300°F + 4 hr at 1500°F, AC, 6 hr at 900°F, AC	239	253	4.0	13.0	10
1 hr at 2200°F, AC, 1 hr at 1500°F, AC	109	152	17.0	77.9	155
1 hr at 2200°F, AC, 1 hr at 1500°F, AC, 6 hr at 900°F, AC	240	267	8.0	42.0	19

*Air-Cooled

152

TABLE 22

Thermal Treatment and Mechanical Properties of an Aluminum-Substituted Steel (Heat No. W-8236)

Thermal Treatment	Yield Strength (0.2% Offset), ksi	Tensile Strength, ksi	Elongation in 1 Inch, %	Reduction of Area, %	Charpy V-Notch Energy Absorbed at +80°F, ft-lb
As-Rolled	107	144	17.0	79.4	171
As-Rolled, 6 hr at 900°F, AC*	277	289	10.8	51.3	21
1 hr at 1500°F, AC	129	149	17.0	81.8	175
1 hr at 1500°F, AC, 6 hr at 900°F, AC	283	289	10.2	47.8	20
1 hr at 2200°F, AC, 6 hr at 900°F, AC	263	280	4.0	13.0	11
1 hr at 2200°F + 1/2 hr at 1500°F, AC	122	144	16.8	76.4	120
1 hr at 2200°F + 1/2 hr at 1500°F, AC, 6 hr at 900°F, AC	259	277	4.2	15.2	9
1 hr at 2200°F + 4 hr at 1500°F, AC	143	144	15.8	70.1	80
1 hr at 2200°F + 4 hr at 1500°F, AC, 6 hr at 900°F, AC	264	282	3.5	11.6	10
1 hr at 2200°F, AC, 1 hr at 1500°F, AC	112	154	17.0	77.2	157
1 hr at 2200°F, AC, 1 hr at 1500°F, AC, 6 hr at 900°F, AC	277	293	6.8	28.6	13

*Air-Cooled.

153

TABLE 23

Chemical Composition of Vanadium-Substituted Steels

Heat No.	C	Mn	P	S	Si	Ni	Mo	Ti	Al	V	Co	N	O (ppm)
					Composition, percent								
W-8133-1A	0.004	0.004	0.0011	0.0026	0.009	18.1	5.14	<0.02	0.005	1.65	7.74	0.008	145
W-8133-1C	0.006	0.003	0.0010	0.0033	0.009	18.1	5.13	<0.02	0.006	1.67	7.73	0.004	120
W-8134-1A	0.007	0.009	0.0014	0.0045	0.007	17.9	4.02	<0.02	0.004	1.02	12.3	0.005	186
W-8134-1C	0.010	0.009	0.0014	0.0039	0.007	17.9	4.02	<0.02	0.005	1.06	12.3	0.005	158

TABLE 24

Thermal Treatment and Mechanical Properties of a Vanadium-Substituted Steel (Heat No. W-8133-1A)

Thermal Treatment	Yield Strength (0.2% Offset), ksi	Tensile Strength, ksi	Elongation in 1 Inch, %	Reduction of Area, %	Charpy V-Notch Energy Absorbed at +80°F ft-lb
As-Rolled	113	1?0	16.0	75.7	102
As-Rolled, 3 hr at 900°F, AC*	237	247	11.8	58.9	24
1 hr at 1500°F, AC	107	147	17.5	74.5	99
1 hr at 1500°F, AC, 3 hr at 900°F, AC	249	255	10.8	55.8	22
1 hr at 2200°F, AC, 3 hr at 900°F, AC	226	236	8.8	37.3	22
1 hr at 2200°F + 1/2 hr at 1500°F, AC	106	136	15.3	69.1	77
1 hr at 2200°F + 1/2 hr at 1500°F, AC, 3 hr at 900°F, AC	232	241	3.8	15.6	10
1 hr at 2200°F + 4 hr at 1500°F, AC	110	134	15.0	66.7	64
1 hr at 2200°F + 4 hr at 1500°F, AC, 3 hr at 900°F, AC	225	235	6.3	22.3	10
1 hr at 2300°F, AC, 3 hr at 900°F, AC	220	231	10.8	40.2	23
1 hr at 2300°F + 1/2 hr at 1500°F, AC	107	135	15.3	68.7	76
1 hr at 2300°F + 1/2 hr at 1500°F, AC, 3 hr at 900°F, AC	230	240	4.8	18.9	10
1 hr at 2300°F + 4 hr at 1500°F, AC	109	134	16.0	67.8	64
1 hr at 2300°F + 4 hr at 1500°F, AC, 3 hr at 900°F, AC	229	233	5.3	16.7	10
1 hr at 2200°F, AC, 1/2 hr at 1500°F, AC	109	148	16.8	71.2	94
1 hr at 2200°F, AC, 1/2 hr at 1500°F, AC, 3 hr at 900°F, AC	253	256	7.5	32.7	18
1 hr at 2200°F, IC, 4 hr at 1500°F, AC	104	144	17.0	72.4	96
1 hr at 2200°F, AC, 4 hr at 1500°F, AC, 3 hr at 900°F, AC	247	255	7.8	30.1	17

*Air-Cooled.

TABLE 25

Thermal Treatment and Mechanical Properties of a Vanadium-Substituted Steel (Heat No. W-8133-1C)

Thermal Treatment	Yield Strength (0.2% Offset), ksi	Tensile Strength, ksi	Elongation in 1 Inch, %	Reduction of Area, %	Charpy V-Notch Energy Absorbed at +80°F, ft-lb
As-Rolled	118	245	16.5	72.9	119
As-Rolled, 3 hr at 900°F, AC*	247	251	11.5	53.2	23
1 hr at 1500°F, AC	111	149	16.8	74.0	113
1 hr at 1500°F, AC, 3 hr at 900°F, AC	257	258	11.5	56.5	22
1 hr at 2200°F, AC, 3 hr at 900°F, AC	233	238.5	9.8	39.0	22
1 hr at 2200°F→1/2 hr at 1500°F, AC	108	139	15.8	67.8	80
1 hr at 2200°F→1/2 hr at 1500°F, AC, 3 hr at 900°F, AC	240	244	4.3	15.9	10
1 hr at 2200°F→4 hr at 1500°F, AC	109	138	15.2	67.4	68
1 hr at 2200°F→4 hr at 1500°F, AC, 3 hr at 900°F, AC	233	239	5.0	19.5	11
1 hr at 2300°F, AC, 3 hr at 900°F, AC	231	235	9.5	41.8	23
1 hr at 2300°F→1/2 hr at 1500°F, AC	108	139	16.0	67.6	79
1 hr at 2300°F→1/2 hr at 1500°F, AC, 3 hr at 900°F, AC	236	243	5.0	16.7	10
1 hr at 2300°F→4 hr at 1500°F, AC	108	138	16.8	68.0	63
1 hr at 2300°F→4 hr at 1500°F, AC, 3 hr at 900°F, AC	237	239	4.0	15.2	10
1 hr at 2200°F, AC, 1/2 hr at 1500°F, AC	107	150	17.5	72.4	122
1 hr at 2200°F, AC, 1/2 hr at 1500°F, AC, 3 hr at 900°F, AC	256	259	7.8	34.2	20
1 hr at 2200°F, AC, 4 hr at 1500°F, AC	109	144	17.0	71.4	121
1 hr at 2200°F, AC, 4 hr at 1500°F, AC, 3 hr at 900°F, AC	252	255	7.0	28.6	17

*Air-Cooled.

156

TABLE 26

Thermal Treatment and Mechanical Properties of a Vanadium-Substituted Steel (Heat No. W-8134-1A)

Thermal Treatment	Yield Strength (0.2% Offset), ksi	Tensile Strength, ksi	Elongation in 1 Inch, %	Reduction of Area, %	Charpy V-Notch Energy Absorbed at +80°F, ft-lb
As-Rolled	117	145	15.5	69.4	84
As-Rolled, 3 hr at 900°F, AC*	246	247	10.0	52.6	22
1 hr at 1500°F, AC	116	147	17.0	75.7	104
1 hr at 1500°F, AC, 3 hr at 900°F, AC	251	260	11.0	53.2	21
1 hr at 2200°F, AC, 3 hr at 900°F, AC	237	249	6.5	15.8	17
1 hr at 2200°F + 1/2 hr at 1500°F, AC	110	141	5.5	66.1	77
1 hr at 2200°F + 1/2 hr at 1500°F, AC, 3 hr at 900°F, AC	240	251	4.0	10.1	10
1 hr at 2200°F + 4 hr at 1500°F, AC	106	140	15.0	67.5	46
1 hr at 2200°F + 4 hr at 1500°F, AC, 3 hr at 900°F, AC	243	250	4.0	7.1	7
1 hr at 2300°F, AC, 3 hr at 900°F, AC	232	247	5.0	13.0	16
1 hr at 2300°F + 1/2 hr at 1500°F, AC	108	139	16.0	67.3	73
1 hr at 2300°F + 1/2 hr at 1500°F, AC, 3 hr at 900°F, AC	239	250	4.0	8.4	10
1 hr at 2300°F + 4 hr at 1500 F, AC	114	140	14.0	57.7	47
1 hr at 2300°F + 4 hr at 1500 F, AC, 3 hr at 900°F, AC	244	249	3.0	9.2	9
1 hr at 2200°F, AC, 1/2 hr at 1500°F, AC	116	156	16.0	69.6	72
1 hr at 2200°F, AC, 1/2 hr at 1500°F, AC, 3 hr at 900°F, AC	263	269	9.3	44.0	17
1 hr at 2200°F, AC, 4 hr at 1500°F, AC	117	149	16.0	67.5	82
1 hr at 2200°F, AC, 4 hr at 1500°F, AC, 3 hr at 900°F, AC	258	261	8.0	38.9	16

*Air-Cooled.

157

TABLE 27

Thermal Treatment and Mechanical Properties of a Vanadium-Substituted Steel (Heat No. W-8134-1C)

Thermal Treatment	Yield Strength (0.2% Offset), ksi	Tensile Strength, ksi	Elongation in 1 Inch, %	Reduction of Area, %	Charpy V-Notch Energy Absorbed at +80°F, ft-lb
As-Rolled	131	151	16.0	79.1	69
As-Rolled, 3 hr at 900°F, AC*	259	260	12.0	55.8	21
1 hr at 1500°F, AC	132	149	17.0	72.8	98
1 hr at 1500°F, AC, 3 hr at 900°F, AC	258	262	11.0	52.2	19
1 hr at 2200°F, AC, 3 hr at 900°F, AC	245	250	6.0	22.5	18
1 hr at 2200°F+ 1/2 hr at 1500°F, AC	113	144	16.0	66.2	68
1 hr at 2200°F+ 1/2 hr at 1500°F, AC, 3 hr at 900°F, AC	249	253	4.0	12.3	9
1 hr at 2200°F+ 4 hr at 1500°F, AC	119	144	15.0	62.8	48
1 hr at 2200°F+ 4 hr at 1500°F, AC, 3 hr at 900°F, AC	238	252	4.0	14.5	8
1 hr at 2300°F, AC, 3 hr at 900°F, AC	234	251	6.0	18.5	17
1 hr at 2300°F+ 1/2 hr at 1500°F, AC	114	144	17.0	69.4	72
1 hr at 2300°F+ 1/2 hr at 1500°F, AC, 3 hr at 900°F, AC	238	254	4.5	11.5	10
1 hr at 2300°F+ 4 hr at 1500°F, AC	109	144	13.5	59.5	47
1 hr at 2300°F+ 4 hr at 1500°F, AC, 3 hr at 900°F, AC	241	253	4.0	12.3	8
1 hr at 2200°F, AC, 1/2 hr at 1500°F, AC	114	158	15.0	72.0	74
1 hr at 2200°F, AC, 1/2 hr at 1500°F, AC, 3 hr at 900°F, AC	259	269	8.0	32.4	16
1 hr at 2200°F, AC, 4 hr at 1500°F, AC	119	152	16.0	70.2	84
1 hr at 2200°F, AC, 4 hr at 1500°F, AC, 3 hr at 900°F, AC	255	262	6.5	32.1	15

*Air-Cooled.

158

TABLE 28

Electron Diffraction Data Obtained from Fracture Surface Extraction Replicas of Steel W-8133-1A* and Steel W-8134-1A*

Miller Indices	Replica of Steel W-8133-1A		Replica of Steel W-8134-1A		VC**		VN+	
	I/I_o	$d(Å)$	I/I_o	$d(Å)$	I/I_o	$d(Å)$	I/I_o	$d(Å)$
(111)	S	2.38	M	2.39	100	2.40	100	2.47
(200)	S	2.07	S	2.05	100	2.07	100	2.14
(220)	M	1.45	S	1.45	50	1.47	70	1.52
(311)	W	1.23	W	1.24	25	1.25	50	1.29
(222)	VW	1.18	W	1.19	10	1.20	50	1.24
(400)	VVW	1.03	VVW	1.03	5	1.04	-	-
(331)	VW	0.935	VW	0.945	5	0.95	70	0.98
(420)	W	0.92	W	0.92	10	0.93	100	0.96
(422)	W	0.84	-	-	5	0.85	100	0.88
(511),(333)	W	0.78	VW	0.83	3	0.80	100	0.83

*Heat Treatment of 1 Hour at 2200°F → 4 Hours at 1500°F, Air-Cooled, 3 Hours at 900°F, Air-Cooled.

**ASTM X-Ray Powder Data File, Card No. 1-1159.

+ASTM X-Ray Powder Data File, Card No. 2-1064.

TABLE 29

Chemical Composition of Experimental Columbium-Tantalum Heats

Heat No.	Composition, percent													O (ppm)
	C	Mn	P	S	Si	Ni	Mo	Ti	Al	Co	Cb	Ta	N	
W-8196	0.003	0.002	0.001	0.0012	0.004	17.8	4.9	0.40	0.08	7.8	0.20		<0.001	18
W-8197	0.003	0.003	0.0006	0.0013	0.003	18.2	4.9	0.39	0.08	7.9		0.21	<0.001	25
W-8198	0.004	0.002	0.0006	0.0016	0.003	17.7	4.9	0.39	0.07	7.9			<0.001	17

TABLE 30

Mechanical Properties of Columbium Heat No. W-8196

Heat Treatment	Yield Strength (0.2% Offset), ksi	Tensile Strength, ksi	Elongation in 1 Inch, %	Reduction of Area, %	CVN Energy Absorbed at +80°F, ft-lb
As-rolled					
As-rolled, 3 hr at 900°F, AC*	105	142	18.0	82.8	173
	246	260	13.0	64.8	37
1 hr at 1500°F, AC	100	146	17.5	78.7	179
1 hr at 1500°F, AC, 3 hr at 900°F, AC	245	258	12.0	61.4	25
1 hr at 2200°F, AC, 3 hr at 900°F, AC	233	247	11.0	49.3	20
1 hr at 2200°F → 1/2 hr at 1500°F, AC	110	139	18.0	78.8	143
1 hr at 2200°F → 1/2 hr at 1500°F, AC, 3 hr at 900°F, AC	236	249	10.5	39.2	15
1 hr at 2200°F → 4 hr at 1500°F, AC	108	138	15.5	73.2	38
1 hr at 2200°F → 4 hr at 1500°F, AC, 3 hr at 900°F, AC	232	243	5.0	17.0	11
1 hr at 2300°F, AC, 3 hr at 900°F, AC	235	244	11.0	46.7	21
1 hr at 2300°F → 1/2 hr at 1500°F, AC	105	139	17.8	59.5	127
1 hr at 2300°F → 1/2 hr at 1500°F, AC, 3 hr at 900°F, AC	237	245	8.5	34.8	16
1 hr at 2300°F → 4 hr at 1500°F, AC	102	138	17.0	72.7	37
1 hr at 2300°F → 4 hr at 1500°F, AC, 3 hr at 900°F, AC	229	243	6.0	19.2	10

*Air-Cooled.

TABLE 31

Mechanical Properties of Tantalum Heat No. W-8197

Heat Treatment	Yield Strength (0.2% Offset), ksi	Tensile Strength, ksi	Elongation in 1 Inch, %	Reduction of Area, %	CVN Energy Absorbed at +80°F, ft-lb
As-rolled	105	144	18.0	83.2	172
As-rolled, 3 hr at 900°F, AC*	258	269	12.0	64.2	26
1 hr at 1500°F, AC	107	145	17.5	80.2	184
1 hr at 1500°F, AC, 3 hr at 900°F, AC	257	270	12.0	63.2	24
1 hr at 2200°F, AC, 3 hr at 900°F, AC	250	263	8.0	39.9	15
1 hr at 2200°F → 1/2 hr at 1500°F, AC	105	139	16.5	79.1	135
1 hr at 2200°F → 1/2 hr at 1500°F, AC, 3 hr at 900°F, AC	249	262	7.5	33.2	11
1 hr at 2200°F → 4 hr at 1500°F, AC	104	139	15.5	70.1	40
1 hr at 2200°F → 4 hr at 1500°F, AC, 3 hr at 900°F, AC	245	257	3.0	8.2	7
1 hr at 2300°F, AC, 3 hr at 900°F, AC	247	259	6.0	25.5	17
1 hr at 2300°F → 1/2 hr at 1500°F, AC	100	138	17.5	76.4	116
1 hr at 2300°F → 1/2 hr at 1500°F, AC, 3 hr at 900°F, AC	247	259	7.8	24.3	12
1 hr at 2300°F → 4 hr at 1500°F, AC	95	137	15.8	68.8	45
1 hr at 2300°F → 4 hr at 1500°F, AC, 3 hr at 900°F, AC	244	255	3.0	8.0	7

*Air-Cooled.

TABLE 32

Mechanical Properties of Control Heat No. W-8198

Heat Treatment	Yield Strength (0.2% Offset), ksi	Tensile Strength, ksi	Elongation in 1 Inch, %	Reduction of Area, %	CVN Energy Absorbed at +80°F, ft-lb
As-rolled	109	142	18.5	82.3	178
As-rolled, 3 hr at 900°F, AC*	252	261	12.8	64.1	32
1 hr at 1500°F, AC	97	141	19.0	82.2	197
1 hr at 1500°F, AC, 3 hr at 900°F, AC	249	259	14.0	65.6	37
1 hr at 2200°F, AC, 3 hr at 900°F, AC	243	256	9.0	33.5	17
1 hr at 2200°F + 1/2 hr at 1500°F, AC	100	140	17.0	75.0	143
1 hr at 2200°F + 1/2 hr at 1500°F, AC, 3 hr at 900°F, AC	245	257	5.0	18.2	13
1 hr at 2200°F + 4 hr at 1500°F, AC	98	138	15.0	64.8	82
1 hr at 2200°F + 4 hr at 1500°F, AC, 3 hr at 900°F, AC	241	253	2.8	7.4	7
1 hr at 2300°F, AC, 3 hr at 900°F, AC	242	254	5.7	22.7	16
1 hr at 2300°F + 1/2 hr at 1500°F, AC	101	140	17.8	77.4	142
1 hr at 2300°F + 1/2 hr at 1500°F, AC, 3 hr at 900°F, AC	243	254	5.0	19.0	13
1 hr at 2300°F + 4 hr at 1500°F, AC	109	139	15.0	67.2	83
1 hr at 2300°F + 4 hr at 1500°F, AC, 3 hr at 900°F, AC	239	250	2.5	7.0	7

*Air-Cooled.

TABLE 33

Electron Diffraction Data Obtained from Fracture Surface Extraction Replicas of Steels W-8196, W-8197, and W-8198

Miller Indices	Interplanar Spacings (d), $\mathring{A}$				
	W-8196[*] (Columbium)	W-8197[*] (Tantalum)	W-8198[*] (Control)	TiC[**]	TiN[+]
(111)	2.53	2.52	2.42	2.51	2.44
(200)	**	2.15	2.10	2.18	2.12
(220)	1.54	1.55	1.49	1.54	1.50
(113)	1.32	1.32	1.27	1.31	1.28
(222)	1.28	1.26	1.22	1.26	1.22
(400)	**	1.07	**	1.09	1.06
(331)	1.00	1.00	0.97	1.00	0.97
(420)	0.98	0.98	0.94	0.97	0.95
(224)	-	0.89	0.86	0.88	0.87

[*]Heat Treatment of 1 Hour at 2200°F ÷ 4 Hours at 1500°F, Air-Cooled, 3 Hours at 900°F, Air-Cooled.

[**]ASTM X-Ray Powder Data File, Card No. 6-0642.

[+]ASTM X-Ray Powder Data File, Card No. 6-0614.

TABLE 34

Chemical Composition of Experimental Silicon Heats

Composition, percent

Heat No.	C	Mn	P	S	Si	Ni	Mo	Ti	Al	Co	N
W-8202-A	0.003	0.001	0.0007	0.0027	0.017	18.0	4.92	0.41	0.15	7.98	<0.001
W-8202-B	0.002	0.001	0.0010	0.0023	0.056	18.0	4.93	0.41	0.08	7.98	<0.001
W-8202-C	0.002	0.001	0.0007	0.0024	0.11	18.1	4.92	0.40	0.07	7.96	<0.001

TABLE 35

Mechanical Properties of Heat W-8202-A
(Silicon = 0.017%)

Heat Treatment	Yield Strength (0.2% Offset), ksi	Tensile Strength, ksi	Elongation in 1 Inch, %	Reduction of Area, %	CVN Energy Absorbed at +80°F, ft-lb
As-rolled	107	143	17.2	79.2	126
As-rolled, 3 hr at 900°F, AC*	245	258	12.5	62.6	27
1 hr at 1500°F, AC	107	147	17.0	79.0	141
1 hr at 1500°F, AC, 3 hr at 900°F, AC	259	269	11.5	59.2	24
1 hr at 2200°F, AC, 3 hr at 900°F, AC	238	253	7.7	35.2	25
1 hr at 2200°F + 1/2 hr at 1500°F, AC	108	140	16.5	77.4	124
1 hr at 2200°F + 1/2 hr at 1500°F, AC, 3 hr at 900°F, AC	240	254	5.5	24.8	8
1 hr at 2200°F + 4 hr at 1500°F, AC	106	139	17.2	76.4	101
1 hr at 2200°F + 4 hr at 1500°F, AC, 3 hr at 900°F, AC	239	252	4.0	14.8	8
1 hr at 2300°F, AC, 3 hr at 900°F, AC	237	253	5.5	23.8	13
1 hr at 2300°F + 1/2 hr at 1500°F, AC	112	138	17.0	75.4	102
1 hr at 2300°F + 1/2 hr at 1500°F, AC, 3 hr at 900°F, AC	238	252	4.0	16.0	7
1 hr at 2300°F + 4 hr at 1500°F, AC	104	139	16.0	73.1	65
1 hr at 2300°F + 4 hr at 1500°F, AC, 3 hr at 900°F, AC	240	255	3.0	8.0	6

*Air-Cooled.

TABLE 36

Mechanical Properties of Heat W-8202-B
(Silicon = 0.056%)

Heat Treatment	Yield Strength (0.2% Offset), ksi	Tensile Strength, ksi	Elongation in 1 Inch, %	Reduction of Area, %	CVN Energy Absorbed at +80°F, ft-lb
As-rolled	110	145	18.0	77.9	165
As-rolled, 3 hr at 900°F, AC*	240	253	11.0	58.4	26
1 hr at 1500°F, AC	116	152	17.0	75.3	156
1 hr at 1500°F, AC, 3 hr at 900°F, AC	257	268	11.5	57.8	25
1 hr at 2200°F, AC, 3 hr at 900°F, AC	233	249	10.5	46.7	18
1 hr at 2200°F + 1/2 hr at 1500°F, AC	109	143	17.0	72.2	79
1 hr at 2200°F + 1/2 hr at 1500°F, AC, 3 hr at 900°F, AC	233	249	5.0	17.6	7
1 hr at 2200°F + 4 hr at 1500°F, AC	108	141	15.0	68.5	33
1 hr at 2200°F + 4 hr at 1500°F, AC, 3 hr at 900°F, AC	231	247	3.0	14.5	5
1 hr at 2300°F, AC, 3 hr at 900°F, AC	223	241	9.0	38.1	15
1 hr at 2300°F + 1/2 hr at 1500°F, AC	104	143	16.0	72.9	33
1 hr at 2300°F + 1/2 hr at 1500°F, AC, 3 hr at 900°F, AC	225	242	2.2	6.9	5
1 hr at 2300°F + 4 hr at 1500°F, AC	103	140	15.2	66.7	25
1 hr at 2300°F + 4 hr at 1500°F, AC, 3 hr at 900°F, AC	229	245	1.0	4.6	5

*Air-Cooled.

167

TABLE 37

Mechanical Properties of Heat W-8202-C
(Silicon = 0.11%)

Heat Treatment	Yield Strength (0.2% Offset), ksi	Tensile Strength, ksi	Elongation in 1 Inch, %	Reduction of Area, %	CVN Energy Absorbed at +80°F, ft-lb
As-rolled	120	147	16.0	79.1	140
As-rolled, 3 hr at 900°F, AC*	249	256	11.0	61.0	29
1 hr at 1500°F, AC	132	149	16.0	76.9	159
1 hr at 1500°F, AC, 3 hr at 900°F, AC	260	268	12.0	59.4	21
1 hr at 2200°F, AC, 3 hr at 900°F, AC	234	252	10.0	47.3	16
1 hr at 2200°F + 1/2 hr at 1500°F, AC	109	143	15.5	70.8	34
1 hr at 2200°F + 1/2 hr at 1500°F, AC, 3 hr at 900°F, AC	241	252	2.0	6.2	5
1 hr at 2200°F + 4 hr at 1500°F, AC	125	141	14.5	63.2	22
1 hr at 2200°F + 4 hr at 1500°F, AC, 3 hr at 900°F, AC	230	249	2.0	5.8	4
1 hr at 2300°F, AC, 3 hr at 900°F, AC	221	249	7.0	30.0	13
1 hr at 2300°F + 1/2 hr at 1500°F, AC	114	144	15.5	69.8	17
1 hr at 2300°F + 1/2 hr at 1500°F, AC, 3 hr at 900°F, AC	229	248	1.5	4.4	4
1 hr at 2300°F + 4 hr at 1500°F, AC	111	141	13.0	56.2	14
1 hr at 2300°F + 4 hr at 1500°F, AC, 3 hr at 900°F, AC	232	247	1.0	2.4	3

*Air-Cooled.

168

TABLE 38

**Electron Diffraction Data Obtained from Fracture Surface
Extraction Replicas of Steels W-8202-A, W-8202-B, and W-8202-C**

| Miller Indices | Interplanar Spacings (d), Å | | | | |
	W-8202-A[*] (0.017% Si)	W-8202-B[*] (0.056% Si)	W-8202-C[*] (0.11% Si)	TiC[**]	TiN[+]
(111)	2.51 2.26[++]	2.51	2.51	2.51	2.44
(200)	2.17 1.60[++]	2.18	2.17 1.62[+]	2.18	2.12
(220)	1.54	1.54	1.54	1.54	1.50
(113)	1.31	1.31	1.31	1.31	1.28
(222)	1.25	1.25	1.26	1.26	1.22
(400)			1.09	1.09	1.06
(331)	0.99	0.99	1.00	1.00	0.97
(420)	0.97	0.97	0.97	0.97	0.95
(224)	0.88	0.88	0.89	0.88	0.87

[*]Heat Treatment of 1 Hour at 2200°F → 4 Hours at 1500°F,
Air-Cooled, 3 Hours at 900°F, Air-Cooled.

[**]ASTM X-Ray Powder Data File, Card No. 6-0642.

[+]ASTM X-Ray Powder Data File, Card No. 6-0614.

[++]τ-Ti$_2$S (VW) — ASTM X-Ray Powder Data File, Card No. 11-664.

TABLE 39

Chemical Composition of Experimental Cerium Heats

Heat No.	C	Mn	P	S	Si	Ni	Mo	Ti	Al	Co	Ce	N
W-8199	0.002	0.012	0.005	0.010	0.010	18.0	5.04	0.24	0.03	7.94	<0.01*	<0.001
W-8200	0.002	0.001	0.003	0.004	0.008	18.2	5.10	0.43	0.09	7.96	0.04**	<0.001
W-8201	0.004	0.001	0.0005	0.008	0.001	17.9	4.91	0.40	0.11	7.89	-	0.001

*Aimed for 0.15 percent.

**Aimed for 0.5 percent.

DOCUMENT CONTROL DATA - R&D

(Security classification of title, body of abstract and indexing annotation must be entered when the overall report is classified)

1. ORIGINATING ACTIVITY (Corporate author)	2a. REPORT SECURITY CLASSIFICATION
U. S. Steel Corporation Applied Research Laboratory Monroeville, Pa.	Unclassified
	2b GROUP

3. REPORT TITLE Investigation of Thermal Embrittlement in 18Ni (250) Maraging Steel.

4. DESCRIPTIVE NOTES (Type of report and inclusive dates)
Final Technical Report 30 June, 1965 to 31 October, 1966

5. AUTHOR(S) (Last name, first name, initial)

Barton, C. J., Reisdorf, B. G., Cox, P. H. Salmon, Chilton, J. M., Oskin, C. E. Jr.

6. REPORT DATE	7a. TOTAL NO. OF PAGES	7b. NO. OF REFS
March 1967	170	7

8a. CONTRACT OR GRANT NO.	9a. ORIGINATOR'S REPORT NUMBER(S)
AF 33(615)-2780	
b. PROJECT NO. 7351	
c. Task No. 735105	9b. OTHER REPORT NO(S) (Any other numbers that may be assigned this report)
d.	AFML-TR-67-34

10. AVAILABILITY/LIMITATION NOTICES This document is subject to special export controls and each transmittal to foreign governments or foreign nationals may be made only with prior approval of the Metals and Ceramics Division (MAM), Air Force Materials Laboratory, Wright-Patterson AFB, Ohio 45433.

11. SUPPLEMENTARY NOTES	12. SPONSORING MILITARY ACTIVITY
	AF Materials Laboratory (MAMP) Wright-Patterson AFB, Ohio 45433

13. ABSTRACT The ultrahigh-strength 18Ni maraging steels may be severely embrittled by certain high-temperature thermal treatments involved in processing and fabrication. Investigation objectives were to (1) survey the thermal embrittlement characteristics of a commercial 18Ni (250) maraging steel, (2) determine the thermal treatments that result in a maximum degree of embrittlement, (3) discover the metallurgical sources of the embrittlement, and (4) improve the resistance of the steel to thermal embrittlement by alloy modification.

This abstract is subject to special export controls and each transmittal to foreign governments or foreign nationals may be made only with prior approval of the Metals and Ceramics Division (MAM), Air Force Materials Laboratory, Wright-Patterson AFB, Ohio 45433.

14.	LINK A		LINK B		LINK C	
KEY WORDS	ROLE	WT	ROLE	WT	ROLE	WT

INSTRUCTIONS

1. **ORIGINATING ACTIVITY:** Enter the name and address of the contractor, subcontractor, grantee, Department of Defense activity or other organization *(corporate author)* issuing the report.

2a. **REPORT SECURITY CLASSIFICATION:** Enter the overall security classification of the report. Indicate whether "Restricted Data" is included. Marking is to be in accordance with appropriate security regulations.

2b. **GROUP:** Automatic downgrading is specified in DoD Directive 5200.10 and Armed Forces Industrial Manual. Enter the group number. Also, when applicable, show that optional markings have been used for Group 3 and Group 4 as authorized.

3. **REPORT TITLE:** Enter the complete report title in all capital letters. Titles in all cases should be unclassified. If a meaningful title cannot be selected without classification, show title classification in all capitals in parenthesis immediately following the title.

4. **DESCRIPTIVE NOTES:** If appropriate, enter the type of report, e.g., interim, progress, summary, annual, or final. Give the inclusive dates when a specific reporting period is covered.

5. **AUTHOR(S):** Enter the name(s) of author(s) as shown on or in the report. Enter last name, first name, middle initial. If military, show rank and branch of service. The name of the principal author is an absolute minimum requirement.

6. **REPORT DATE:** Enter the date of the report as day, month, year; or month, year. If more than one date appears on the report, use date of publication.

7a. **TOTAL NUMBER OF PAGES:** The total page count should follow normal pagination procedures, i.e., enter the number of pages containing information.

7b. **NUMBER OF REFERENCES:** Enter the total number of references cited in the report.

8a. **CONTRACT OR GRANT NUMBER:** If appropriate, enter the applicable number of the contract or grant under which the report was written.

8b, 8c, & 8d. **PROJECT NUMBER:** Enter the appropriate military department identification, such as project number, subproject number, system numbers, task number, etc.

9a. **ORIGINATOR'S REPORT NUMBER(S):** Enter the official report number by which the document will be identified and controlled by the originating activity. This number must be unique to this report.

9b. **OTHER REPORT NUMBER(S):** If the report has been assigned any other report numbers *(either by the originator or by the sponsor),* also enter this number(s).

10. **AVAILABILITY/LIMITATION NOTICES:** Enter any limitations on further dissemination of the report, other than those imposed by security classification, using standard statements such as:

(1) "Qualified requesters may obtain copies of this report from DDC."

(2) "Foreign announcement and dissemination of this report by DDC is not authorized."

(3) "U. S. Government agencies may obtain copies of this report directly from DDC. Other qualified DDC users shall request through

_____ ."

(4) "U. S. military agencies may obtain copies of this report directly from DDC. Other qualified users shall request through

_____ ."

(5) "All distribution of this report is controlled. Qualified DDC users shall request through

_____ ."

If the report has been furnished to the Office of Technical Services, Department of Commerce, for sale to the public, indicate this fact and enter the price, if known.

11. **SUPPLEMENTARY NOTES:** Use for additional explanatory notes.

12. **SPONSORING MILITARY ACTIVITY:** Enter the name of the departmental project office or laboratory sponsoring *(paying for)* the research and development. Include address.

13. **ABSTRACT:** Enter an abstract giving a brief and factual summary of the document indicative of the report, even though it may also appear elsewhere in the body of the technical report. If additional space is required, a continuation sheet shall be attached.

It is highly desirable that the abstract of classified reports be unclassified. Each paragraph of the abstract shall end with an indication of the military security classification of the information in the paragraph, represented as *(TS), (S), (C),* or *(U).*

There is no limitation on the length of the abstract. However, the suggested length is from 150 to 225 words.

14. **KEY WORDS:** Key words are technically meaningful terms or short phrases that characterize a report and may be used as index entries for cataloging the report. Key words must be selected so that no security classification is required. Identifiers, such as equipment model designation, trade name, military project code name, geographic location, may be used as key words but will be followed by an indication of technical context. The assignment of links, rules, and weights is optional.